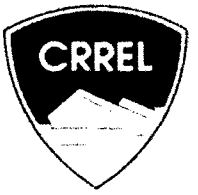

SPECIAL REPORT 93-21

A Mathematical Model for Oil Slick Transport and Mixing in Rivers

Hung Tao Shen, Poojitha D. Yapa, De Sheng Wang and Xiao Qing Yang

August 1993

Abstract

The growing concern over the impacts of oil spills on aquatic environments has led to the development of many computer models for simulating the transport and spreading of oil slicks in surface waters. Almost all of these models were developed for coastal environments. A few river models exist. These models only considered the movement of surface oil slicks. In this study a two-layer model, ROSS2, is developed for simulating oil spills in rivers. This model considers the oil in the river to consist of a surface slick and suspended oil droplets entrained over the depth of the flow. The oil transformation processes considered in the model include advection, mechanical spreading, turbulent diffusion and mixing, evaporation, dissolution, emulsification, shoreline deposition and sinking. The model can be used for simulating instantaneous or continuous spills either on or under the water surface in rivers with or without an ice cover. The model has been implemented for the Ohio–Monongahela–Allegheny river system and the upper St. Lawrence River. This report describes the model formulation and implementation. A case study is presented along with detailed explanations of the program structure and its input and output. Although it is developed for simulating oil spills, the model can be applied to spills of other hazardous materials.

For conversion of SI metric units to U.S./British customary units of measurement consult *Standard Practice for Use of the International System of Units (SI)*, ASTM Standard E380-89a, published by the American Society for Testing and Materials, 1916 Race St., Philadelphia, Pa. 19103.

This report is printed on paper that contains a minimum of 50% recycled material.

Special Report 93-21

US Army Corps of Engineers
Cold Regions Research & Engineering Laboratory

A Mathematical Model for Oil Slick Transport and Mixing in Rivers

Hung Tao Shen, Poojitha D. Yapa, De Sheng Wang and Xiao Qing Yang

August 1993

Prepared for
U.S. ARMY COLD REGIONS RESEARCH AND ENGINEERING LABORATORY
and
ST. LAWRENCE SEAWAY DEVELOPMENT CORPORATION

PREFACE

This report was prepared by Hung Tao Shen, Professor; Poojitha D. Yapa, Assistant Professor; De Sheng Wang, Research Assistant; and Xiao Qing Yang, Visiting Scholar, Department of Civil and Environmental Engineering, Clarkson University, Potsdam, New York.

This study was supported in part by the U.S. Army Cold Regions Research and Engineering Laboratory (CRREL), Hanover, New Hampshire, under Contract No. DACA 89-SS-K0019, and the St. Lawrence Seaway Development Corporation, Department of Transportation, under Contract No. DTSL55-89-C-C0549. Part of the work during the final phase of this study was carried out at the Water Resources Engineering Department, Luleå University of Technology. Support provided by the Swedish Natural Science Research Council (NFR) and the Luleå University of Technology for Dr. Shen and Mr. Wang is appreciated.

The authors thank Steven F. Daly of CRREL, Robert Schmitt and Lewis Kwett of the U.S. Army Engineer District, Pittsburgh, Stephen C. Hung of the St. Lawrence Seaway Development Corporation, and Anders Sellgren and Annika Andersson of the Luleå University of Technology *for their cooperation and assistance.*

This report is one of a series of reports on numerical simulation of oil slicks in inland waterways. The series coordinator is Steven F. Daly, CRREL.

CONTENTS

ILLUSTRATIONS

TABLES

A Mathematical Model for Oil Slick Transport and Mixing in Rivers

HUNG TAO SHEN, POOJITHA D. YAPA, DE SHENG WANG AND XIAO QING YANG

INTRODUCTION

In recent years there has been a growing concern over the increasing contamination of waterways and shoreline areas caused by oil spills. Oil spills in inland waterways can have enormous environmental and economic impacts. Oil pollution in rivers can not only cause long-term damage to the aquatic environment for fish and wildlife but also pose threats to water supplies for areas along the river. With heavy industrial development in areas along rivers and inland navigation activities, major rivers in the United States are vulnerable to oil spills. For example, in January 1988, an oil storage tank at West Elizabeth, Pennsylvania, collapsed, spilling over 17,000 barrels of diesel oil into the Monongahela River. The oil slick reached the Ohio River near Pittsburgh, which is 25 miles downstream of the spill site, within a day and drifted farther downstream, affecting water supply intakes along the river (Miklaucic and Saseen 1989).

Concern over the adverse impacts of oil spills has led government agencies and private industries to develop oil spill emergency response plans (e.g. Hung 1991). An important element in these programs is the use of computer models to predict the movement and possible impact of an oil spill. In the event of a real oil spill, a model can be used on a real-time basis to assist the containment and recovery of the oil, and it can also help to guide the field data collection for detailed environmental impact analysis. These objectives can be achieved by using the model to forecast the location and distribution of the oil. A computer model can also be used to study scenarios of possible spills to assist in developing contingency plans and assessing likely environmental impacts.

Numerous oil spill models have been developed during the last two decades, as reviewed by Stolzenbach et al. (1977), Huang and Monastero (1982) and Spaulding (1988). Almost all of these models were developed for coastal marine environments. In a recent study Shen and Yapa (1988) developed a model, ROSS, for surface oil slick transport in rivers. Oil slick transformation processes considered in the model include advection, mechanical spreading, horizontal turbulent diffusion, evaporation, dissolution and shoreline deposition. In this study, a two-layer model, ROSS2, is developed to take into consideration the dispersion of oil droplets into the water column, as well as related processes including subsurface transport, mass exchanges between the surface slick and the suspended oil droplets in the water column, and deposition of oil to the channel bottom due to sedimentation.

Transport and fate of spilled oil

In addition to the location, size and physical–chemical properties of the spill, the fate of an oil spill is affected by complex interrelated transport and weathering processes (Mackay and McAuliffe 1988).

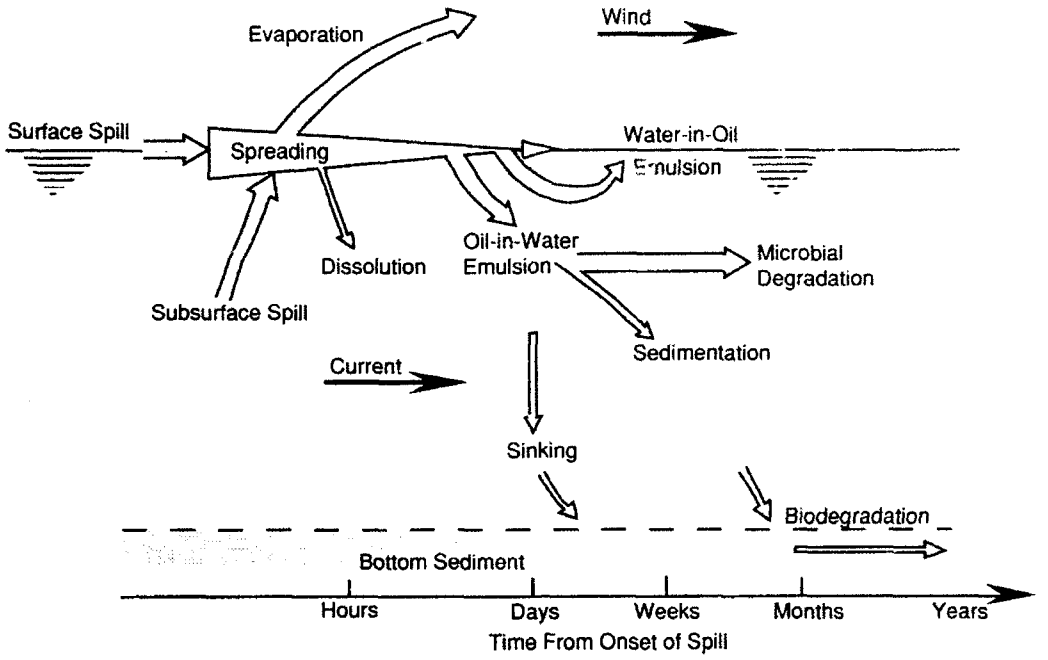

Figure 1. Physical, chemical and biological processes affecting the oil slick transformation.

Figure 1 shows a schematic representation of the fate of oil spilled in a surface water body. Oil may enter a water body either through a surface spill or an underwater discharge. A part of the spilled oil will form a surface slick on the water surface and can be moved about by the action of winds, currents or waves. Some low-molecular-weight hydrocarbons can dissolve into the underlying water column, but most of these are lost to the atmosphere through evaporation. Evaporation of volatile components will reduce the volume of spilled oil by as much as 50% during the first few days after the spill (Butler et al. 1976). In turbulent waters some of the oil is emulsified and dispersed into the water column as suspended droplets. Some of the oil droplets in the suspension may become attached to suspended particulate matter and slowly settle to the bottom; some will rise to the water surface due to buoyancy to form a water-in-oil emulsion. Current and waves may also drive oil onto beaches or riverbanks. For spills in rivers the transport of oil is also affected by hydraulic structures, such as locks and dams, as shown in Figure 2. In addition, photochemical reactions and microbial biodegradation can change the character of the oil and reduce the amount of oil present.

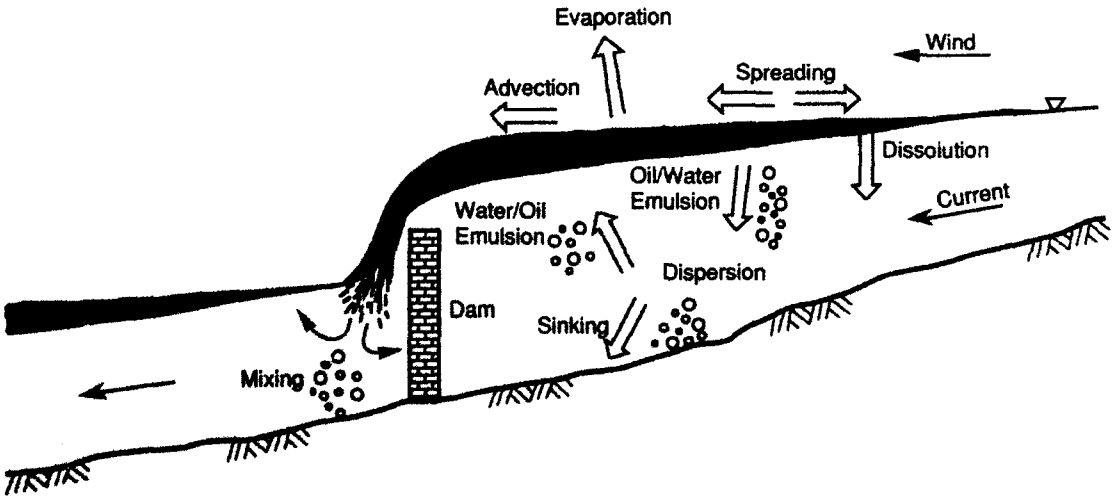

Figure 2. Oil slick transformation in rivers.

Advection

Advection is a physical process that involves drifting of the surface oil slick and the subsurface oil. It is the main mechanism that governs the location of the oil following its discharge into the river. Once spilled into the river, the oil will be transported downstream by the flow, with the influence of wind. The advection of surface oil is caused by the combined effects of surface current and wind drag. The advection of subsurface oil is the movement of suspended oil droplets entrained in the flow due to the subsurface current.

Spreading

Spreading is the physical process that involves drifting of the surface oil slick and the subsurface oil as it is being transported in the river. The spreading phenomena include mechanical spreading and horizontal diffusion. Mechanical spreading is the horizontal spreading of the surface oil slick due to the balancing forces of inertia, gravity, viscosity and surface tension. This mechanism terminates when the thickness of the slick is reduced and the thin oil slick ruptures into small patches. Horizontal diffusion is the spreading of oil due to the turbulent fluctuations of wind and current velocities. This is the main mechanism that causes the spreading of both the surface and subsurface oils. Since the spreading of oil enhances other weather processes, such as evaporation, dissolution and emulsification, it is one of the most important processes affecting the fate of the spilled oil.

Evaporation

Evaporation occurs immediately after the spill. As the surface slick spreads, more of the hydrocarbons are exposed to the atmosphere, causing the evaporation rate to increase. The amount and rate of evaporation depend on the percentage of light, or volatile, components in oil. Evaporation is the most significant physical–chemical process causing the reduction in oil volume. Highly refined oil can lose 75% or more of its volume through evaporation within a matter of days.

Dissolution

Some of the same oil components that are subjected to evaporation can also dissolve into the water column from a surface slick. Only the low-molecular-weight hydrocarbons have an appreciable solubility in water. The fraction of oil dissolved is very small compared to the oil that is evaporated. However, this extraction process can be important because of the toxicity of the dissolved fraction.

Emulsification

Dispersion, or oil-in-water emulsification, is the mixing of surface oil into the water column. Breaking waves and other surface turbulence can mix the surface oil into the water column by forming many small globules of oil that can be rapidly dispersed over the depth of the river flow and transported by the current. Some of the fine oil droplets in the water column may dissolve in the water column, attach to solid particles and biodegrade. A significant portion of suspended oil droplets will rise to the water surface when the buoyancy force is large enough to overcome the vertical mixing. This resurfacing mechanism can increase the area of oil on the water surface and the duration of oil passage at any particular site along the river.

Water-in-oil emulsions can also be formed, particularly with heavy crudes and residual oil. The resulting emulsions contain a large percentage of water but have a semisolid texture, often referred to as "mousse" because of their appearance. The formation of mousse is a process of dispersion of emulsified water into the oil. This process will increase the viscosity and volume of the slick. Stable emulsions can have a water content of up to 80%. The mechanism of water-in-oil emulsification is not clear, although it is believed that this is due to the presence of asphaltenes, waxes and surfactants and the turbulence associated with dispersion and resurfacing processes.

Photo-oxidation

In the presence of atmospheric oxygen, natural sunlight has sufficient energy to change the composition of the oil. This photo-oxidation process is very slow and usually becomes important a few days after the spill. The extent and rate of photo-oxidation depends primarily on the chemical composition and optical density of the oil. The photochemical reactions can change the interfacial properties of the oil and may dissolve toxic organic species into the water column. However, its effect on the oil slick transport process is not very important.

Shoreline deposition and sedimentation

Oil may be brought to the riverbanks and deposited along the shoreline, to be later re-entrained into the river current. This process can significantly affect the distribution of oil and should be modeled Some of the suspended oil droplets may also sink to the riverbed. This sinking or sedimentation process occurs due to an increase in density of the oil, resulting from either the evaporation and dissolution of lighter fractions of the oil, or adherence of the oil droplets onto suspended sediment. The oil deposited on the channel bottom may be moved laterally or resuspended, or it may undergo further biological or physical–chemical reaction. Little is known about the ultimate fate of the sedimented oil.

Biodegradation

All of the processes just described, except possibly photo-oxidation, can only redistribute the oil. They cannot remove the hydrocarbon from the environment. Real degradation takes place only through biochemical oxidation. This biodegradation process, which may continue for years after a spill, is the principal long-term means of removing the spilled oil from the environment.

Oil spill models

Most of the existing oil spill models simulate only the advection and spreading of a surface slick. Other models deal extensively with physical–chemical processes but lack the component for simulating the movement of the slick. Only in recent models have the incorporation of both transport and weathering processes been attempted (Huang and Monastero 1982, Spaulding 1988). Since there is a significant lack of data for a reliable analytical formulation to be established for many of the weathering processes, it is impractical to include all of them into an oil spill simulation model. It would be more useful to include the most significant processes, i.e. those accounting for the bulk of the oil, while omitting others so that uncertainty in the outcome can be reduced. Almost all of the existing oil slick models were developed for coastal marine environments.

Only a few models were developed for inland waters (Huang and Monastero 1982). Tsahalis (1979b) developed a simulation model for predicting the transport, spreading and associated shoreline contamination of a surface oil slick in a river. In his model the current velocity distribution in the river is calculated by empirical relationships determined from field data with some modifications for the secondary current in river bends. The oil slick is assumed to remain circular, with its radius calculated according to Fay's spreading laws (Fay 1969, 1971). The drift velocity of the slick center is determined by formulas derived by Tsahalis (1979a) from laboratory experiments. Fingas and Sydor (1980) developed a two-dimensional model for surface oil slicks in a short river reach. The current distribution was determined using the finite-difference scheme of Leendertse (1970). The entire oil slick volume is represented by a large number of individual parcels. The drift velocities of these parcels are determined by the wind factor approach. A random fluctuation component is included to represent horizontal diffusion. The area of each oil parcel is calculated by Fay's spreading laws for circular slicks.

Recently Shen and Yapa (1988) developed a computer model, ROSS, for surface slicks in rivers. The model considered the effect of ice covers. In this model the oil slick is considered to be composed of a large number of discrete parcels with equal volume. These parcels are tracked for their positions and subjected to an equal mass loss rate during the simulation. The two-dimensional velocity distribution of the river water is computed using a separate hydrodynamic model. The advection of each parcel in

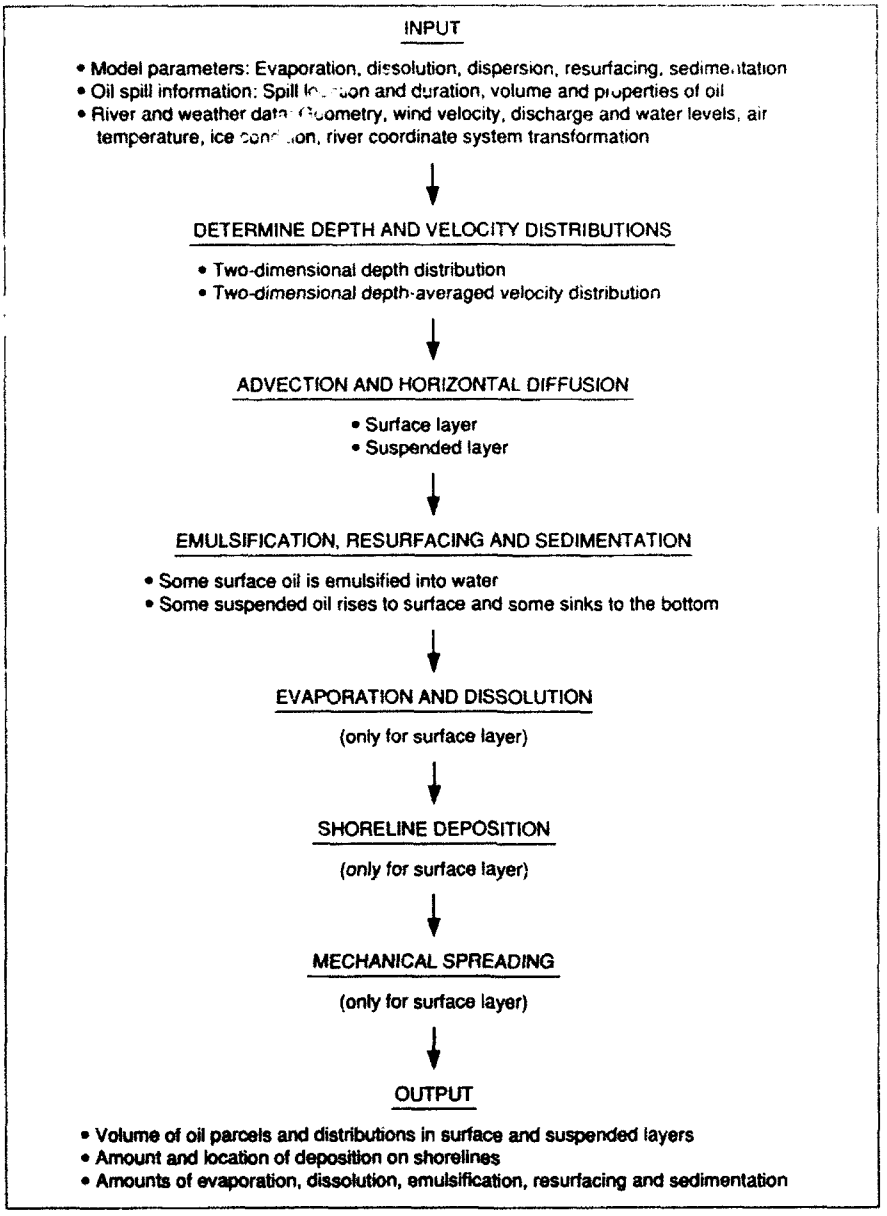

Figure 3. Structure of the simulation model

the slick is determined from the wind velocity and the computed current velocity, using the wind factor approach. The spreading of the slick is simulated by considering both mechanical spreading and horizontal turbulent diffusion. The model developed by Fay (1969, 1971) is used to simulate mechanical spreading, while a random-walk simulation is used to simulate spreading due to surface turbulence. The loss of oil due to the shoreline deposition is calculated according to the oil-retention capability of the shorelines. The losses of oil due to evaporation and dissolution are calculated based on empirical formulations that consider the effects of slick area, wind velocity, temperature and oil properties. None of the above models considered the motion of oil in suspension and the exchange between the surface oil and the suspended oil. Sedimentation of oil to the bottom was also not considered.

In the present study the model ROSS is generalized by considering the movement of oil both on and under the water surface. The present model, ROSS2, is primarily designed for the transport of oil spilled in rivers; however, it can also be used for spills of other hazardous materials. A brief outline of the structure of the model is presented in Figure 3.

In ROSS2 the spilled oil is divided into a surface layer and a suspended layer, with continuous exchanges of oil mass between the two layers. In the simulation, oil in both layers is discretized into a large number of parcels that are tracked for their positions and volumes at each time step during the simulation. Besides the two-dimensional velocity distribution, the distribution of flow depth is also determined for simulating transport in the suspended layer. Because of the exchange between the surface layer and the suspended layer, the number of oil parcels, as well as the volume of each parcel, will change from time to time. The advection of oil parcels in the suspended layer is determined by the depth-averaged current velocity, and those on the surface are determined by the wind factor approach. The model developed by Fay (1969, 1971) is used to simulate mechanical spreading, and a random-walk simulation is used to account for horizontal spreading due to turbulent diffusion. The loss of oil in the surface layer due to evaporation and dissolution is calculated based on analytical and empirical formulations, which consider the effects of slick area, wind velocity, temperature and oil properties. The loss of oil due to shoreline deposition is calculated according to the oil-retention capability of the shorelines. The amounts of vertical dispersion into the water column, resurfacing and deposition to the channel bottom are calculated based on the depth-averaged oil concentration in the suspended layer. Weathering processes that occur long after the onset of the spill are not well understood and less significant, so they are not considered in this model. This is also justified from the operational point of view, since the main objective of the model is for short-term tactical forecasts to assist in designing response measures in the event of a major spill.

The present simulation model has been applied to the upper St. Lawrence River and the Ohio–Monongahela–Allegheny river system. This report will use the Ohio–Monongahela–Allegheny river system as an example to illustrate the model implementation in detail. The Ohio–Monongahela–Allegheny river system is more complex and difficult to implement, so it serves as a better example.

MODEL FORMULATION

Governing equations

In the present model, oil in the river is considered to consist of a surface slick coating on the water surface and a mixed layer containing suspended oil droplets extending over the depth of the flow, with continuous exchange between the two layers. The thickness of the surface layer is assumed to be negligible in comparison to the suspended layer. The equation of motion for oil in the surface layer can be written as:

$$\frac{\partial C_s}{\partial t} + \frac{\partial}{\partial x}(u_s C_s) + \frac{\partial}{\partial y}(v_s C_s) = \frac{\partial}{\partial x}\left(D_x \frac{\partial C_s}{\partial x}\right) + \frac{\partial}{\partial y}\left(D_y \frac{\partial C_s}{\partial y}\right)$$

$$+ \alpha_1 V_b c_v|_{z=0} - \gamma C_s - C_a S_E + M_s(x, y) - D_s(x, y) \qquad (1)$$

where x, y, t = space and time variables

z = vertical coordinate measured downward from the water surface

C_s = local volumetric oil concentration in the surface layer per unit surface area

c_v = local volumetric concentration of oil in the suspended layer per unit volume of water

u_s, v_s = components of surface drift velocity in x and y directions, respectively

D_x, D_y = diffusion coefficients in the x and y directions, respectively

α_1 = coefficient representing the probability of deposition of an oil droplet reaching the water surface

V_b = buoyant velocity of suspended oil globules

γ = coefficient describing the rate at which the surface oil is dispersed into the water column

C_a = area concentration of oil in the surface layer

S_E = rate of evaporation and dissolution per unit area of the surface slick
M_s = effect on the distribution of surface oil by mechanical spreading
D_s = effect on the distribution of surface oil by shoreline deposition.

The concentration distribution in the suspended layer can be described by:

$$\frac{\partial (C_v h)}{\partial t} + \frac{\partial}{\partial x}(uC_v h) + \frac{\partial}{\partial y}(vC_v h)$$

$$= \frac{\partial}{\partial x}\left(hD_x \frac{\partial C_v}{\partial x}\right) + \frac{\partial}{\partial y}\left(hD_y \frac{\partial C_v}{\partial y}\right) - \alpha_1 V_b c_v|_{z=0} + \gamma C_s - \beta_1 c_v|_{z=-h} \quad (2)$$

where C_v = depth-averaged volumetric concentration of oil in the suspended layer
h = flow depth
u, v = components of depth-averaged river current in x and y directions, respectively
β_1 = coefficient defining the rate of net oil deposition on the riverbed per unit area.

Equation 2 can be simplified by introducing the mass conservation equation of water:

$$\frac{\partial h}{\partial t} + \frac{\partial}{\partial x}(uh) + \frac{\partial}{\partial y}(vh) = 0. \quad (3)$$

In Lagrangian form the simplified equation for the suspended layer becomes:

$$\frac{DC_v}{Dt} = \frac{1}{h}\left[\frac{\partial}{\partial x}\left(hD_x \frac{\partial C_v}{\partial x}\right) + \frac{\partial}{\partial y}\left(hD_y \frac{\partial C_v}{\partial y}\right)\right] - \frac{\alpha}{h} V_b C_v + \frac{\gamma}{h} C_s - \beta C_v \quad (4)$$

where $\frac{D}{Dt} = \frac{1}{\partial t} + u\frac{\partial}{\partial x} + v\frac{\partial}{\partial y}$;

$\alpha C_v = \alpha_1 c_v|_{z=0}$;

$\beta C_v = \left(\beta_1 c_v|_{z=-h}\right)/h$.

The movement of spilled oil in the river as described by eq 1 and 4 is mainly governed by advection and diffusion. These equations can be solved when the flow condition is known. Finite-difference and finite-element methods for solving advection–diffusion equations exist. These methods, however, often suffer from numerical diffusion problems and demand excessive computational time and memory when applied to long river reaches. In this study a modified Lagrangian discrete-parcel method is used. The method is a generalization of the method used in the ROSS model (Shen et al. 1990).

Lagrangian discrete-parcel algorithm

In the Lagrangian discrete-parcel algorithm, both the oil on the water surface and the oil in the suspension are represented as ensembles of a large number of small parcels. Each parcel has a set of time-dependent spatial coordinates and a mass associated with it. The movement of each parcel in the river is affected by the wind, the water current and the concentration of surrounding parcels. During each time step, all the oil parcels are first displaced according to the current velocity and a fluctuation component at their respective locations. The turbulent fluctuation component, which represents the effect of horizontal diffusion, is related to the diffusion coefficient based on the random-walk analogy. After all the oil parcels are displaced according to advection and diffusion, further modifications are introduced to account for all other transport and weathering processes. Due to these processes, especially the exchanges between the two layers, the mass of each oil parcel will be different and will change from

time to time. The number of parcels will also increase with time during the simulation. If a large number of parcels are released in the river, and their discrete paths and masses are followed and recorded as functions of time relative to a reference grid system in space, then the density distribution of the particles in the water body can be interpreted to give the concentration of the oil.

The approach requires an efficient bookkeeping procedure rather than the solution of a large matrix associated with a conventional Eulerian finite-difference or finite-element method. The algorithm is inherently stable with respect to time, although the time step should be compatible with the grid size and velocity for numerical accuracy. Since the movement of each parcel in the river depends on the distribution of the entire ensemble on the water surface and in the suspension, all parcels must be traced at each time level before proceeding to the next.

The detailed structure and implementation of the present numerical model will be discussed and presented later. In the following sections the analytical formulations used for each component of the model will be discussed.

Model formulation

Current velocity

Since the water current affects advection, spreading and the exchange of oil between the two layers, the distribution of the magnitude and direction of the current and the flow depth must be determined first. Numerous numerical methods exist in the literature for determining the two-dimensional flow distribution in shallow waters (Leendretse 1970, Hamilton et al. 1982). However, this type of method is time consuming and impractical for long rivers. A quasi-two-dimensional stream-tube method is used in the present study. In the present approach the time-dependent discharge distribution $Q(x,t)$ along the river is first obtained through the use of a one-dimensional hydraulic transient model, which was developed based on the St. Venant equations:

$$\frac{\partial Q}{\partial x} + \frac{\partial A}{\partial t} = 0 \tag{5}$$

$$\frac{\partial Q}{\partial t} - \left(\frac{Q}{A}\right)^2 \frac{\partial A}{\partial x} + \frac{2Q}{A}\frac{\partial Q}{\partial x} + gA\frac{\partial H}{\partial x} - gA\left(S_o - S_f\right) = 0 \tag{6}$$

where x = longitudinal distance along the river
A = flow cross-sectional area
H = water level
S_o = bed slope
S_f = friction slope.

The friction slope can be calculated by Manning's equation:

$$S_f = \frac{n_b^2 Q^2}{2.21\, A^2 R^{4/3}} \tag{7}$$

in which R is the hydraulic radius and n_b is the Manning's roughness coefficient of the bed. For an ice-covered reach, the composite Manning's coefficient, which accounts for the resistance of ice cover and the riverbed, should be used instead of n_b. The composite Manning's coefficient can be calculated by the Belokon–Sabaneev formula (Larsen 1969):

$$n = \left[\frac{n_i^{3/2} + n_b^{3/2}}{2}\right]^{2/3} \tag{8}$$

The hydraulic radius can be assumed to be half of the flow depth for an ice-covered reach in wide rivers.

Once the one-dimensional solution is obtained, the discharge Q can then be distributed across the width of the river using a stream-tube model (Shen and Ackermann 1980) to give the two-dimensional velocity distribution at selected cross sections.

For a channel cross section, as shown in Figure 4, the transverse distribution of the flow can be determined using the stream-tube method. The cross section is first discretized into trapezoidal elements. By applying Manning's equation, the ratio of discharges between the entire cross section and a partial cross section can be written as:

$$\frac{Q_P}{Q} = \frac{\sum_{p=1}^{P} A_p R_p^{2/3}}{\sum_{p=1}^{N} A_p R_p^{2/3}} \tag{9}$$

where P = number of trapezoids in the partial cross section
N = total number of trapezoids describing the entire cross section
Q_P = cumulative discharge up to and including the P^{th} trapezoid
Q = total discharge through the entire cross section
A_p, R_p = area and hydraulic radius of the p^{th} trapezoid, respectively.

The cumulative discharge Q_P can be computed by first rewriting eq 9 as:

$$Q_p = F_Q \sum_{p=1}^{P} A_p R_p^{2/3} \tag{10}$$

with

$$F_Q = \frac{Q}{\sum_{p=1}^{N} A_p R_p^{2/3}} \tag{11}$$

and

$$Q_P - Q_{P-1} = F_Q A_P R_P^{2/3} \tag{12}$$

Based on the computed distribution of Q_p, stream-tube boundaries within the cross section can be determined by simple interpolation. Once the stream-tube boundaries are located, the flow through each stream tube is then divided by the cross-sectional area of the stream tube to obtain the depth-averaged velocity, and the area of the stream tube is divided by its width to obtain the width-averaged depth. The velocity and depth are then assigned to the center of the stream tube. By applying this procedure to successive cross sections along the river, a two-dimensional depth-averaged velocity and

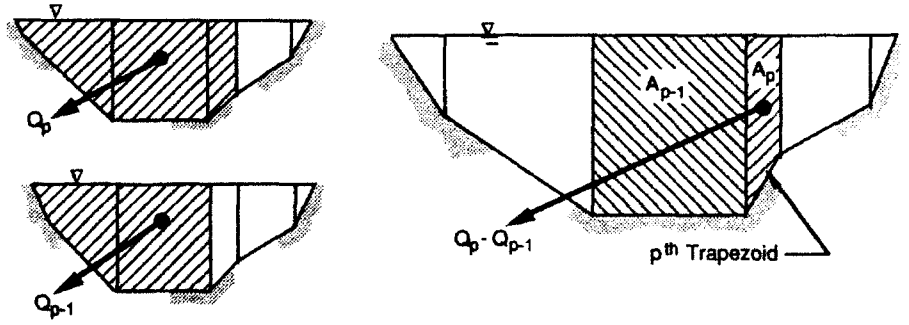

a. Cumulative discharges over a partial cross section.

b. Area and discharge for the Pth trapezoid.

Figure 4. Method for determining the transverse distribution of the flow in a cross section.

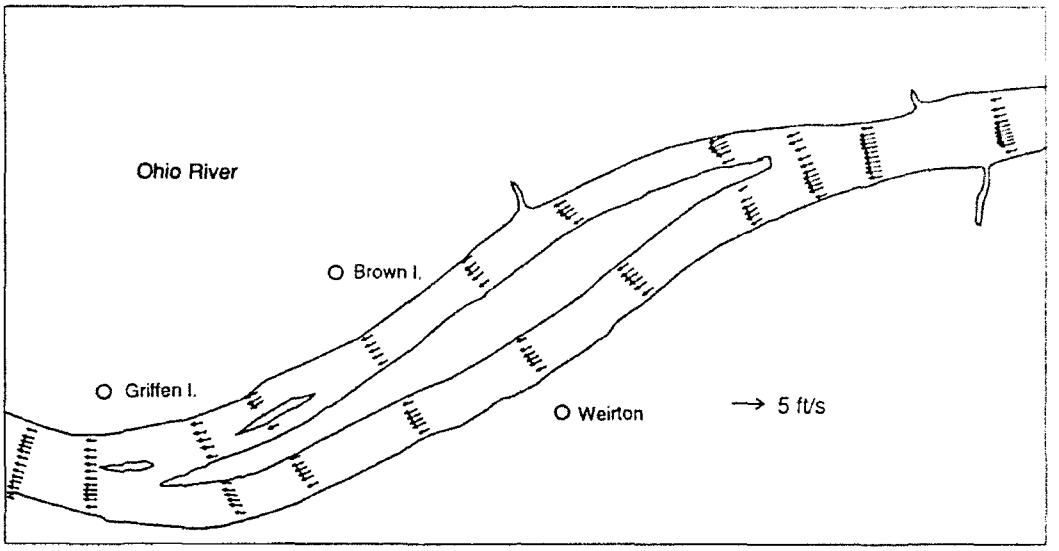

Figure 5. Stream-tube velocity distributions for a reach of the Ohio River.

width-averaged depth distributions can be obtained. The direction of a velocity vector is the same as the vector connecting center points of a stream tube at successive cross sections in a relatively straight reach, or perpendicular to the cross section in a river bend. As an example, the simulated depth-averaged velocity distribution for a reach of the Ohio River is shown in Figure 5.

Once the velocity and depth distributions along stream tubes are established, the distribution of velocity for all the points in a predefined grid system can be obtained through linear interpolations. Samples of calculated velocity and depth distributions are shown in Figures 6 and 7. The validity of the stream-tube method has been examined by Shen and Ackermann (1980).

Advection

During each time step Δt of the oil spill simulation, the displacement $\Delta\vec{S}$ of an oil parcel is calculated by numerically integrating the drift velocity V_t over the time period Δt. When the Δt value is large, subintervals δt_k are needed for numerical accuracy. In this case the displacement during the time interval Δt is

$$\Delta\vec{S} = \sum_{k=1}^{K} \vec{V}_k \, \delta t_k \tag{13}$$

where $\vec{V}_k$ = drift velocity of the oil parcel during the time interval δt_k

$\Delta\vec{S}$ = displacement during the time interval Δt

$\sum_{k=1}^{K} \delta t_k = \Delta t.$

The values of δt_k should satisfy the condition (Roache 1972, Cheng et al. 1984)

$$\delta t_k \leq \left[\frac{u_k}{\Delta x} + \frac{v_k}{\Delta y}\right]^{-1} \tag{14}$$

where u_k and v_k are the x and y components of the velocity.

Open water condition. In the present model the advective velocity of each oil parcel is computed as:

$$\vec{V}_t = \vec{V} + \vec{V}' \tag{15}$$

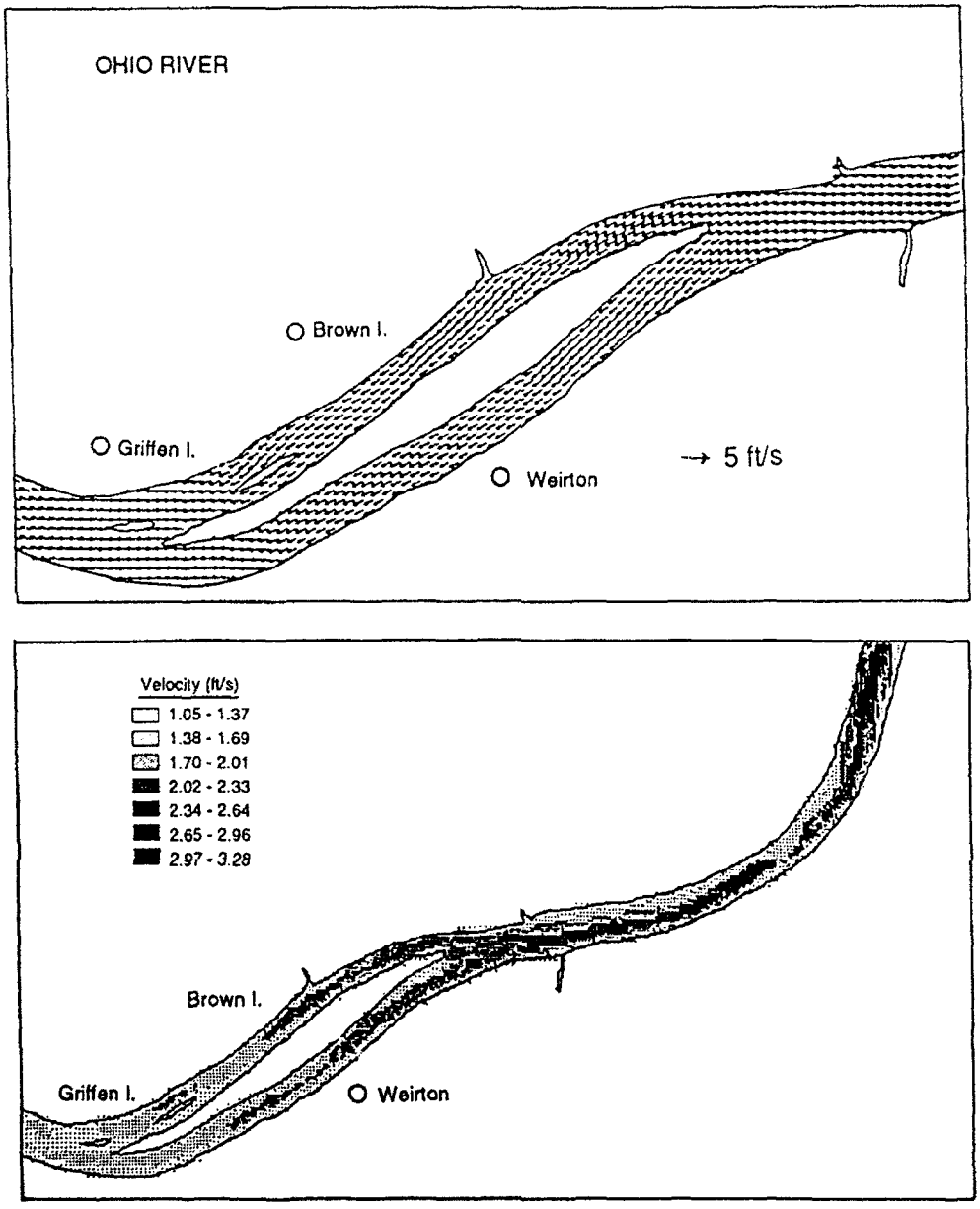

Figure 6. Velocity distribution in the grid system for a reach of the Ohio River.

where $\vec{V}_t$ is the drift velocity of an oil parcel and $\vec{V}$ and $\vec{V}'$ are the mean and turbulent fluctuation components of the drift velocity. The component $\vec{V}'$ is included to simulate the horizontal diffusion of the oil parcels. The formulation for $\vec{V}'$ will be discussed later. In the suspended layer the mean drift velocity is equal to the depth-averaged current velocity $\vec{V}_c$, determined from the stream-tube simulation. On the surface layer the mean drift velocity is considered to be a vector sum of a wind-induced and water-current-induced drift (Stolzenbach et al. 1977). The mean drift velocity $\vec{V}_s$ on the surface can be calculated by the formula:

$$\vec{V}_s = \alpha_w \vec{V}_w + \alpha_c \vec{V}_c \tag{16}$$

where $\vec{V}_w$ = wind velocity at 10 m above the water surface

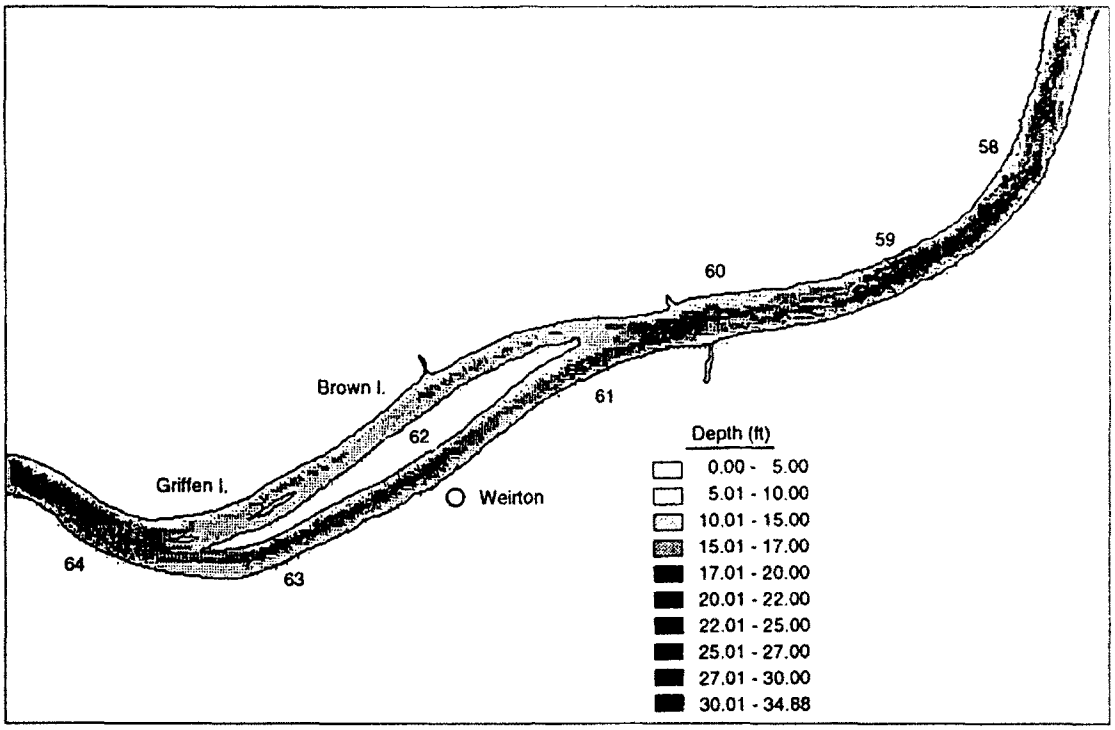

Figure 7. Depth distribution of the channel for a reach of the Ohio River.

$\vec{V}_c$ = depth-averaged current velocity
α_w = wind drift factor to account for the drift of the surface slick due to wind
α_c = correction factor for the current on the surface.

A value of 0.03 has been commonly used for α_u (Huang and Monastero 1982). The wind speed on the river is usually different from that at a nearby meteorological station (Weeks and Dingman 1972). A correction factor should be used when the meteorological station is situated away from the river.

Assuming a logarithmic velocity profile, the surface velocity of the water current can be related to the depth-averaged current velocity by the relationship:

$$\alpha_c = \frac{\vec{V}_o}{\vec{V}_c} = 1 + \frac{\vec{u}_*}{\kappa \vec{V}_c} \tag{17}$$

where $\vec{V}_o$ = surface velocity
u_* = shear velocity
κ = Karman constant (0.4).

The ratio α_c usually varies between 1.1 and 1.2.

Ice-covered condition. Oil spill movement under ice is a topic that has received little theoretical or laboratory treatment. For the suspended layer the transport of oil droplets can be treated by the advective diffusion formulation, as described in eq 4. The advection velocity is equal to the depth-averaged current velocity. The advection of surface oil on the underside of the ice cover is, however, more complicated. As suggested by the experimental study of Cox and Schultz (1981), an ice cover may be classified into three categories for slick advection. The ice cover may be smooth, contain small roughness elements, or contain large roughness elements. The following discussion summarizes the results of their limited experimental studies and serves as the basis of the present simulation.

Under smooth ice covers with no current, the oil will rest at an equilibrium thickness that is described by the empirical equation

$$\delta_{eq} = 1.67 - 8.5(\Delta\rho_w) \tag{18}$$

where δ_{eq} = static equilibrium slick thickness (cm)
$\Delta = (\rho_w - \rho_o)/\rho_w$, the relative density difference between oil and water
ρ_w and ρ_o = water and oil densities, respectively (g/cm^3).

An ice cover is considered to be smooth when the height of the ice roughness is smaller than the equilibrium thickness of the oil, δ_{eq}.

The current velocity at which the oil begins to move along an ice cover is called threshold velocity, U_{th}. For a smooth cover the value of U_{th} was empirically determined to be a function of the oil viscosity μ_o and is given as

$$U_{th} = 305.79/(88.68 - \mu_o) \tag{19}$$

where U_{th} has the units of cm/s and μ_o has units of g/cm-s. Viscosities for crude and fuel oils fall in the range of 5–50 centipoises (1 cp = 1.0×10^{-2} g/cm-s = 2.4 lb/ft-hr).

A rough ice cover has the ability to retain the oil between the roughness elements. As the current velocity is increased, the oil will creep along the upstream face of the roughness element until it spills over the element and moves downstream. The threshold current velocity at which the oil will move downstream under a rough ice cover is called the failure velocity, U_{fl}:

$$U_{fl} = 1.5\left\{2\left(\frac{\rho_o + \rho_w}{\rho_o \rho_w}\right)[\sigma_{o/w} g\ (\rho_w + \rho_o)]^{1/2}\right\}^{1/2} \tag{20}$$

where $\sigma_{o/w}$ is the oil–water interfacial tension. The failure velocity U_{fl} is the velocity above which no oil can be contained upstream of a large roughness element.

If the depth-averaged current velocity is larger than the threshold velocity, U_{th} or U_{fl}, the relationship between the current velocity and the slick velocity is given as:

$$\left(1 - \frac{V}{V_c}\right)^2 = \frac{K}{0.115\ F_\delta^2 + 1.105} \tag{21}$$

with

$$F_\delta = \frac{V_c}{(\Delta g \delta_{eq})^{1/2}} \tag{22}$$

where V = mean oil drift velocity
V_c = current speed
K = friction amplification factor
F_δ = slick densimetric Froude number
g = gravitational acceleration.

The value of K is a function of the roughness height of the cover. With the limited data available, K is assumed to vary linearly between 1.0 for a smooth cover and 2.6 for an ice cover with Manning's roughness coefficient $n_i = 0.055$.

Horizontal diffusion

The term V' in eq 15 accounts for the horizontal turbulent diffusion due to the turbulent fluctuation of the drift velocity. Based on the random-walk analysis (Fischer et al. 1979):

$$V' = \left(4D_T/\delta t\right)^{1/2} \tag{23}$$

and

$$\vec{V}' = V' R_n e^{i\theta'} \tag{24}$$

where δt = time step

D_T = diffusion coefficient

R_n = normally distributed random number with a mean value of 0 and a standard deviation of 1.

The directional angle θ' is assumed to be a uniformly distributed random angle ranging between 0 and π.

In rivers the diffusion coefficient is affected by the shear velocity u_* and the depth of flow h (Fischer et al. 1979):

$$D_T = 0.6h\,U_*. \tag{25}$$

Flume experiments by Sayre and Chang (1969) indicated that D_T for surface dispersants can also be calculated by eq 25. Using Manning's equation, we can rewrite eq 25 as:

$$D_T = 0.40 n_b V g^{1/2} h^{5/6} \tag{26}$$

for free surface flow (ft^2/s) and

$$D_T = 0.64\,\bar{n}\,V g^{1/2}\,h^{5/6} \tag{27}$$

for ice-covered flows (ft^2/s).

Mechanical spreading

The mechanical spreading process only affects the spreading of surface slicks. Formulations used in the model will be discussed in this section.

Spreading in open water. A number of theories have been proposed for the process of mechanical spreading in open waters (Blokker 1964, Fay 1969, 1971, Hoult and Suchon 1970, Mackay et al. 1980b). In this study Fay's spreading theory (1971) is used because this theory is based on a rather comprehensive description of the spreading mechanism and has been verified by laboratory experiments (Fay 1971, Hoult and Suchon 1970) and other analytical solutions (Fannelop and Waldman 1972).

Fay's spreading theory is derived for single-component, constant-volume slicks with idealized configurations in quiescent water. This theory considers the spreading of oil as a result of two driving forces—gravity and surface tension—counterbalanced by inertia and viscous forces. The spreading of an oil slick is considered to pass through three phases. In the beginning phase, only gravity and inertia forces are important. In the intermediate phase, gravity and viscous forces dominate. The final phase is governed by the balance between surface tension and viscous forces.

Formulas for both one-dimensional spreading and radial spreading at different stages are summarized in Table 1. The spreading rate during each phase can be obtained by taking time derivatives of the formulas given in Table 1. The equations for spreading rates are summarized in Table 2. The time rate of change of the oil volume in these equations represents the change due to weathering, including

Table 1. Spreading law for oil slicks. (After Fay 1971, Hoult 1979, Waldman et al. 1973.)

Spreading phase	*Width* L_e	*Radius* R_e
Gravity–inertia	$1.39\ (\Delta g A t^2)^{1/3}$	$1.14\ (\Delta g \forall t^2)^{1/4}$
Gravity–viscous	$1.39\ (\Delta g A^2 t^{3/2} \nu^{-1/2})^{1/4}$	$0.98\ (\Delta g \forall^2 t^{3/2} \nu^{-1/2})^{1/6}$
Surface tension–viscous	$1.43\ (\sigma^2 t^3 \rho_w^{-2} \nu^{-1})^{1/4}$	$1.60\ (\sigma^2 t^3 \rho_w^{-2} \nu^{-1})^{1/4}$

A = 0.5 volume of the oil per unit length of oil slick.

$\Delta = 1 - \frac{\rho_o}{\rho_w}$.

ν = kinematic viscosity of water.

evaporation and vertical mixing, and the changes in oil volume distribution in various parts of the slick. In addition to the rates of spreading at different phases, the times at which phase transitions occur also need to be determined. These transition times can be obtained by letting equations in the appropriate phases equal each other and solving for the time. Equations for the transition times are summarized in Table 2.

Fay (1969, 1971) observed that the changes in slick properties caused by weathering may result in the eventual cessation of mechanical spreading. Based on a number of fields observations, Fay suggested that

$$A_f = 10^5 \forall^{3/4} \tag{28}$$

where A_f is the final slick area in m^2 and $\forall$ is the total volume of the slick in m^3. In this study the cessation of mechanical spreading is considered to occur when the slick thickness reduces to $10^{-5} \forall^{1/4}$ m.

The formulas presented in Tables 1 and 2 were derived for simple slick geometries that exist under idealized conditions. In the simulation model the radial spreading formulas are used when the slick is nearly circular, and the one-dimensional formulas are used when the slick area is elongated. A slick is considered to be elongated when the aspect ratio of the slick area is greater than 3. The aspect ratio refers to the length-to-width ratio of the slick and the orientation refers to the angle θ between the major axis of the slick and the x axis, as shown in Figure 8.

The orientation of the slick is computed using the moments of inertia and the product of inertia of the slick. The angle θ can be calculated using:

$$\tan(2\theta) = \frac{-2P_{xy}}{I_x - I_y} \tag{29}$$

where

$$I_x = \Sigma y^2,\ I_y = \Sigma x^2,\ P_{xy} = \Sigma_{xy} \tag{30}$$

where I_x and I_y are the moments of inertia of the oil slick with respect to the x and y axes, respectively, and P_{xy} is the product of inertia. Once the orientation is known, the x and y coordinates of all the particles in the slick are transformed into coordinates in an x' and y' coordinate system in which the x' axis is the major axis of the slick. The aspect ratio is computed by the following equation, with x' and y' coordinates of all oil particles:

$$\text{Aspect ratio} = \frac{\Sigma x'}{\Sigma y'}. \tag{31}$$

Table 2. Spread rates of oil slicks and phase transition times. (After Shen et al. 1990.)

One-dimensional slicks, dL_e/dt

Spreading phase	*Spreading rate*
Gravity–inertia	$\frac{2}{3} k_{10} (\Delta g)^{1/3} \left(L^{-1/3} \frac{dL}{dt} t^{2/3} + L^{2/3} t^{-1/3} \right)$
Gravity–viscous	$k_{20} \left(\Delta g \nu^{-1/2} \right)^{1/4} \left(\frac{3}{8} L t^{-5/8} + \frac{dL}{dt} t^{3/8} \right)$
Surface tension–viscous	$\frac{3}{4} k_{30} \left(\sigma \rho_w^{-1} \right)^{1/2} (t\nu)^{-1/4}$

Circular slicks, dR_e/dt

Spreading phase	*Spreading rate*
Gravity–inertia	$\frac{k_{2i}}{4} (\Delta g)^{1/4} \left(t^{1/2} \forall^{-3/4} \right) \left(\frac{d\forall}{dt} + \frac{2\forall}{t} \right)$
Gravity–viscous	$k_{2v} \left(\Delta g \nu^{-1/2} \right)^{1/6} \left(\frac{1}{3} \frac{d\forall}{dt} + \frac{\forall}{4t} \right) \frac{t^{1/4}}{\forall^{2/3}}$
Surface tension–viscous	$\frac{3}{4} k_{2t} \left(\sigma \rho_w^{-1} \right)^{-1/2} (t\nu)^{-1/4}$

Times of phase transition

Transition	*One-dimensional spreading*	*Radial spreading*
Gravity–inertia to gravity–viscous	$\left(L^8 \nu^{-3} [\Delta g]^{-2} \right)^{1/7}$	$\frac{(k_{2v})^4}{(k_{2i})} \left(\frac{\forall}{\nu \Delta g} \right)^{1/3}$
Gravity–viscous to Surface tension–viscous	$\left(\frac{k_{20}}{k_{30}} \right)^{8/3} \left(\Delta g L^4 \sigma^{-2} \rho_w^2 \nu^{1/2} \right)^{2/3}$	$\frac{(k_{2v})^2}{(k_{2t})} \left(\frac{\rho_w}{\sigma} \right) \left(\forall^2 \nu \Delta g \right)^{1/3}$

Note:

L^2 = 0.5 volume of oil per unit length along the major axis of the slick (L is a characteristic length); $k_{10} = 1.39$, $k_{20} = 1.39$, $k_{30} = 1.43$.

$\forall$ = Total volume of oil slick; $k_{2i} = 1.14$, $k_{2v} = 0.98$, $k_{2t} = 1.60$.

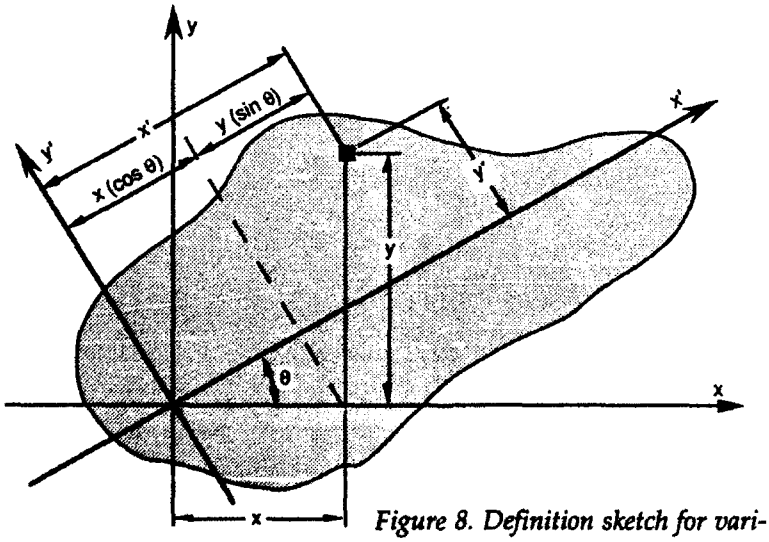

Figure 8. Definition sketch for variables used to compute the slick's aspect ratio and orientation.

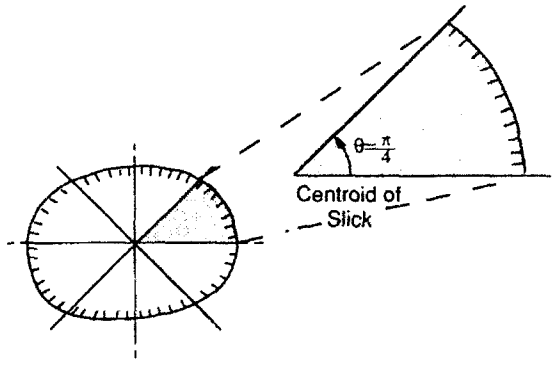

Figure 9. Division of a nearly circular slick into pie-shaped segments.

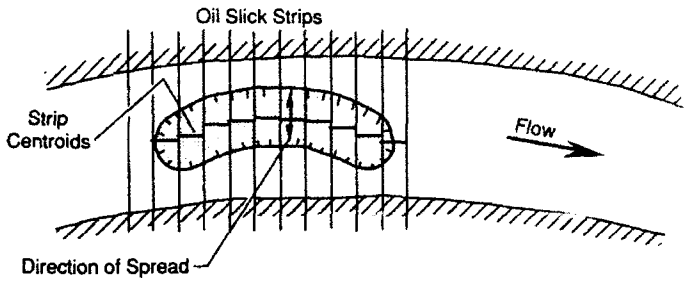

Figure 10. Division of an elongated slick into strips.

This aspect ratio is used to determine whether the spreading of the oil slick is radial or one-dimensional. The use of 3 as the aspect ratio for transition from radial spreading to one-dimensional spreading is subjective but gives reasonable results. For a nearly circular slick the slick area is divided into eight pie-shaped sectors, as shown in Figure 9. For an elongated slick the entire slick is segmentized into a series of strips, as shown in Figure 10. For both cases the spreading rate of each segment is calculated using Fay's formula shown in Table 2, independent of other segments in the slick. This simplification assumes that concentration gradients at the boundaries between neighboring segments are negligible for mechanical spreading (Shen and Yapa 1988). The segmentization also allows for different spreading rates in different regions of the slick, thus providing a more realistic description of the field situation. For a nearly circular slick the rate of outward movement of an oil parcel along the radial direction in a particular pie-shaped sector located at a distance r from the centroid of the slick can be calculated from the spreading rate of the mean radius $\bar{r}$ of the sector:

$$\frac{dr}{dt} = \frac{r}{\bar{r}} \frac{d\bar{r}}{dt}. \tag{32}$$

Parcels scattered at distances far away from the main slick will be excluded from this process since small isolated patches of oil will not be subjected to mechanical spreading. In this study, parcels that account for the outer 5% of the total slick volume are excluded. This is equivalent to excluding the parcels located at a radial distance greater than 2.2 $\bar{r}$ from the centroid of the slick, as determined from numerical experiments for the spreading of circular slicks.

For an elongated slick the rate of outward movement in the width direction of an oil parcel in a segment with mean length $\bar{l}$, located at distance l from the centroid of the segment, can be calculated from the rate of spreading of the mean length of the segment as:

$$\frac{dl}{dt} = \frac{l}{\bar{l}} \frac{d\bar{l}}{dt} \tag{33}$$

Parcels for the outer 5% of the slick volume are not subjected to mechanical spreading.

Spreading under an ice cover. Hoult et al. (1975) suggested that appreciable mechanical spreading will only occur during a continuous spill, because the oil thickness is stabilized when the equilibrium thick-

ness for the flow condition is reached. There is no pressure gradient or surface tension force to cause further spreading of the oil. The oil reaches an equilibrium state when cavities formed by the ice roughness contain a volume of oil that can decrease only with a significant increase in the current speed. Since a continuous spill will repeatedly add oil to fill the cavities, the excess oil will effectively spread to the empty neighboring cavities and establish an equilibrium state there.

The formula used to model mechanical spreading for a continuous spill under ice is:

$$r = 0.25\left(\frac{\Delta g Q_o^2}{h'}\right)^{1/6} t^{2/3} \tag{34}$$

where r = slick radius
$\Delta = (\rho_w - \rho_o)/\rho_w$, the relative density difference
g = gravitational acceleration
Q_o = average volume flow rate from the beginning of the spill
h' = half of the root-mean-square roughness height of the ice cover.

This equation is a result of balancing the frictional drag from the ice cover with the pressure drop that occurs as the oil flows into open cavities. In the simulation models it is assumed that no mechanical spreading will occur for an instantaneous spill or after the continuous oil discharge stops. If the oil discharge is in progress and the slick is nearly circular, the mechanical spreading will be calculated by eq 34.

Shoreline boundary conditions

When oil reaches a shoreline, it will deposit along it. The deposited oil may be re-entrained into the river by the current. The rate of re-entrainment can be formulated according to the "vulnerability" index of the shoreline (Gundlach and Hayes 1978). This index is designed to reflect the environmental sensitivity of the shoreline to oil pollution. For beaches of different vulnerability indices, Torgrimson (1984) suggested "half-life" values to describe the ability of the shore to retain the oil. Half-life is a parameter that describes the "absorbency" of the shoreline by describing the rate of re-entrainment of oil after it has landed at a shoreline location. Table 3 presents half-lives for different types of shorelines along with their vulnerability indices. According to the half-life formulation, the fraction of the beached oil re-entrained into the water body during each time step $d\forall_b$ is calculated from:

$$\frac{d\forall_b}{\forall_b} = 1 - e^{-k\Delta t} = 1 - 0.5^{\Delta t/\lambda} \tag{35}$$

where $\forall_b$ is the volume of oil on the beach. The decay constant k can be expressed in terms of the half-life λ as:

$$k = [-\ln(1/2)]/\lambda . \tag{36}$$

For the purpose of calculating evaporation rate, the beached oil is assumed to occupy a predefined width of each computational grid along the shoreline. This width is determined by the user according to the field conditions.

Evaporation and dissolution

Evaporation. Evaporation is the main process that causes the loss in oil volume during weathering. Mackay et al. (1980a) developed a formula for calculating the rate

Table 3. Shoreline descriptor and default parameters.

Shoreline descriptor	*Half-life (hr)*	*Vulnerability index*
Instantaneous rejection*	0	0
Exposed headland	1	1
Wave-cut platform	1	2
Pocket beach	24	3
Sand beach	24	4
Sand and gravel beach	24	5
Sand and cobble beach	8760	6
Exposed tide flats	1	7
Sheltered rock shore	8760	8
Sheltered tide flats	8760	9
Sheltered marsh	8760	10
Land	8760	11

* This option is added in the present computer model.

of evaporation. The volume fraction of oil evaporated is determined as

$$F = \alpha_E (1/C)[\ln P_o + \ln(CK_E t + 1/P_o)] \tag{37}$$

where α_E = modification coefficient introduced in the present study to account for the effect of the change in oil properties on the evaporation rate due to emulsification and other weathering processes

$E = K_E t$ = evaporative exposure term, which varies with time and environmental conditions

$K_E = K_M A v/(RT\forall'_o)$

K_M = mass transfer coefficient (m/s) $(0.0025\, U_{wind}^{0.78})$

A = spill area (m^2)

v = molar volume (m^3/mole)

R = gas constant [82×10^{-6} atm m^3/(mole-K)]

T = surface temperature of the oil (K), which is generally close to the ambient air temperature T_E

$\forall'_o$ = volume (m^3).

The initial vapor pressure P_0 in atm at the temperature T_E is determined from

$$\ln P_0 = 10.6[1 - T_0/T_E] \tag{38}$$

where T_0 is the initial boiling point (K). The constant C can be determined by the relationship $T_E C$ = constant. Values of C for $T_E = 283$ K are given in Table 4. For crude oils of different API index values, C at $T_E = 283$ K are given in Table 5 along with T_0. This table can be replaced by the following functional relationships obtained through curve fitting (Shen et al. 1990):

$$C = 1158.9\, API^{-1.1435} \tag{39}$$

and

$$T_0 = 542.6 - 30.275 API + 1.565 API^2 + 34.39 API^3 + 0.0002604 API^4 \tag{40}$$

The API index and the specific gravity of the oil are related by

$$\text{Specific gravity} = 141.5/(API + 131.5)\,. \tag{41}$$

Table 4. Suggested evaporation parameters for various petroleum fractions (T_E = 283 K). (After Mackay et al. 1980b.)

Oil type	T_o *(K)*	C	P_o *(atm)*
Motor gasoline			
Summer	314	5.99	0.313
Winter	308	6.23	0.39
Aviation gasoline	341	2.81	0.12
Diesel fuel	496	5.57	3.4×10^{-4}
Jet fuel	418	5.06	6.0×10^{-3}
No. 2 furnace oil	465	7.88	1.1×10^{-3}
Lube (heavy and light)	583	8.61	1.32×10^{-3}
Heavy gas oil	633	8.99	2.0×10^{-6}
Residuals	783	3.37	7.35×10^{-9}
Light gas oil	473	6.37	8.1×10^{-4}

Table 5. Suggested evaporation parameters for various crude oils (T_E = 283 K). (After Mackay et al. 1980.)

API	*Specific gravity* ($g\ cm^{-3}$)	C	T_o	P_o
10	1.0	89.2	366	0.044
12	0.986	69.4	348	0.088
15	0.966	52.1	339	0.13
20	0.934	34.7	329	0.18
25	0.904	27.2	330	0.17
30	0.876	22.33	325	0.21
35	0.850	19.5	314	0.31
40	0.825	17.9	304	0.45
45	0.802	16.4	283	1.004

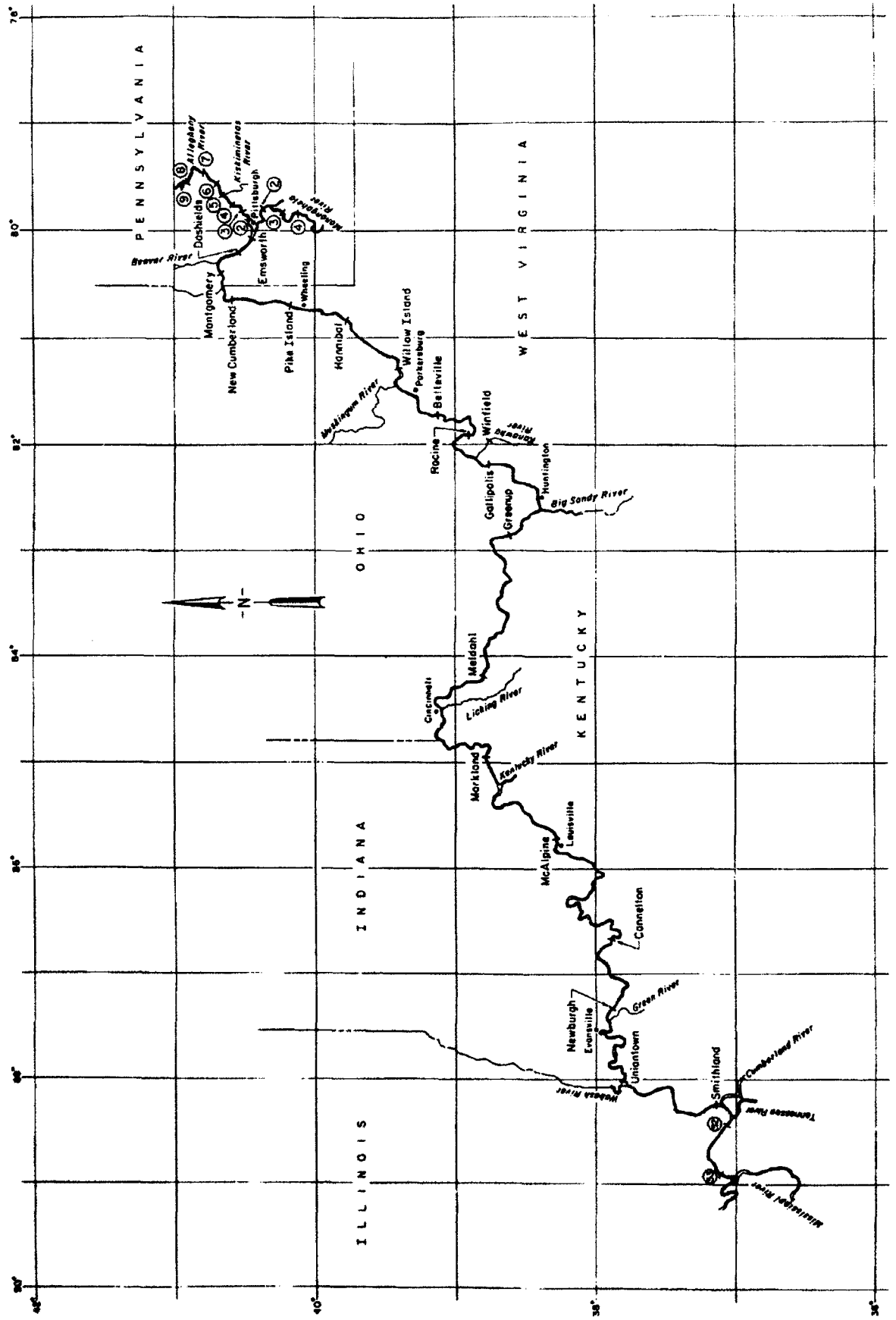

Figure 11. Ohio–Monongahela–Allegheny river system.

The molar volume of oil is required in eq 37. The value of the molar volume can vary between 150×10^{-6} and 600×10^{-6} m^3/mole. Typical values of molecular weight of various oil components are given by Moore et al. (1973). The compositions of several different oils are given along with the concentration and molecular weight M_i of each component. Based on these the molecular volume can be computed (Shen et al. 1990). The volume $\forall_0'$ for each time step is determined by

$$\forall_0' = \forall_0 + \Delta\forall_m \tag{42}$$

where $\forall_0'$ = effective initial volume of surface oil
$\forall_0$ = initial volume of oil spilled on the water surface
$\Delta\forall_m$ = volume increase in the surface layer due to the exchange between the two layers.

Dissolution. Cohen et al. (1980) developed a method to calculate the total dissolution rate N:

$$N = KA_sS \tag{43}$$

where N = total dissolution rate of the slick (g/hr)
K = dissolution mass transfer coefficient, assumed to be 0.01 m/hr
A_s = slick area (m^2)
S = oil solubility in water.

Huang and Monastero (1982) suggested that for a typical oil the solubility can be calculated by

$$S = S_0e^{-0.1t} \tag{44}$$

where S_o is the solubility for fresh oil and t is time in hours. Huang and Monastero suggested a typical value of 30 g/m^3 for S_o. In the present study the formula of Lu and Polak (1973) is used, which provides more information on solubility. In this method the rate of dissolution is calculated as

$$r_d = cde^{-0.1t} \tag{45}$$

where r_d is the rate of dissolution (mg/m^2-day). For three oil samples tested the coefficient c and d are given in Table 6.

Table 6. Dissolution coefficients at 25°C. (After Lu and Polak 1973.)

Oil type	API	c *(mg/m²)*	d *(1/day)*	$KS_o = cd$ *(1/g² hr)*
No. 2 fuel oil	35.5	1043	0.423	0.0184
Crude oil	38.6	8915	2.380	0.884
Bunker C oil	14.8	459	0.503	0.0104

Mixing, emulsification and sedimentation

Terms representing mass exchanges in the surface and the suspended layers in eq 1 and 4 are calculated at the end of each time step. The volume of oil mixing into the suspended layer per time step in a grid is calculated as $\gamma C_s\Delta x\Delta y\Delta t$. Similarly the volume of suspended oil resurfaced is calculated as $\sigma C_v V_b\Delta x\Delta y\Delta t$. The volume of oil settled to the channel bed is calculated as $\beta C_v h\Delta x\Delta y\Delta t$.

COMPUTER MODEL AND CASE STUDY

Based on the analytical formulation presented in the previous chapter, we developed a computer model for the Ohio–Monongahela–Allegheny River (OMA) system (Fig. 11). This chapter describes the

model along with a case study. It should be noted that the following discussions deal with many programming details. For a user to apply the model to the OMA system, a menu-driven model (Yapa et al. 1990a) provides a simple means for spill simulations.

Model implementation

The grid system

In the computer simulation a two-dimensional reference grid is used to discretize the river. This reference grid is required to identify the locations and velocities of oil parcels. The grid boxes in this model are squares of equal size. The location of each grid box is identified by its x and y indices.

The reference grid described is adequate for rivers with only one orientation, e.g. from east to west, or with only small variations in their orientation. Unfortunately the OMA river system has a complicated configuration with changing orientations. Seven sets of local coordinates are introduced, as shown in Figure 12, for different regions in the system to accommodate the changing orientations. During the simulation, transformation between a local coordinate system and the global system is required. The local x-axis is set to be in the main flow direction toward upstream. Relationships between the global and local coordinate systems are given in Table 7.

Table 7. Relationships between local and global coordinate systems.

Region no.	*Origins of local coordinates* (x_0, y_0)	*Rotating angle degrees*	*River*
1	0.0, 0.0	0.0	Ohio
2	348200.0, 138800.0	-90.0	Ohio
3	379400.0, -42200.0	-90.0	Ohio
4	392000.0, -84800.0	-180.0	Monongahela
5	315800.0, -104600.0	-180.0	Monongahela
6	383200.0, -36800.0	360.0	Allegheny
7	592000.0, -768000.0	90.0	Allegheny

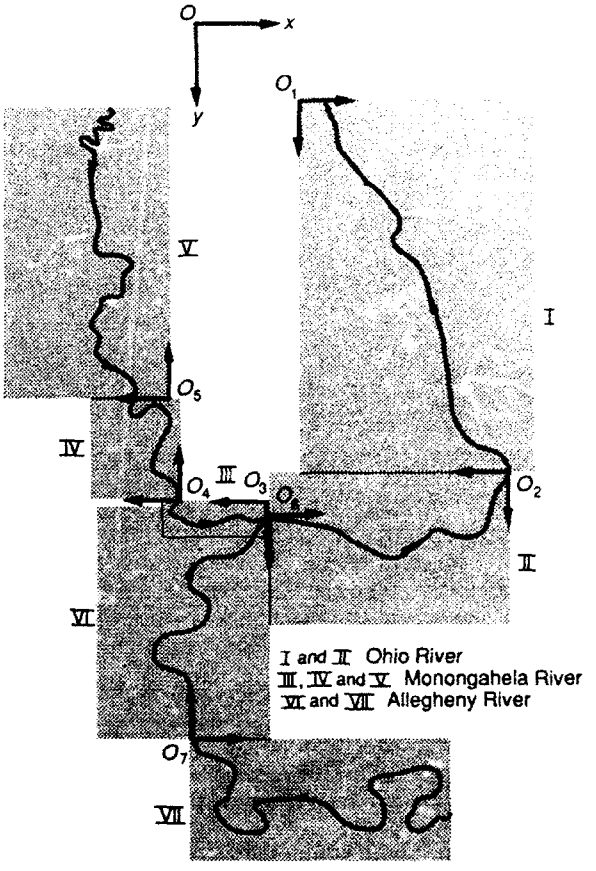

Figure 12. Local and global coordinate systems.

Besides the fixed-grid systems a temporary moving grid system traveling with the slick is used in the model to save memory space. This moving grid system will just be long enough to cover the length of the oil slick and the travel distance in one time step of the Bow computation. In a long simulation the slick may become too long to be covered by the moving grid because of bank deposition and rejection. For this case there are two options, one of which is to make the length of the moving grid long enough to cover the longest slick during the spill or the total length of the river. However, this option is limited by the memory space of microcomputers. Hence, the second option is used. In this option the model selects a reasonable length of moving grid, both for computer memory and for the length of the oil slick, for example, 30 miles long. The moving grid will follow the slick's leading edge and cover a 30-mile-long segment of the river upstream from the leading edge. The oil outside the moving grid, if it exists, will generally be insignificant.

A series of successive river bends can cause difficulty in defining the river boundary. In Figure 13 there are four continuous river bends. There are more than three sets of boundary points that intersect with a local j grid line. In this model all land boundary points, except for the two extreme end points,

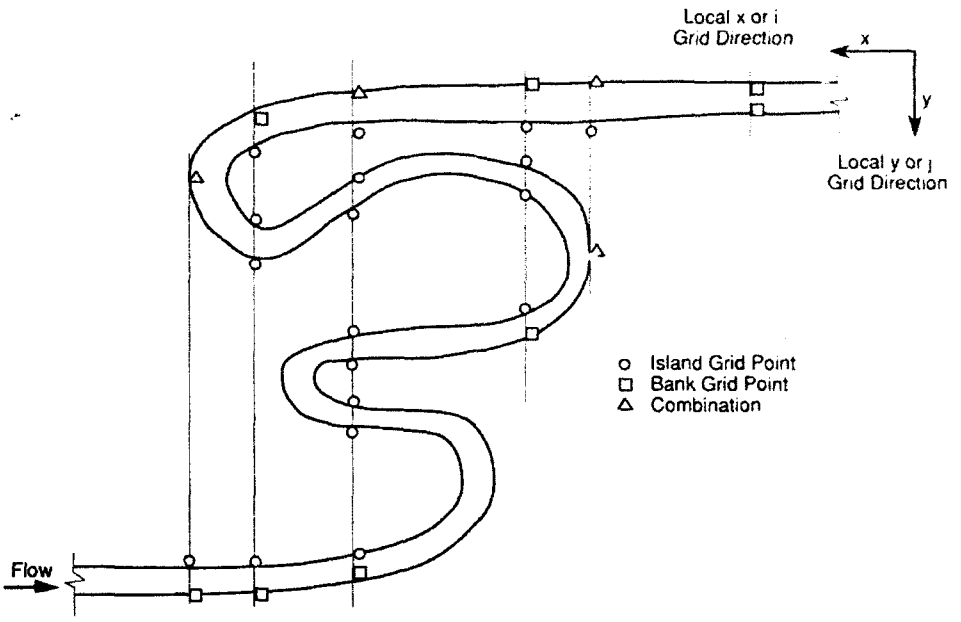

Figure 13. Method for determining the land grid along a series of river bends.

are treated as island boundary points. The boundary grids along a series of bends can be divided into three types, as shown in Figure 13. They are island grids, bank grids and their combinations.

Release of oil

The oil released into the river is represented by a user-specified number of particles. Each particle can be considered as a parcel of oil. The user can select a particle number up to 1000 for each layer at the beginning of the simulation. During the simulation the number may increase to 3000 or even more than 5000 due to the exchanges between the surface and the suspended layers. For simulation accuracy, approximately 500 particles in each layer is suggested to be used at the beginning of the simulation. However, in an emergency situation the user may reduce the particle number to 50 or less to reduce the computing time. The volume of oil released into each layer is determined by the user's input. Parcels in the same layer have the same volume at the beginning. The total number of parcels in each layer is the same at the beginning, so that the oil is released at a constant rate in each layer. For example, consider a spill of 10,000 gallons, with 7000 gallons in the surface layer and 3000 gallons in the suspended layer. If the user chooses 1000 parcels in each layer, then each surface oil parcel will contain 7 gallons, and a suspended one will contain 3 gallons at the beginning.

An oil spill will be treated either as an instantaneous spill or a continuous spill. When the spill duration is zero, the spill will be treated as instantaneous. Otherwise, it will be treated as a continuous spill.

Velocity and depth distributions

Analysis of the transport of oil spill parcels in a river requires well-defined water velocity and depth distributions. To calculate these distributions, various information is needed, including the total discharge, river stage, cross-section geometry, shoreline characteristics, ice condition and wind condition. The velocity and depth distributions in the river are calculated in two stages. First, a one-dimensional unsteady flow model is used to generate discharge and river stages at specified cross sections referred to as nodes. For the OMA model the Flowsed model is used for this purpose (Johnson 1982). The oil spill model uses this information to compute two-dimensional velocity and depth distributions.

In the oil spill model, branches are used to describe the channel configuration. The beginning and end of these branches are generally selected to coincide with nodes of the one-dimensional unsteady flow model. In cases where it is necessary to have more branches in the oil spill model than in the

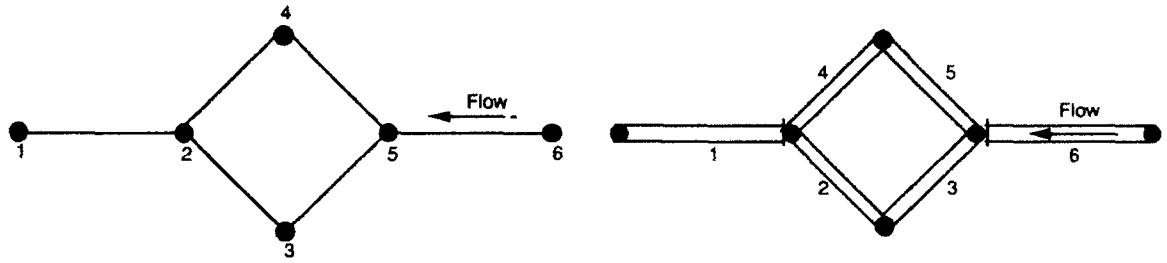

a. Nodes. *b. Branches.*

Figure 14. Schematization of a river reach with an island.

unsteady flow model, water levels at intermediate points are obtained through interpolation. When an island is encountered, there will be branches on each side of the island (Fig. 14). Each of these branches includes a portion of the stream tubes. The information available is the magnitude and direction, i.e. the x and y components, of velocities at stream-tube centers at all cross sections.

The assignment of velocity and depth through the entire river requires the establishment of a grid system, as shown in Figure 15. Velocities and depths obtained from the stream-tube analysis are interpolated to all grid boxes. River boundaries for this grid system are defined by boundary grid boxes. For each grid along the x-direction, two corresponding y-grid boxes are used to define the location of the riverbanks. In places where there are islands, more y-grid boxes are used to define the upper and lower boundaries of islands. The model can handle any number of islands in the river. However, if more islands are intersected by a vertical line along which the x coordinate is constant, more space will be needed for the input data, and simulation speed will be slowed down. Defining islands in the grid system is independent of defining islands in a branch configuration. This allows for a greater flexibility in the simulation of oil slick transformation. For example, a small island that covers only three or four grid boxes, which may be too small to be defined in the branch configuration, can be easily defined in the grid box system. All islands must be defined in the grid box system.

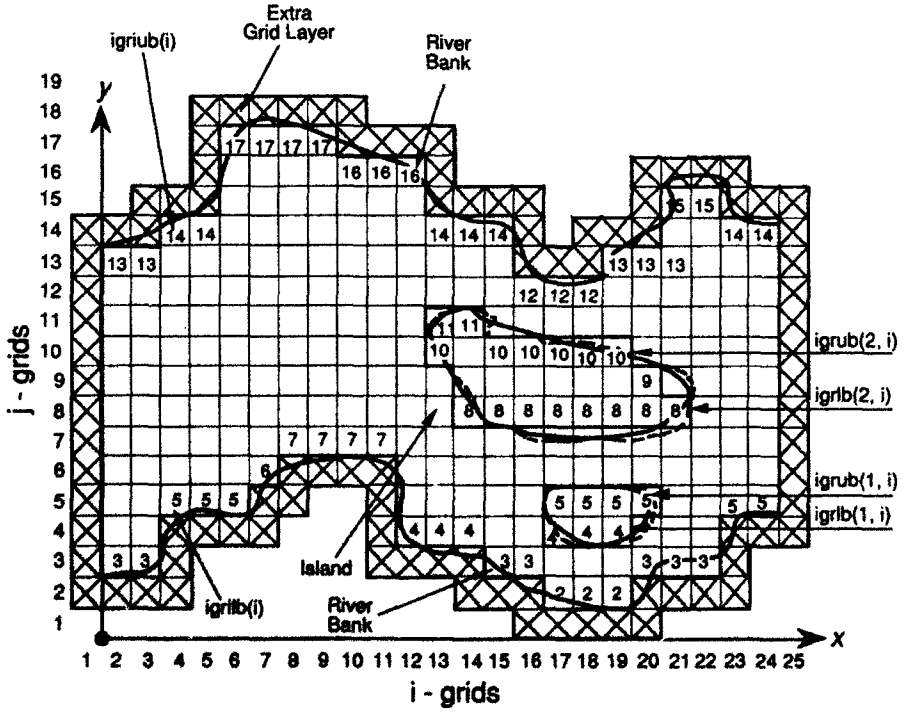

Figure 15. Grid boxes and river boundary representation.

The velocity and depth within a box are assumed to be uniform. Only boxes found within the defined river boundaries are assigned velocities and depths. Generally spacing between cross sections in the stream-tube computation is much larger than the grid size Δx. The following procedure is adopted for assigning velocity and depth to grid boxes based on the velocity and depth at cross sections. In the following discussion the term "velocity/depth point" is used to represent a point at which a computed velocity/depth is located. At first all velocity and depth points computed from the stream-tube analysis will be assigned to the boxes within which they lie. If more than one velocity and depth point fall into a box, the average value of velocity/depth is assigned to that box. In the next step, more velocity/depth points will be obtained through interpolation between two successive cross sections. The number of interpolation points between two successive cross sections can be changed through user-defined input. These velocity/depth points obtained through interpolation will now be assigned to grid boxes using the same method as before. After this, if there is any box without an assigned velocity/depth, an average velocity/depth calculated based on neighboring boxes will be assigned. Upon the completion of these steps, the entire river is scanned to ensure that velocity/depth points are assigned to all boxes.

Oil slick orientation

The surface slick can spread either axisymmetrically or one-dimensionally. The determination of which type of spreading prevails depends on the shape of the slick, i.e. the aspect ratio. Therefore, after the oil particles moved to their new positions, the centroid, aspect ratio and orientation of the oil slick are calculated. These calculations will consider only oil particles in the water grids.

Table 8. Boundary types of locks and dams.

Code no.	*Rejection rate*
13	2
14	3
15	4
16	5
0	6

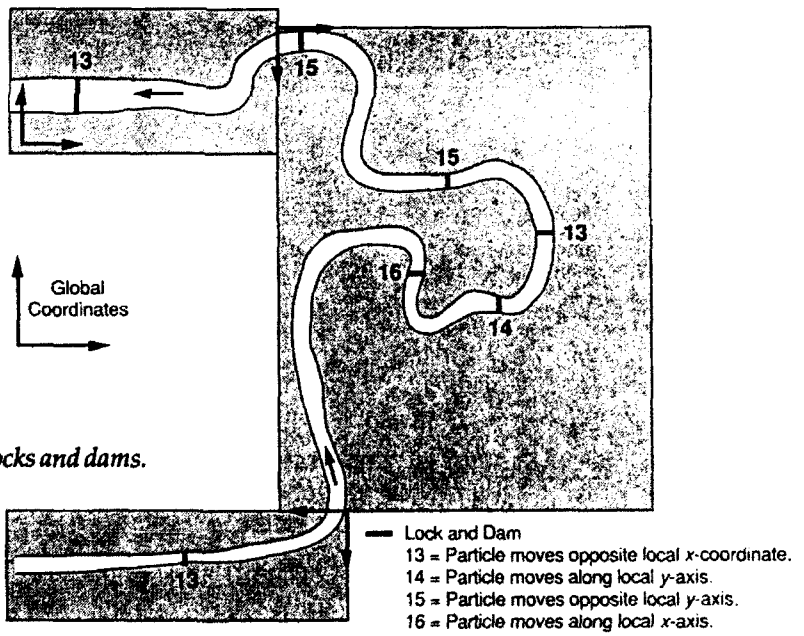

Figure 16. Index system for locks and dams.

Boundary conditions and locks and dams

Twelve half-life values were defined in Table 3 for shoreline boundaries. Oil slicks passing a lock and dam will be completely mixed into the water column. The program is directed to this condition through the use of shoreline boundary codes. Four new boundary condition codes are added. As defined in Table 8, code numbers 13–16 refer to lock and dams with four different orientations (Fig. 16). A set of special rejection rate codes are given for these conditions to direct the program to well-mixed conditions. Oil parcels deposited on the banks at a lock and dam are instantly rejected into the water. This is achieved by using a set of shoreline codes 0 and 6 as in Table 8. This set of codes can also be used at other shoreline locations for instantaneous rejection if needed.

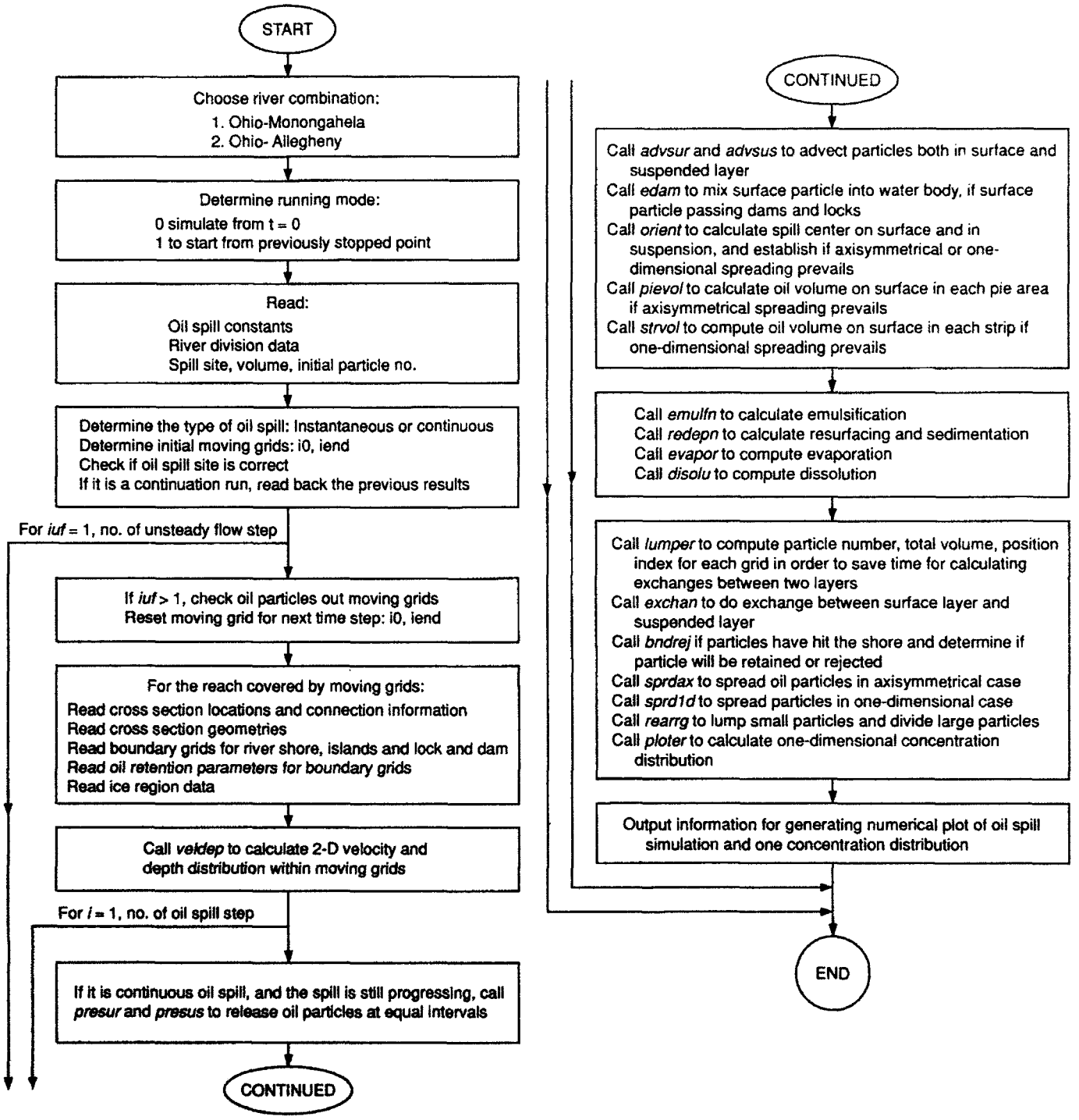

Figure 17. The computer model ROSS2.

Model structure

The computer code is written in standard Fortran 77. No compiler-specific extensions have been used. The code has been tested only on 32-bit machines with Fortran 77 compilers that support 32-bit computations. The program can be run on other machines (e.g. 24-bit) with minor modifications. Appendix B gives a listing of all the subroutines used. The model is named ROSS2, and the model structure is shown in Figure 17. All variables are dimensioned to have sufficient storage to run for each segment of the river system. The velocity and depth distributions will be kept only for a reach long

enough for the oil slick to travel one unsteady flow calculation time step. The model can be run for a new spill simulation or continue from a previously terminated run by changing weather and oil characteristics.

Subroutine cross reference

The model consists of the main program ROSS2 and 37 subroutines, as summarized in Table 9. An alphabetically arranged listing of the subroutines is given in Appendix B.

The common block includes arrays and their definitions shared by subroutines. Sizes or arrays can be adjusted in this block according to the moving grid size, maximum particle number, river segment number, maximum island number and stream-tube number. Table 10 gives definitions of important variables included in the common block. When the model is applied to other rivers, dimensions should be adjusted. Other variables used in the program are presented in Appendix A.

Main program

The main program is used to establish the link between subroutines, besides interactions going through the common block. The major functions of the main program can be summarized as follows:

- Read oil spill information in the data file *xxx.spl*.
- Read boundary grid box numbers and set boundary conditions from *xxx.igr* and *xxx.bnd*.
- Call *con* to read back the simulation results if it continues a job from a previously terminated run.
- Call *ckout* to adjust the moving grid position based on the oil slick position.
- Call *veldep* to calculate velocity and depth distributions of the river reach superimposed by moving grids during every unsteady flow time step.
- Call *presus* and *presur* to release oil particles at equal intervals for the oil spill duration.
- Call *advsus* and *advsur* to advect oil particles in both the suspended layer and the surface layer.
- Call *emdam* to mix oil particles into the water column when passing locks and dams.
- Call *orient* to calculate the oil slick orientation, determining whether the slick is quasi-one-dimensional or quasi-axisymmetric; call *pievol* to calculate the volume of each pie segment for an axisymmetric slick; or call *strvol* to calculate the volume in each small strip for a one-dimensional slick. All of these are for mechanical spreading calculations.
- Call *emulfn* and *redepn* to compute oil volumes into the water column, resurfaced to the water sur-

Table 9. Cross references of subroutines.

Program	*Calls*	*Input files*
ross2	*input, ckout, positn, veldep, ohndc, ohvad, advsur, presus, advsur, advsus, bndloc, check1, ckout, con, rejloc, emdam, orient, pievol, strvol, emulfn, redepn, areacl, evapor, disolu, lumper, exchan, bndrej, shift, sprdax, sprdld, rearrg, ploter*	River division data, spill data, shoreline condition, ice regions
advsur	*gauss, randu, bndrej, rejloc*	None
advsus	*gauss, randu, bndrej, rejloc*	None
areacl	None	None
bndloc	None	None
bndrej	*rejloc*	None
calcij	None	None
calclm	None	None
check1	*calcij*	None
ckout	*calcij,calclm*	None
con	*conchk*	Previous simulation results
conchk	*calcij*	Previous simulation results
disolu	None	None
emdam	None	None
emulfn	None	None
evapor	None	None
exchan	None	None
input	None	Spill constants, river divison data
lumper	None	None
lumper1	None	None
ohndc	None	Flow data
ohvad	None	None
pievol	None	None
ploter	None	None
posit2	None	None
presur	*advsur, gauss, randu, bndrej, rejloc*	None
presus	*advsus, gauss, randu, bndrej, rejloc*	None
rearrg	*lumper1*	None
relca	None	None
reloca	None	None
reloxy	None	None
relxy	None	None
shift	None	None
sprdax	None	None
sprdld	None	None
strvol	None	None
veldep	*ohndc, ohvad*	Geometry data, flow data

Table 10. Definition of variables in the common block (dimension parameters).

Variable	*Value*	*Definition*
numbrn	37	Maximum number of branches of river segments
numdep	66	Maximum number of sounding depth locations at all cross sections
numice	10	Maximum number of ice regions
numpar	15000	Maximum number of oil particles
numpie	8	Number of pies into which the axisymmetrical slick is divided
numv10	2	Number of positions where the velocities are assigned zero
numpos	26000	Maximum number of moving grids
numsec	330	Maximum number of cross sections among river segments
numstb	11	Number of stream tubes
nwth	10	Number of shorelines, including islands, locks and dams
nudxx	1100	Maximum grid number in x direction of moving grids
numxgd	4600	Total number of grids in the x direction
nseg	5	Maximum number of river segments
nisl	4	Maximum number of islands a cross section can meet
nout	800	Maximum number of particles out of moving grids that can be plotted

face and deposited onto the riverbed during the time step, as well as the cumulative values.

- Call *areacl* to calculate the slick area in water, under ice and on land for the calculation of evaporation and dissolution.
- Call *evapor* and *disolu* to calculate evaporation and dissolution.
- Call *lumper* and *exchan* to calculate oil exchanges between the suspended layer and the surface layer.
- Call *sprdax* for an axisymmetrical oil slick, or call *sprd1d* for a one-dimensional slick, to calculate mechanical spreading.
- Call *bndrej* to reject oil particles back into the river according to the bank retarding condition (half-life).
- Call *rearrg* to adjust particle sizes, i.e. lump small particles together and divide large particles to satisfy the requirements of the random-walk simulation and the computer memory space.
- Call *ploter* to calculate the one-dimensional cross-sectional average oil concentration distribution along the river.
- Save the simulation results into corresponding output files at a designated output frequency.

Subroutines

Since all subroutines and related variables are listed in Appendices A and B, and some simple subroutines can be easily understood with comments in the listing, no further explanation will be given. Block diagrams for some main subroutines are given in Figure 18 to assist in understanding the program.

Case study

The model is applied to the oil spill in the Monongahela River on 2 January 1988 (Miklaucic and Saseen 1989). Simulation results for the leading edge and concentration distribution of the oil plume will be compared with the field data.

Model parameters

A number of empirical parameters, which can affect the simulation results, are to be selected by the user. In this section the effects of these parameters will be discussed to assist the user in making appropriate selections.

One of the parameters that will affect the movement of the slick is the shoreline boundary condition. Under an instantaneous-rejection shoreline boundary condition, oil will not deposit on riverbanks. Particles moved to the shore will be rejected to water instantly. This will give a shorter slick, and its leading edge will advance at a faster rate.

Theoretically the simulation should not be affected by the spill time step. However, numerically a

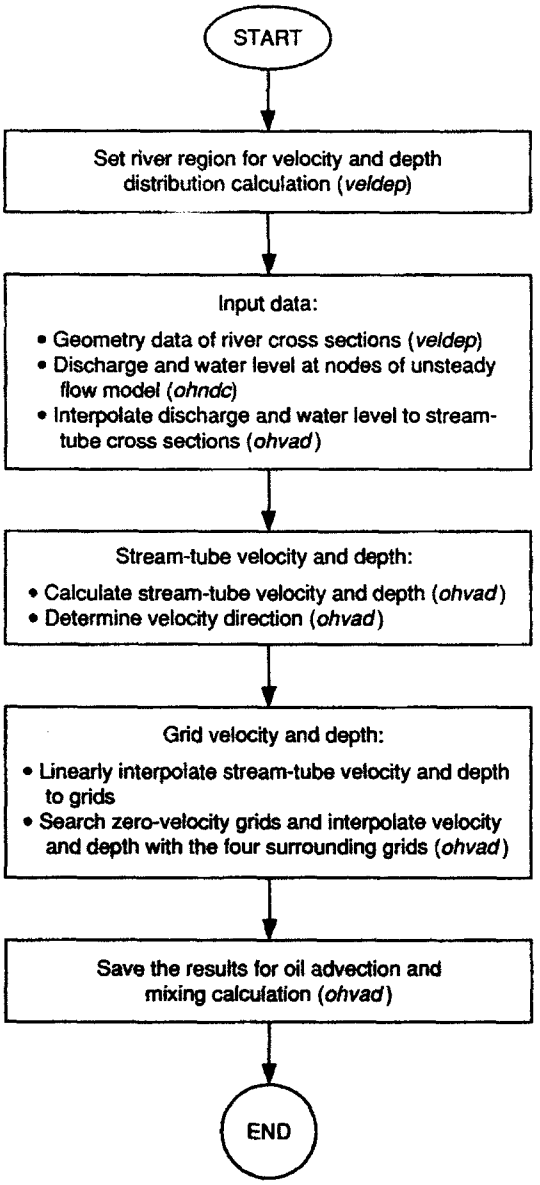

a. Velocity and depth computations.

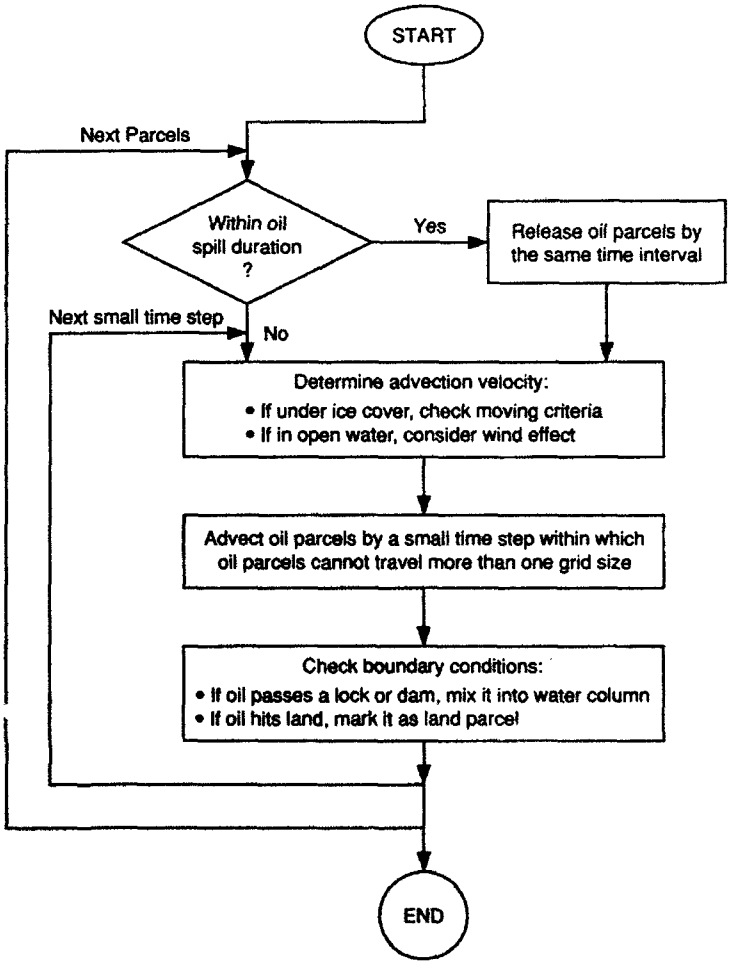

b. Release and advection of oil parcels.

Figure 18. Subroutines.

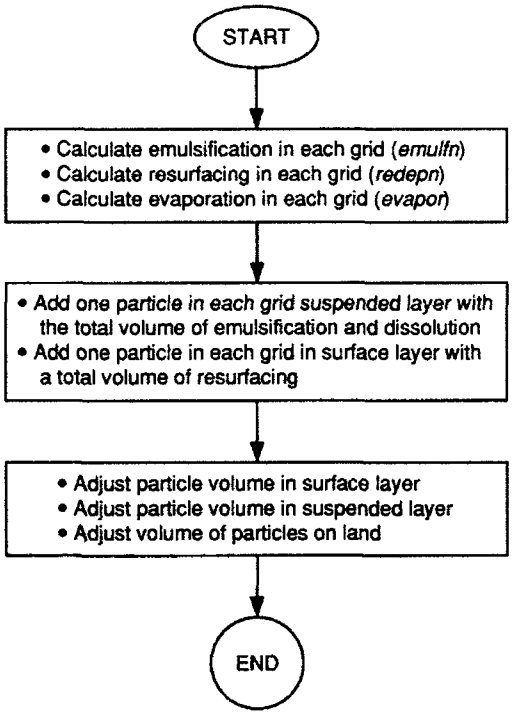

c. Mixing computation.

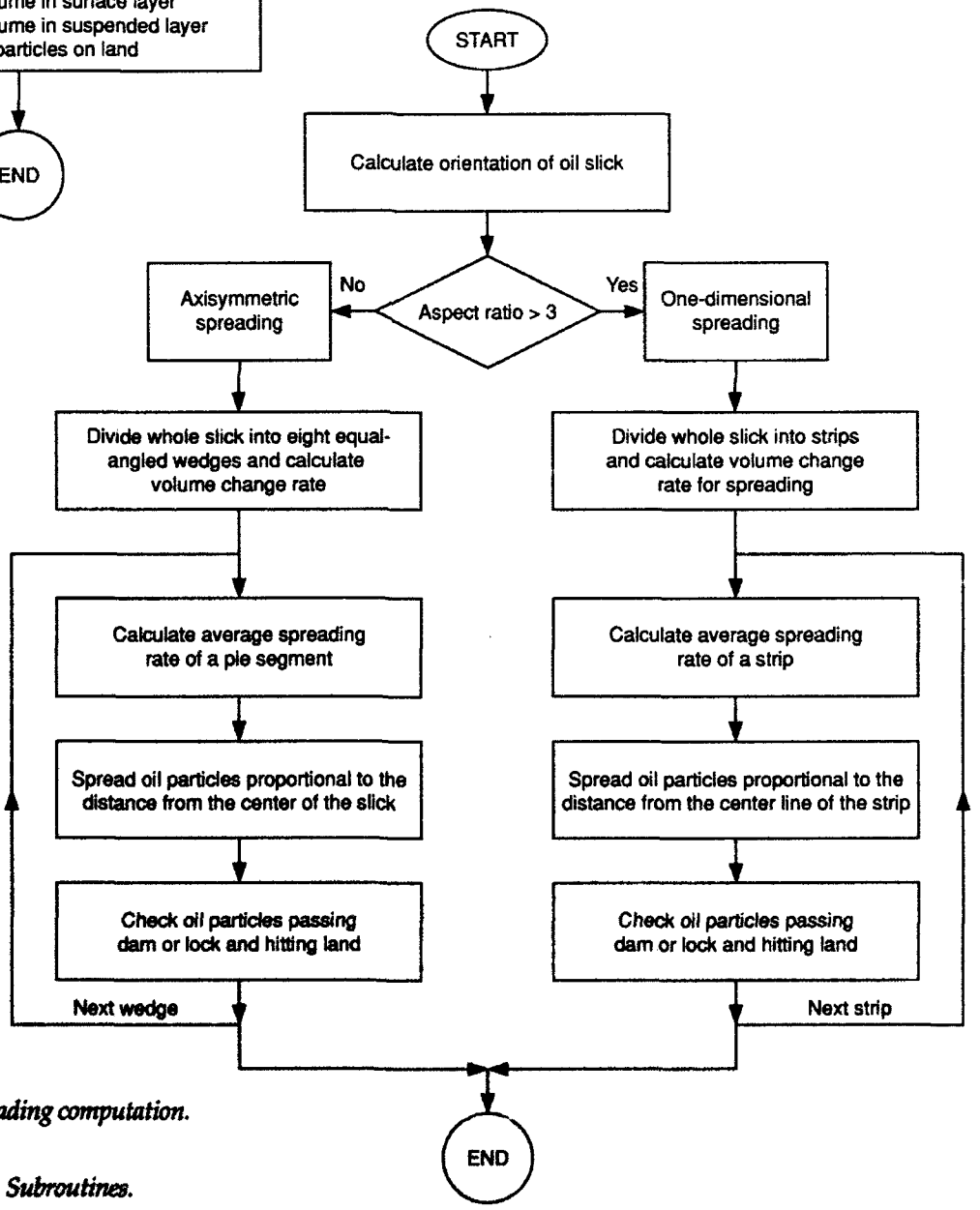

d. Mechanical spreading computation.

Figure 18 (cont'd). Subroutines.

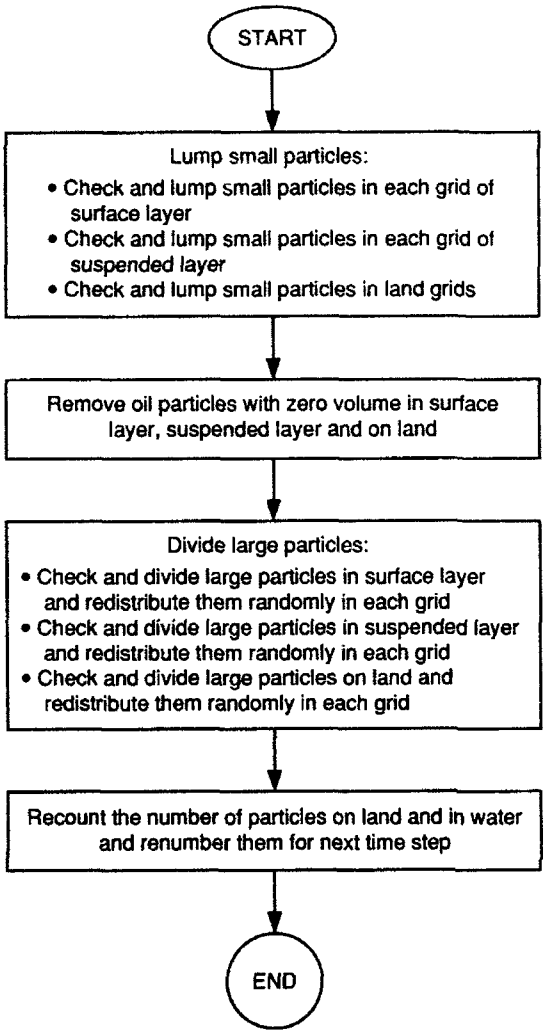

e. Particle size adjustment.

Figure 18 (cont'd).

large time step can lead to inaccurate results, especially for the non-instantaneous-rejection condition. In the model, boundary rejection, exchange between layers, mechanical spreading, evaporation and dissolution are done once every spill time step to save computation time and memory. The spill time step can affect the slick length through all of these simulation components. If the time step is too large, discontinuous distributions of the portions of oil deposited on shoreline, on the water surface and in the suspension will appear. When the instantaneous-rejection condition is used, the effect of the spill time step is small.

The random-walk theory requires a large number of particles with equal mass. Numerical experiments show that the equal mass requirement can be relaxed if the particle number is large enough. In the present model the particle number increases when the particle mass becomes more uneven due to the exchange between the surface and suspended layers The model also keeps at least one particle in each grid that contains oil.

To demonstrate the effects of the shoreline condition, simulations for the time step Δt and the initial particle number N_0 are carried out for the 1988 oil spill in the Monongahela River for a duration of 10 days. The model parameters used in these simulations are:

- **Buoyant velocity:** $v_b = 0.01$ ft/s;
- **Resurfacing coefficient:** $\alpha = 1.0$;
- **Emulsification coefficient:** $\beta = 10^{-5}$/s;
- **Riverbed deposition coefficient:** $\gamma = 10^{-5}$/s;

- Initial particle number: $N_o = 40$, or 400 each layer;
- Spill time step: $\Delta t = 5$, 15 or 30 minutes; and
- Evaporation modification coefficient: $\alpha_E = 0.3$.

Ice covers can affect the movement of oil in the river. According to the model the advection velocity of the oil slick under a smooth ice cover will only be reduced by 10–15%. The ice cover has very little effect in the advection of suspended oil. For the 1988 spill the air temperature was below freezing, as shown in Figure 19. Ice may have existed in the Ohio River during the later part of the simulation period. However, since the ice covers formed in the Ohio River are generally smooth, the existence of an ice cover will be neglected in the sample simulations for simplicity.

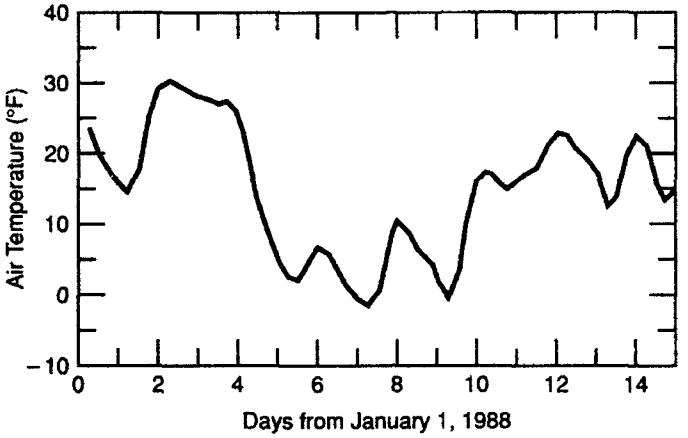

Figure 19. Air temperature variation during the simulation period, Pittsburgh, Pennsylvania.

Figure 20 shows simulation results with the idealized instantaneous-rejection shoreline condition and a partial-rejection shoreline condition determined for the OMA system. Table 11 and Figures 21 and 22 compare simulated and observed locations of the leading edge of the slick and the concentration peak. These results show that the slick locations simulated using the instantaneous-rejection shoreline condition do not agree with the observed locations, although the errors are relatively small. Simulations using the partial-rejection shoreline condition compared well with the field observation. Simu-

Table 11. Observed and simulated locations of the leading edge and the concentration peak.*

	Leading edge (river mile)		*Concentration peak (river mile)*	
Date	*Observed*	*Simulated*	*Observed*	*Simulated*
	Instantaneous shoreline rejection			
2 Jan	−25.0	−25.0	−25.0	−25.0
3 Jan	0.0	−1.21	−4.5	−2.54
4 Jan	25.0	22.24	no	19.04
5 Jan	45.0	52.14	no	49.90
6 Jan	65†	74.32	no	72.58
	78**	74.32	60.0	72.58
7 Jan	73†	98.89	65.0	96.07
	88**	98.89	77.0	96.07
8 Jan	89.0†	115.8	77.0	112.9
	99.0**	115.8	84.0	112.9
9 Jan	94.0†	125.1	no	122.6
	108**	125.1	86.0	122.6
10 Jan	112.0	125.2+	96.0	125.1+

	Leading edge (river mile)		*Concentration peak (river mile)*	
Date	*Observed*	*Simulated*	*Observed*	*Simulated*
	Partial shoreline rejection			
2 Jan	−25.0	−25.0	−25.0	−25.0
3 Jan	0.0	0.41	−4.5	−2.11
4 Jan	25.0	21.06	no	14.06
5 Jan	45.0	43.11	no	32.34
6 Jan	65†	58.82	60.0	52.43
	78**	58.82	60.0	52.43
7 Jan	73†	77.62	65.0	64.06
	88**	77.62	77.0	64.06
8 Jan	89.0†	90.43	77.0	78.41
	99.0**	90.43	84.0	78.41
9 Jan	94.0†	101.5	86.0	85.39
	108**	101.5	86.0	85.39
10 Jan	112.0	109.7	96.0	93.51

* Initial particle number in each layer is 400; spill time step is 900 s.
† Vicory and Ahles-Kedziora (1989).
** Berkey et al. (1989).

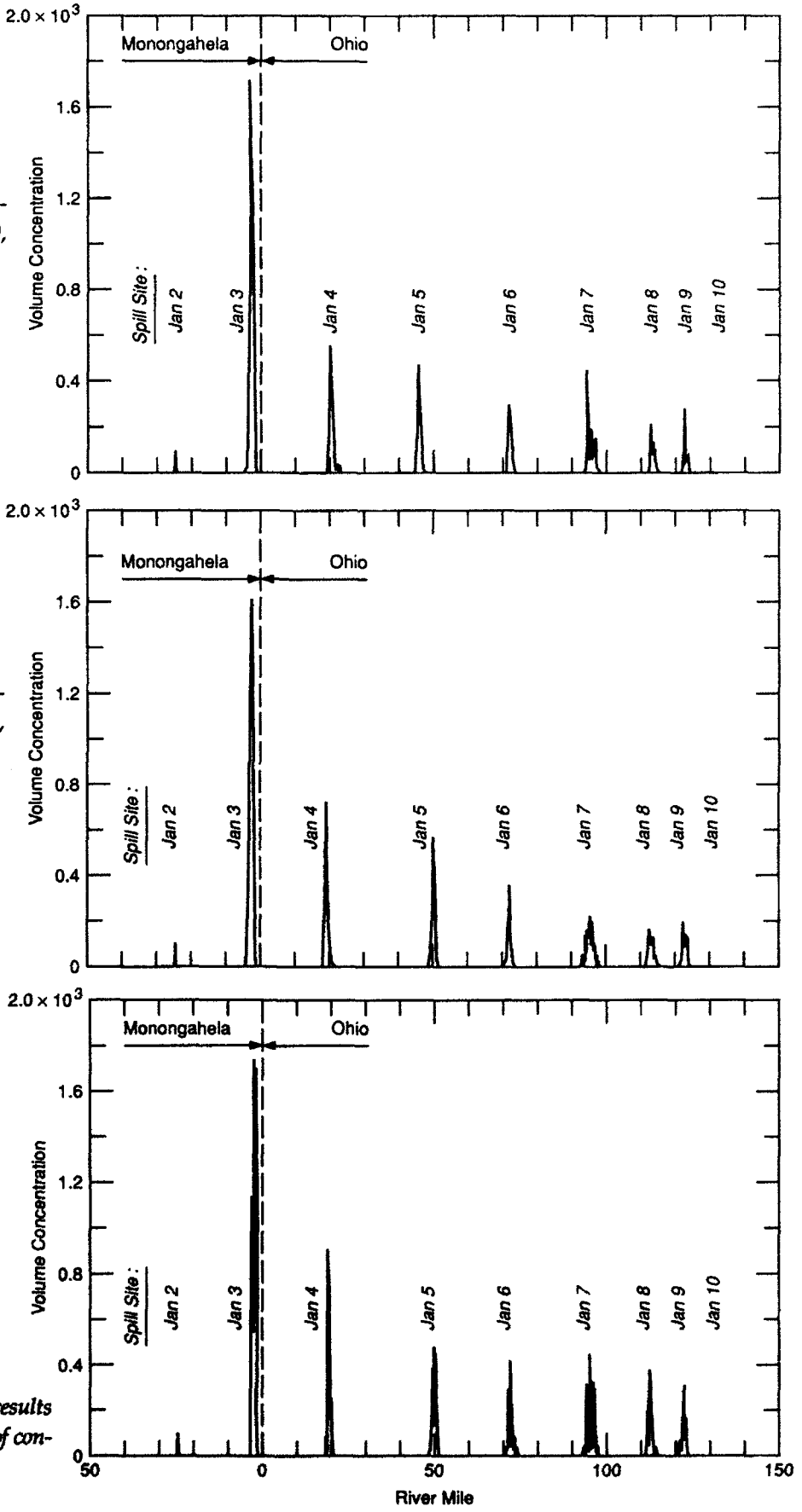

a. Instantaneous shoreline rejection, $N_o = 400$, $\Delta t = 5$ min.

b. Instantaneous shoreline rejection, $N_o = 400$, $\Delta t = 15$ min.

c. Instantaneous shoreline rejection, $N_o = 40$, $\Delta t = 30$ min.

Figure 20. Simulation results showing the variation of concentration distribution.

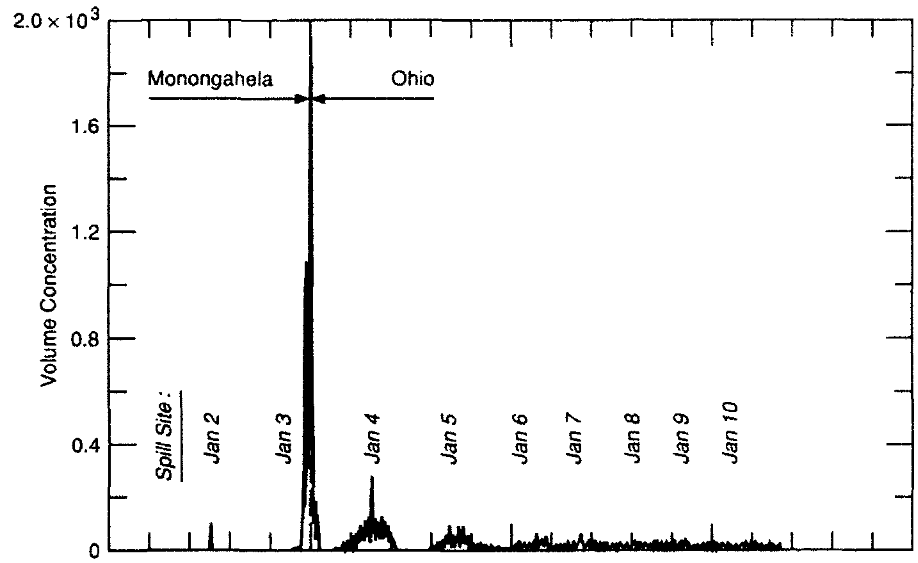

d. Partial shoreline rejection, N_0 = 400, Δt = 5 min.

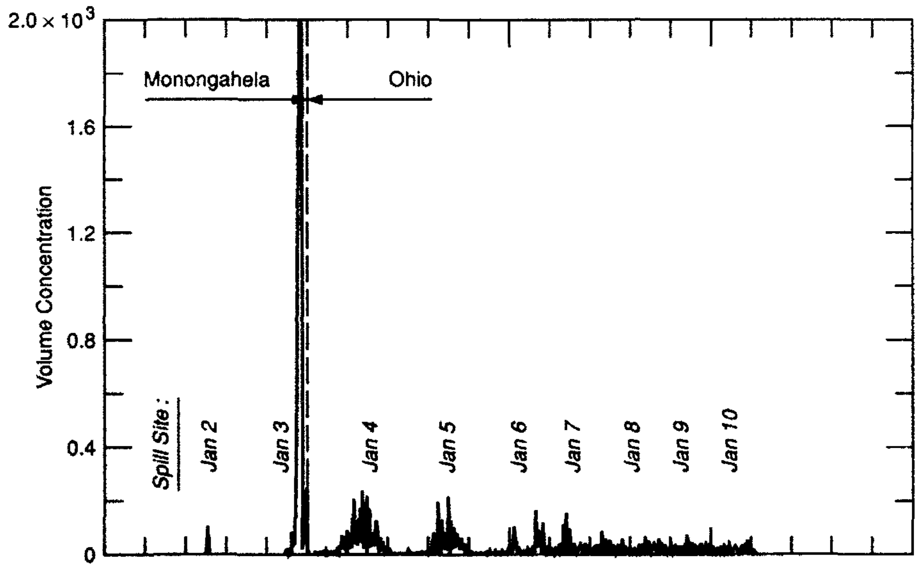

e. Partial shoreline rejection, N_0 = 400, Δt = 15 min.

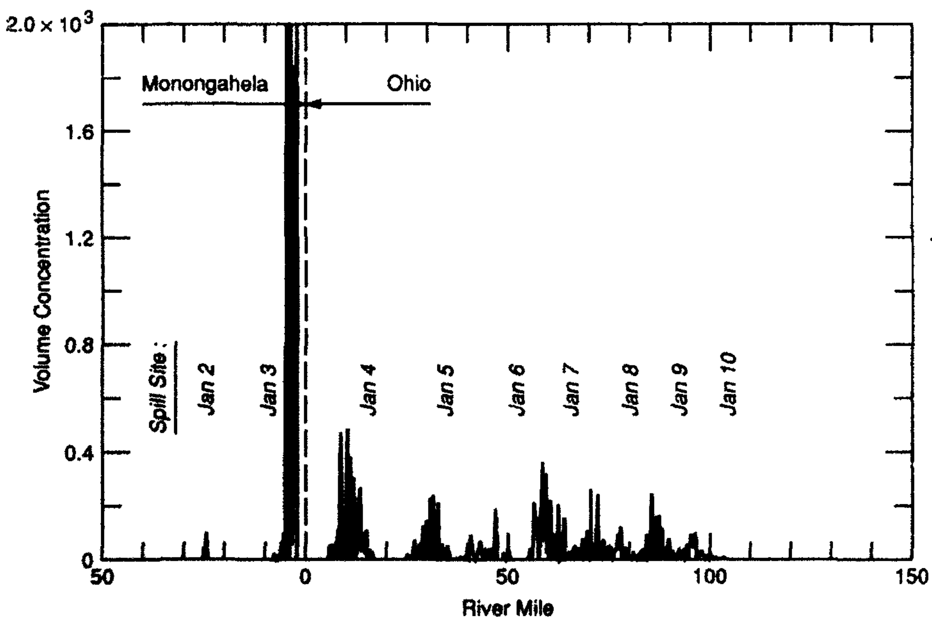

f. Partial shoreline rejection, N_0 = 400, Δt = 30 min.

Figure 20 (cont'd). Simulation results showing the variation of concentration distribution.

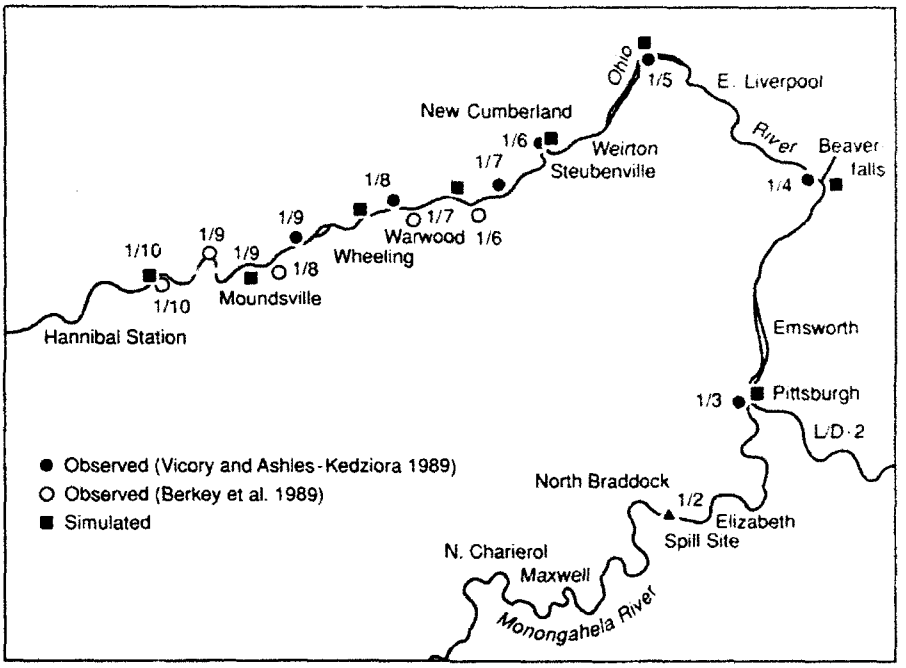

Figure 21. Comparison of simulated and observed leading edge positions; $N_o = 400$, $\Delta t = 300$ s.

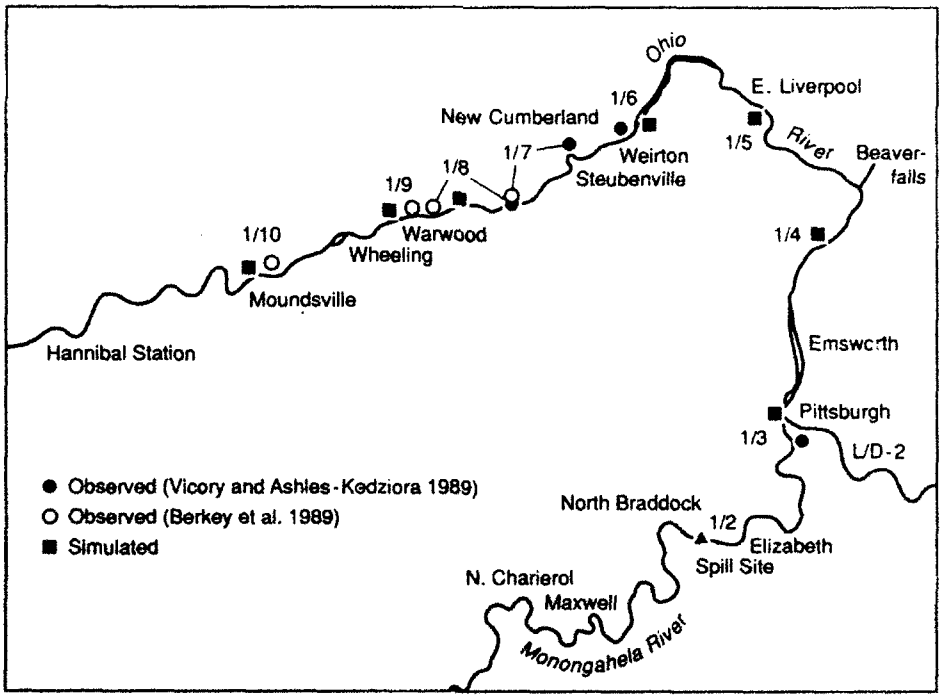

Figure 22. Comparison of simulated and observed concentration peak locations; $N_o = 400$, $\Delta t = 300$ s.

lations using small particle numbers generally resulted in shorter slicks with higher concentration. The effect of time step Δt is shown in Figure 23. This figure shows that the slick slowed down with the increase in Δt. However, this effect is small.

A summary of computing time used for all of the sample simulations run on a SUN SPAC station1+ is given in Table 12. This t[illegible] shows that the computing time decreases with a reduction in particle

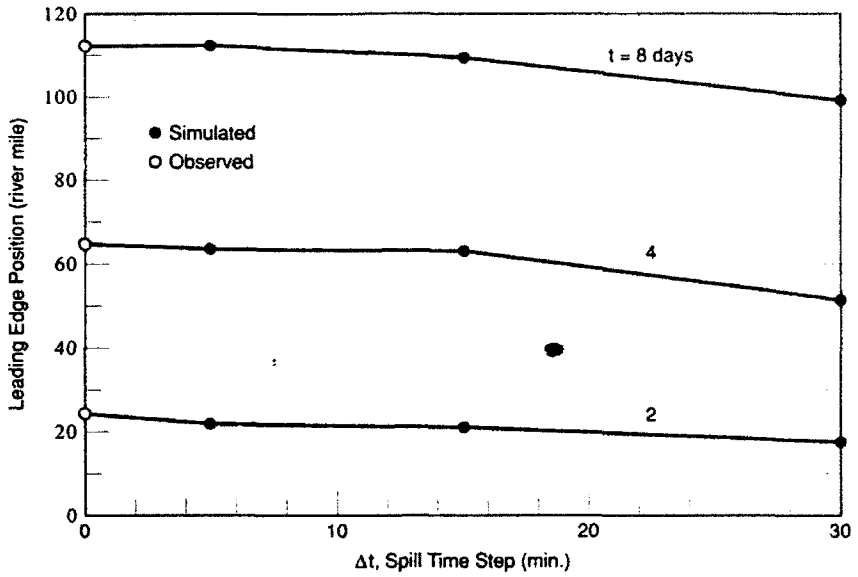

Figure 23. Effect of time step Δt on leading edge positions.

Table 12. Comparison of computing time.

Parameters	*CPU time (s)*	*Parameters*	*CPU time (s)*
Instantaneous rejection		**Partial rejection**	
$N_o = 400$; $\Delta t = 300$ s	23,855	$N_o = 400$; $\Delta t = 300$ s	67,354
$N_o = 400$; $\Delta t = 900$ s	10,797	$N_o = 400$; $\Delta t = 900$ s	32,248
$N_o = 400$; $\Delta t = 1800$ s	3,612	$N_o = 400$; $\Delta t = 1800$ s	19,258

number and an increase in Δt. The use of the instantaneous-rejection shoreline condition reduces the computing time by approximately 60%. It is recommended that, for field applications in the OMA river system, the partial-rejection shoreline condition with $\Delta t = 900$ s and $N_o = 400$ be used, considering the simulation accuracy and computing time. The ratio between the real time and the computing time is about 1:12. This ratio is smaller at the early stages of simulation. For emergency applications an instantaneous-rejection shoreline condition along with a smaller N_o and a larger Δt should be used. The ratio between the real time and the computing time is about 1:240 when $\Delta t = 30$ minutes and $N_o = 40$ are used.

Applications to non-oil spills

As mentioned earlier the model can be applied to non-oil spills. Non-oil spills can be simulated by inputting appropriate values for the spill parameters described earlier. For neutrally buoyant miscible materials, the buoyant velocity should be set to zero.

INPUT DATA FILES

There are two categories of inputs that are required to run the model. The first category can be considered to be fixed data for a given river reach. This is the information required to describe the shoreline and cross-sectional geometry of the river. Normally there is no need to adjust these data. The second category includes various parameters that may be adjusted according to the flow condition and spill characteristics. To completely understand the setup of the data files, it is helpful to go through the step-by-step procedure that follows. Sample input data files are given later. If the user is only interested in adjusting parameters, changing the spill location or establishing new stage and discharge conditions on a previously modeled river, no new data files need be created.

Data file creation

For demonstration purposes the Ohio–Monongahela river combination will be used as an example. This river shows the complexity of a river system that the model can handle. Where the data files for the Ohio–Monongahela river combination are not sufficient to describe the detail, other river data will be presented. Eight data files exist for inputting information into the computer model:

xxx.geo River geometry, cross sections and branch geometry
xxx.igr Boundary grid box numbers
xxx.ice Ice regions, ice roughness and oil viscosity
xxx.flo Water level and discharge at nodes determined from the unsteady flow model
xxx.bnd Index for half-life value assignments to shore grids
xxx.spl Oil parameters, spill location, wind condition and ambient temperature.
xxx.ndc Information to transform computed unsteady flow results to what are needed in the oil spill model flow computation
xxx.msc River segment definitions, parameters for exchange between two layers and information needed to coordinate transformation data.

The first step in preparing the data file is to make a sketch similar to Figure 24 to describe the branch and cross-section numbering system used in the data file. The procedure for obtaining this sketch is as follows:

1. Determine the number of river segments. In this model the entire Ohio–Monongahela–Allegheny river system is divided into seven segments, as described earlier. The numbering of segments depends on the river combination. The Ohio–Monongahela has five river segments numbered from downstream to upstream. Each segment has its own local coordinate system, which can be transformed to the global coordinate system using the transformation data in data file *ohmon.int*. All geometry data will be prepared segment by segment with independent numbering. To ensure that all water grids are covered, cross-section numbers will have overlaps in the vicinity of the division line between river segments.
2. Determine the number of branches. Each branch must contain at least two unsteady flow nodes and one stream-tube cross section.
3. Number the cross sections in consecutive order from the downstream end to the upstream end of the segment. Around islands, first number the bottom side up to the last cross section prior to the confluence into a single channel, then go back to the top side and continue the numbering sequence.

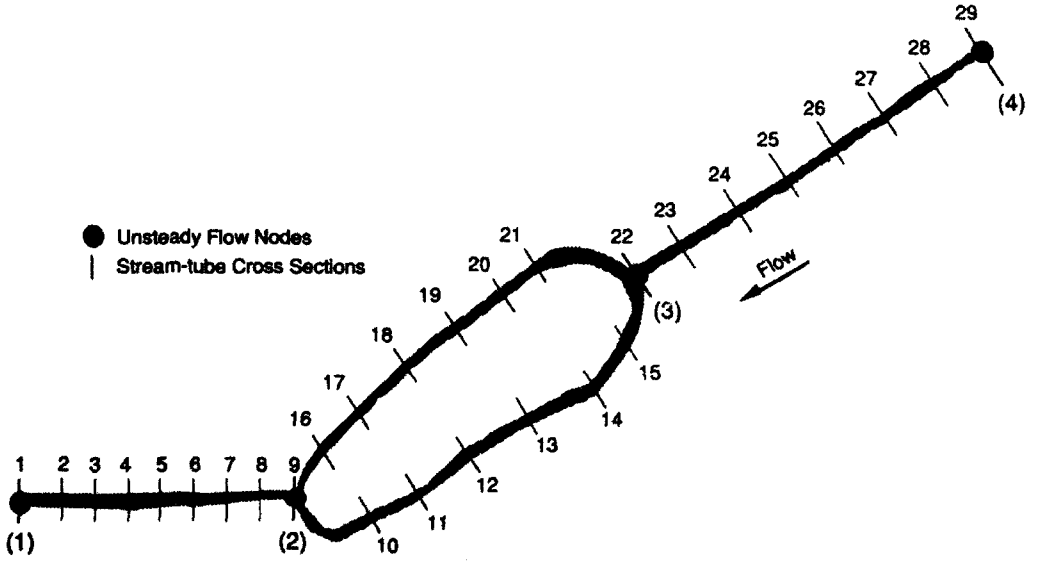

Figure 24. Definition sketch of the river numbering system.

4. Determine the number of stream tubes in each branch. The total number of stream tubes always remains the same. The stream tubes must be divided according to the ratio of the flow split around the island.

Once the branches and cross sections for the river are established, scaled maps of the river and cross sections are used to:

1. Establish the global x–y Cartesian coordinates, to be superimposed over the river.
2. Establish the reference coordinates on the left bank (looking downstream).
3. Digitize the entire river boundary and cross-section locations simultaneously.
4. Digitize the cross-section geometries by measuring a transverse distance from the reference point on the left bank to a corresponding sounding point.
5. Determine the way to assign flow direction to each cross section. For the cross sections along river bends, use 1 as the direction index, which implies that the flow directions will be perpendicular to the cross section. Along straight reaches, especially in reaches with islands, 0 is chosen as the flow direction index. This implies that the flow direction will be along the line connecting corresponding stream-tube centers in two neighboring cross sections.
6. Schematize boundary boxes, i.e. for every x-grid there exists corresponding upper and lower riverbanks and island boundary boxes.

The files are generally broken up into blocks and cards. A block covers a group of data that may contain one or more card types. A card type is one line of specific data, which is sometimes repeated. (For example, Block 4 in *xxx.geo* has Cards 1 and 2, where Card 2 is repeated as many times as needed.) By inspecting the example of a card and comparing it to the complete sample data set, it is easy to see how the entire file comes together.

Most of the data read into the model are in list-directed I/O (free format). If column numbers are shown, the data must be formatted accordingly. Otherwise it is necessary to put only one space or comma between each number in a card.

In the following sections, data files of the Ohio–Monongahela river combination will be used as examples to explain the setup of data cards.

Geometry data: ohmon.geo

Ohmon.geo consists of five segments of geometry data for the five corresponding river segments. Each segment has four blocks. None of the data in this file needs to be adjusted from one spill to the next. The user may choose to add additional cross sections, change the number of branches, etc. *However, the user is cautioned to consult this section before making such changes.* Since all segments have the same format, only one will be explained here.

ohmon.geo: Block 1, branch and grid information

Card 1
Example:
24 16

Variable name	*Type and length*	*Column number*	*Description*
nbrnch	Integer	–	Number of branches
kintm	Integer	–	Number of velocity interpolations between cross sections in a stream tube

Card 2 (one number for each branch)
Example:

12 22 32 44 45 64 89 104 105 121 131 138 139 141 150 208 210 218 228 233

Variable name	*Type and length*	*Column number*	*Description*
lcstsq(i)	Integer	–	Last cross section in each branch. In the last branch, use the second to last cross section. There must be a total of *nbranch* data. If the line is not long enough, continue to the next line

ohmon.geo: Block 2, cross section and connection information

Card 1 (one card for each cross section)
Example:

1 16840.66 7741.73 –0.44720 0.89443 11 11 2 0 0.0 0

Variable name	*Type and length*	*Column number*	*Description*
j	Integer	–	Cross-section number
x	Real	–	*x* coordinate (in global coordinate system) of reference point on left bank
y	Real	–	*y* coordinate (in global coordinate system) of reference point on left bank
cst	Real	–	Cosine value that the angle cross section makes with positive *x*-axis (global)
snt	Real	–	Sine value that the angle cross section makes with positive *x*-axis (global)
nstube(i)	Integer	–	Number of stream tubes at current cross section
numcon(i)	Integer	–	If all stream tubes continue to next cross section undivided, = 11; if stream tubes divided into two channels from a main channel, = 12; if stream tubes from this channel and another channel connect to next section that is in the main channel, = 21
nfirco(i)	Integer	–	Next cross section connecting to the current cross section. For a divided channel around an island, this represents the first cross section connected to in the lower division from the main channel cross section
nseco(i)	Integer	–	For a divided channel around an island, this represents the first cross section connected to the upper division from the main channel cross section (if no island, = 0). If this is the first cross section in the upper branch, = 888. If this is the last in the upper branch, = 999.
stub(i)	Real	–	If a branch has small islands, = discharge fraction on left side of the island; if no island, = 0.0
ibend(i)	Integer	–	Flow direction index; for cross sections in a river bend, = 1; otherwise = 0

ohmon.geo: Block 3, cross-section geometry

Card 1
Example:
6 39

Variable name	*Type and length*	*Column number*	*Description*
j	Integer	–	Cross-section number (for checking)
nslsct(j)	Integer	–	Number of sounding depths (points along the bed in the transverse direction) used to describe the cross-section geometry

Card 2 (as many cards as required to input all sets of ywid.z)
Example:
0.0 660.0 540.0 660.0 540.0 596.0 ...

Variable name	*Type and length*	*Column number*	*Description*
ywid(i,j)	Real	–	Transverse distance from the reference shore to the j^{th} sounding depth in i^{th} cross section
z(i,j)	Real	–	Bed elevation at the j^{th} transverse point (sounding depth) for the j^{th} transverse point (sounding depth) for the j^{th} cross section

Note: Block 3 must be repeated lcstsq(nbrnch) times (i.e. number of cross sections defined).

ohmon.geo: Block 4, defines all grid boxes that are to be assigned zero velocity

Card 1
Example:
0

Variable name	*Type and length*	*Column number*	*Description*
nzrvb	Integer	–	Number of boxes to assign zero velocities

Card 2

Variable name	*Type and length*	*Column number*	*Description*
izrbx	Integer	–	x-grid number of i^{th} box to have zero velocity
izrby	Integer	–	y-grid number of i^{th} box to have zero velocity

Note: There are must be nzrvb pairs of izrbx(i) and izrby(i). Data can be continued to as many lines as needed.

For the other river segment, just repeat block 1 to block 4. This is the end of data file *ohmon.geo*.

***Ice condition data:* ohmon.ice**

The *ohmon.ice* file contains information identifying ice regions. An ice region is defined by a range of grid boxes that are ice-covered; using the example in Figure 25 an ice region may be identified as extending from grid (14,8) to grid (18,7). The ice region then covers every grid from (14,8) to (18,7) as shown in the figure. This information is used when determining if spreading and advection takes place under an ice cover or on open water.

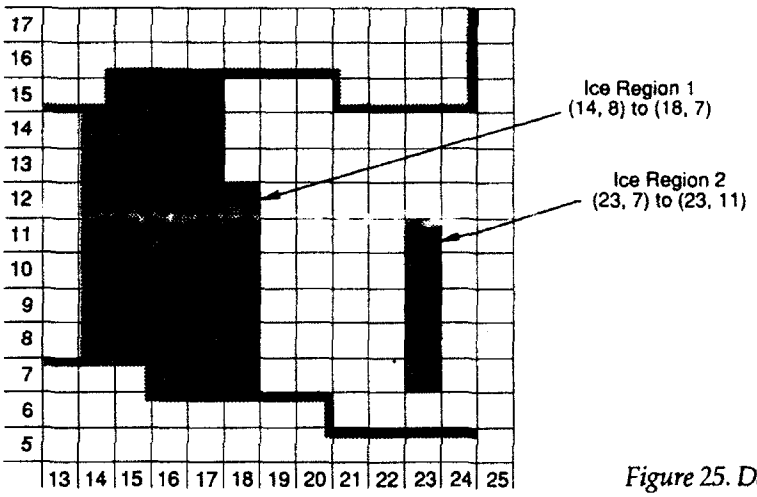

Figure 25. Defining ice regions.

ohmon.ice: Block 1

Card 1
Example:
0 035 12.5

Variable name	*Type and length*	*Column number*	*Description*
anice	Real	–	Manning's *n* for ice roughness
amiuo	Real	–	Viscosity of oil (gm-cm/s) (poise)

Card 2
Example:
2

Variable name	*Type and length*	*Column number*	*Description*
nicerg	Integer	–	Total number of ice regions

Card 3
Example:
14 8 18 7

Variable name	*Type and length*	*Column number*	*Description*
nicexl(i)	Integer	–	*x* grid at the beginning of ice region
niceyl(i)	Integer	–	*y* grid at the beginning of ice region
nicex2(i)	Integer	–	*x* grid at the end of ice region
nicey2(i)	Integer	–	*y* grid at the end of ice region

This is the end of data file *ohmon.ice*.

Flow data: ohmon.flo

The *ohmon.flo* file contains the unsteady flow time step, the water level and the discharge at each node in the river as defined by the one-dimensional unsteady flow model (Yang et al. 1990). Also in-

cluded are the ice conditions for each cross section in the river. These data are separated from the ice region data in *ohmon.ice*. The oil spill simulation model converts this information into boundary conditions for each river branch.

This file consists of three blocks of information. All blocks are listed below with descriptions and corresponding components. Blocks 2 and 3 must be repeated every time when the velocities and depths are updated in the model, i.e. every time step of the one-dimensional flow model. Therefore, the data in this file need to be adjusted on a more regular basis.

If the format or column numbers are shown, the data must be formatted accordingly. Otherwise it is necessary to have only one space or comma between the data.

For the Ohio–Monongahela–Allegheny river system, the difference in branch configuration between the oil spill model and the unsteady flow model is built into the oil spill model through subroutine *ohndc*. The number of branches in this data file is the same as the number of branches in the unsteady flow model. The discharges and water levels at the nodes of the branches of this data file should be interpolated to the cross sections of the oil spill model. If the two models have the same number of branches, then subroutine *ohndc* should be changed to the following three lines, which are already in the program. These lines are presently given as comments, which can easily be activated:

```
do 230 i=l, nsect
read(7,*) wlsct(i), qsct(i)
230 continue
```

ohmon.flo: Block 1, time step in one-dimensional model

Card 1
Example:
6.0

Variable name	*Type and length*	*Column number*	*Description*
ufdt	Real	–	Unsteady flow time step (hr)

Card 2 (Comments line)
Example:
branch qu qd hu hd region 1 1/1/88 hour=0.0

These are the variable name, date and time of the data to be given in the following block.

ohmon.flo: Block 2, discharge and water level.

Card 1 (one card for one branch)
Example:

```
1   52810.  52810.  625.19  625.00
2   51761.  52810.  625.25  625.19
```

Variable name	*Type and length*	*Column number*	*Description*
i	Integer	–	Branch number for checking
qu(i)	Real	–	Discharge at upstream end of each branch (cfs)
qd(i)	Real	–	Discharge at downstream end of each anch (cfs)
wu(i)	Real	–	Water level at upstream end of each branch (ft)
wd(i)	Real	–	Water level at upstream end of each branch (ft)

Note: Card 1 needs to be repeated as many times as the number of branches of this river segment.

ohmon.flo: Block 3, ice conditions (thickness information)

Card 1
Example:
1

Variable name	*Type and length*	*Column number*	*Description*
icinfo	Integer	–	Number of cross sections with ice-covered condition. If no ice-covered section exist, set icinfo =1 and then in card 2, define the section to be open

Card 2
Example:
2 open

Variable name	*Type and length*	*Column number*	*Description*
is	i4	–	ID number of the cross section with ice-covered conditions
word	a4	–	Cross-section ice cover condition, "full" = fully covered, "part" = partially covered, "open" = open water. If word = "full," then the card has only one value and that is the ice thickness across the river for that *x*-section. If word = "part," then card 3 must have an ice thickness defined at each vertical line defining the *x*-section = nslsct(is). If all numbers don't fit into one card, as many cards as necessary may be used.

Card 3 (for fully covered cross section)
Card 3 must follow every card 2 if word = "full" or "part." If word = "open," card 3 is not needed.

Example:
0.6

Variable name	*Type and length*	*Column number*	*Description*
fulti	Real	–	Ice thickness (ft) of fully covered cross section. Only one value is read as input, and it will be assigned to the entire cross section

Card 3 (for partially covered cross section)
Example:
0.3 0.4 0.5 0.5 0.4 0.2

Variable name	*Type and length*	*Column number*	*Description*
tice(i,j)	Real	–	Ice thickness (ft) of partially covered cross section. There must be one value for each sounding depth of the cross section with one additional value for the extreme left of the cross section where depth sounding is not input through data because it is always assumed to be zero

Note: Block 2 followed by 3 must be repeated for every one-dimensional unsteady flow time step.

This is the end of data file *ohmon.flo*.

Boundary grid data: ohmon.igr

ohmon.igr: Block 1, boundary grid boxes

Card 1
Example:
343 121 130 125 125

Variable name	*Type and length*	*Column number*	*Description*
i	i4	–	*x*-grid box number
igrilb(i)	i5	–	*y*-direction grid box number of lower river boundary for i^{th} *x*-grid (water-side grid)
igriub(i)	i5	–	*y*-direction grid box number of upper river boundary for i^{th} *x*-grid (water-side grid)
igrlb(j,i)	i5	–	*y*-direction grid box number of lower boundary of j^{th} island for i^{th} *x*-grid (land-side grid)
igrub(j,i)	i5	–	*y*-direction grid box number of upper boundary of j^{th} island for i^{th} *x*-grid (land-side grid)

Note: Block 1 must repeat ntogridx (no. of grids in *x*-direction) times.

This is the end of data file *ohmon.igr*.

Shoreline boundary condition data: ohmon.bnd

The *ohmon.bnd* file consists of three blocks of information. All blocks are listed below with components and description. Most of the data read into the model are in free format. If the format or column numbers are shown, the data must be formatted accordingly. Otherwise it is necessary to have only one space or comma between the data. All files with the *bnd* extension follow the same format.

ohmon.bnd: Block 1, half-life index.

Card 1 (one card for each range of grid boxes)
Example:
1 1 81 1

Variable name	*Type and length*	*Column number*	*Description*
k	Integer	–	Shore number. Lower *y* (river) = 1; upper *y* (river) = 2; lower *y* (first island) = 3; upper *y* (first island) = 4; etc.
lfrom	Integer	–	Beginning limit (grid box number) for half-life designation to shore
lto	Integer	–	Ending limit (grid box number) for half-life designation to shore
icode	Integer	–	Integer identifying which of the 16 half-life values are to be assigned to a grid; for determining the value for lock and dams, refer to Figures 15 and 16

Card last (must be included)

0 0 0 0

This is the end of data file *ohmon.bnd*.

Oil spill data, ohmon.spl

The *ohmon.spl* file consists of two blocks of information with a varying or constant number of cards in each block. All blocks are listed below with the components and description. Most of the data read

into the model are in free format. If the format or column numbers are shown, the data must be formatted accordingly. Otherwise it is necessary to have only one space or comma between the data. All files with the *spl* extension follow the same format.

ohmon.spl: Block 1, Oil spill and simulation parameters.

Card 1 (river name—for identification only)
Example:
Ohio Monongahela

Variable name	*Type and length*	*Column number*	*Description*
text	a20	–	Any text to identify the river system

Card 2 (Type of oil, for identification only)
Example:
Fuel No. 2

Variable name	*Type and length*	*Column number*	*Description*
fueltp	a20	–	Text for identifying the oil type

Card 3
Example:
24.0 4 1 1 1 0 1800.0 –1.0

Variable name	*Type and length*	*Column number*	*Description*
totime	Real	–	Time of oil spill simulation (hr)
ievery	Integer	–	Frequency of obtaining output from simulation results from ohmon and plotter. For example, if ievery = 4, output is written every four time steps
ipot1	Integer	–	Two options: one (1) results in output of fixed data, such as cross-section geometry data and shoreline conditions; zero (0) results in no output
ipot2	Integer	–	Two options: one (1) results in output of computed velocities to a data file for plotting; zero (0) results in no printout
ipot3	Integer	–	Two options: one (1) results in output of particle location to a data file for plotting; zero (0) results in no printout
ipot4	Integer	–	Two options: one (1) results in output of number plot of particle distribution to a data file for plotting; zero (0) results in no printout
spltim	Real	–	Duration of oil spill in seconds. If = 0, the spill will be treated as instantaneous; otherwise it will be continuous
diffur	Real	–	Horizontal diffusion coefficient (ft^2/s) for river. If the default formulation is desired, set this value to –1.0

Card 4
Example:
400 705000. 900. .84 1.411e–5 7.55e–4 1.14 1.1 1.6 1.4 1.4 1.4

Variable name	*Type and length*	*Column number*	*Description*
ntotal	Integer	–	Number of parcels defined in each layer at the beginning of the simulation (currently 400)
spvol	Real	–	Total volume of oil spilled (gal.)
spgoil	Real	–	Specific gravity of oil
aniu	Real	–	Kinematic viscosity of water (ft^2/s)
sigma	Real	–	Surface tension of oil (lb/ft)
ak2i	Real	–	Fay's gravity–inertia phase spreading coefficient (axisymmetrical)
ak2v	Real	–	Fay's gravity–viscous phase spreading coefficient (axisymmetrical)
ak2t	Real	–	Fay's surface tension–viscous spreading coefficient (axisymmetrical)
akc10	Real	–	Fay's or Waldman's gravity–inertia spreading phase coefficient (one-dimensional)
akc20	Real	–	Gravity–viscous phase spreading coefficient (one-dimensional)
akc30	Real	–	Surface tension–viscous phase spreading coefficient (one-dimensional)

Card 5
Example:
342650. –97800. .7063e–2 .1873e–2 7.88 465.0

Variable name	*Type and length*	*Column number*	*Description*
spx	Real	–	*x*-coordinate of spill site (ft)
spy	Real	–	*y*-coordinate of spill site (ft)
vmuni	Real	–	Molar volume of oil (ft^3/mol)
soluni	Real	–	Solubility of fresh oil (lb/ft^3)
cevp	Real	–	Coefficient C of evaporation characteristics of oil
toevp	Real	–	Boiling point temperature of oil (K). If you define a value of less than 1.0 for toevp, the program will define the evaporation characteristics, using fitted curves. Therefore, the input values of cevp and toevp have no influence on computations, although they are read

ohmon.spl: Block 2, wind and temperature data.

Card 1 (1 card for each time step
Example:
0.2 11.80 21.50 24.00

Variable name	*Type and length*	*Column number*	*Description*
vwc	Real	–	Empirical coefficient for modifying the wind speed on land to that on river
vwmag	Real	–	Wind speed (ft/s)
theta	Real	–	Wind direction (angle measured clockwise from the north in degrees)
tenvf	Real	–	Air temperature (°F)

Note: Card 5 must be repeated for every time step of the simulation.

This is the end of data file *ohmon.spl*.

Bridging data between the unsteady flow model and the oil spill model: ohmon.ndc

The *ohmon.ndc* file consists of two blocks of information with a varying or nonvarying number of cards in each block. All blocks are listed below with the components and description. Most of the data read into the model are in free format. If the format or column numbers are shown, the data must be formatted accordingly. Otherwise it is necessary to have only one space or comma between the data. All files with the *ndc* extension follow the same format.

ohmon.ndc: Block 1, stream-tube cross-section distribution

Card 1 (Comments)
Example:
Region 1: part 1

Variable name	*Type and length*	*Column number*	*Description*
dummy	a4	–	Dummy variable for skipping a line in the data file

Card 2
Example:
5 1 45

Variable name	*Type and length*	*Column number*	*Description*
j	Integer	–	Branch number in this river segment
ns	Integer	–	Number of stream-tube cross sections in this branch
jar(j)	Integer	–	List of numbers of all stream-tube cross sections in the branch

Note: Card 2 must repeat for all branches in this segment.

ohmon.ndc: Block 2, location of stream-tube cross sections

Card 1
Example:
2 2.11 1 0.09

Variable name	*Type and length*	*Column number*	*Description*
j	Integer	–	Cross-section number
ihup	Integer	–	Number of upstream unsteady flow node
xup	Real	–	Distance between cross section and upstream node
ihdp	Integer	–	Number of downstream unsteady flow node
xdp	Real	–	Distance between cross section and downstream node

Note: Card 2 must repeat as many times as the number of cross sections in this river segment.

Repeat blocks 1 and 2 as many times as the number of river segments. This is the end of data file *ohmon.ndc*.

Miscellaneous data: ohmon.msc

The *ohmon.msc* file consists of two blocks of information with a varying or nonvarying number of cards in each block. All blocks are listed below with the components and description. Most of the data read into the model are in free format. If the format or column numbers are shown, the data must be formatted accordingly. Otherwise it is necessary to have only one space or comma between the data. All files with the *msc* extension follow the same format.

ohmon.msc: Block 1, some miscellaneous data.

Card 1 (Bank rejection options)
Example:
inst

Variable name	*Type and length*	*Column number*	*Description*
rejp	a4	–	Bank rejection parameter; for instantaneous rejection, = "inst;" if = "full," then the oil deposited on the shoreline during each time step will be rejected completely at the end of the time step; for other rejection rates, = "part"

Card 2 (Output options)
Example:
0

Variable name	*Type and length*	*Column number*	*Description*
ipropt	Integer	–	Two options: larger than 1, output grid locity, stream-tube velocity to data files for plotting; less than 1, no output to data files

Card 3
Example:
1.0

Variable name	*Type and length*	*Column number*	*Description*
alpha	Real	–	Resurfacing coefficient, a; if all particles that rise to the surface layer stay in surface layer, = 1; otherwise, less than 1.0

Card 4
Example:
1.e–5

Variable name	*Type and length*	*Column number*	*Description*
beta	Real	–	Deposition coefficient

Card 5
Example:
0.001

Variable name	*Type and length*	*Column number*	*Description*
gama	Real	–	Emulsification coefficient (1/s)

Card 6
Example:
0.028

Variable name	*Type and length*	*Column number*	*Description*
amngn	Real	–	Manning's coefficient of riverbed

Card 7
Example:
32.2

Variable name	*Type and length*	*Column number*	*Description*
gravac	Real	–	Gravitational acceleration (ft/s^2)

Card 8
Example:
0.01

Variable name	*Type and length*	*Column number*	*Description*
vbuoy	Real	–	Buoyant velocity (ft/s)

Card 9
Example:
1.1

Variable name	*Type and length*	*Column number*	*Description*
alpc	Real	–	Coefficient for converting depth-averaged velocity to surface velocity, a_c

Card 10
Example:
0.03

Variable name	*Type and length*	*Column number*	*Description*
alpw	Real	–	Wind effect coefficient on water surface velocity, a_w

Card 11
Example:
0.5 0.5

Variable name	*Type and length*	*Column number*	*Description*
ratsur	Real	–	Fraction of oil spilled on water surface
ratsus	Real	–	Fraction of oil spilled in the suspended layer

Card 12
Example:
0.3

Variable name	*Type and length*	*Column number*	*Description*
alevp	Real	–	Coefficient for modifying evaporation due to emulsification, a_E

Card 13
Example:
1000 200.

Variable name	*Type and length*	*Column number*	*Description*
ntxgrid	Integer	–	Total x-grid of moving grids
dx	Real	–	Grid size (ft)

Card 14
Example:
5

Variable name	*Type and length*	*Column number*	*Description*
nr	Integer	–	Total number of river segments

ohmon.msc: Block 2, coordinate transformation information.

Card 1
Example:
129.

Variable name	*Type and length*	*Column number*	*Description*
s0	Real	–	River mileage of the downstream boundary of the study reach

Card 2
Example:
0.0 0.0 348200.0 144000.

Variable name	*Type and length*	*Column number*	*Description*
xmin(i)	Real	–	Minimum x-coordinate of i^{th} river segment
ymin(i)	Real	–	Minimum y-coordinate of i^{th} river segment
xmax(i)	Real	–	Maximum x-coordinate of i^{th} river segment
ymax(i)	Real	–	Maximum y-coordinate of i^{th} river segment

Card 3
Example:
0.0 0.0 0.0

Variable name	*Type and length*	*Column number*	*Description*
x0(i)	Real	–	x-origin (coordinate) of the i^{th} local coordinate system
y0(i)	Real	–	y-origin (coordinate) of the i^{th} local coordinate system
beta0(i)	Real	–	Rotation angle of the i^{th} local coordinate x positive with global x positive; "–" for clockwise and "+" for counterclockwise

Card 4
Example:
1741 46.

Variable name	*Type and length*	*Column number*	*Description*
ngrid(i)	Integer	–	Maximum *x*-grid number in the i^{th} river segment
sbrn(i)	Real	–	River mileage at the end of the i^{th} river segment

Note: Repeat cards 3 and 4 times as many times as the number of river segments.

This is the end of data file *ohmon.msc*.

Input adjustments

For a river that already has the necessary input files, very little modification in input is needed to run the model with different field conditions, such as new river discharge, different oil properties, new spill location, etc. Input data that are most likely to require modification are cited below with some guidelines and suggested values. Readers should refer to the preceding section for the format of the data.

Velocity

Interpolating stream-tube velocities to boxes depends on the variable kintm (*ohmon.geo*, Block 1, Card 1) and ibend(i) (*ohmon.geo*, Block 2, Card 1). As kintm increases, more velocity interpolations are made between cross sections. If the cross sections are spaced far apart, kintm should be in the range of 5–8 or more; otherwise kintm can be 5 or less. The problem with using too small a value for kintm is that more grid boxes will end up without assigned velocities after the interpolation stage. They will be assigned a velocity based on their neighboring boxes. This is less accurate than assigning a velocity based on interpolation. One should try to assign as many boxes as possible in the interpolation stage. On the other hand, if the value of kintm is too large, it will take more computation time. Besides the value of velocities, appropriate simulation of the direction of velocity is also important. Ibend(i) supplies two options for determining velocity directions. When ibend(i) = 0, the velocity will be along the line connecting two corresponding stream-tube centers in neighboring cross sections. This usually gives a fairly accurate flow direction. However, for cross sections in a river bend, as shown in Figure 26, ibend(i) should be 1. This makes the velocity direction perpendicular to the cross section.

Another factor that affects assigning velocities to grid boxes is the number of stream tubes selected. The choice of the number of stream tubes (nstube, *ohmon.geo*, Block 2, Card 1) will affect the computer time and the accuracy. For a river with highly irregular cross sections or when a high degree of accuracy is required, more stream tubes should be used.

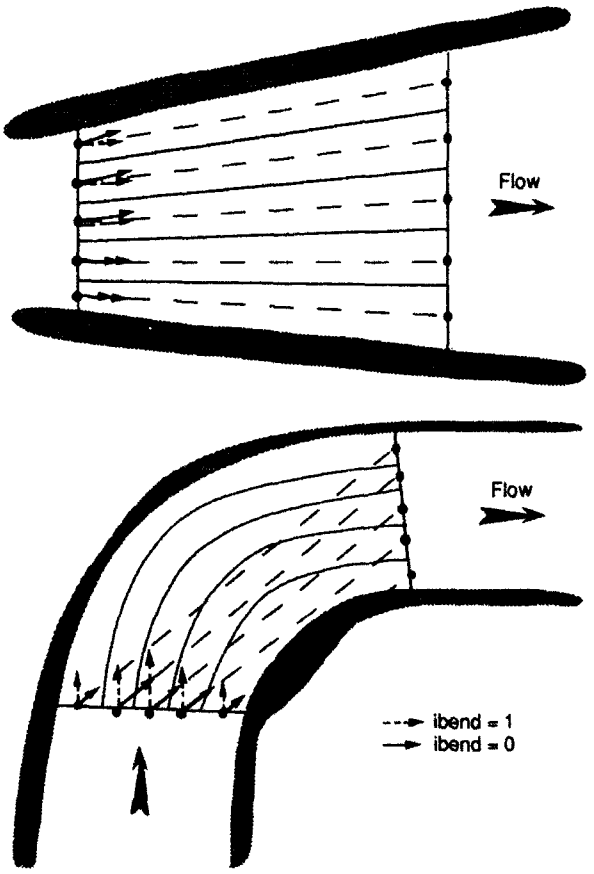

Figure 26. Simulation of flow direction in stream tubes.

Stage-discharge data

Stage and discharges (*ohmon.flo*, Block 1, Card 2) in river branches are unlikely to remain constant over time. Therefore, this information will require updates as the need arises. The one-dimensional unsteady flow model can be used to obtain this information.

Oil spill parameters

The oil spill parameters (*ohmon.spl*, Block 1, Cards 2, 3, 4, 5) will require the most modification from spill to spill. Each spill will have its own simulation duration, simulation time step, printing options, number of particles, volume, physical properties and location, so it will be necessary to adjust these data each time the simulation is done for a new spin. The suggested guidelines for these parameters follow.

The initial total particle number, ntotal, is about 500; a maximum of 1000 is possible in the current version. During the simulation the number may increase to several thousand because of the exchange between the two layers. A larger particle number will give a better result at the expense of a longer execution time. The time step suggested for spildt is 900 s (15 minutes).

For other spill parameters the following values may be used:

spgoil = 0.7–0.98
aniu = 1.411×10^{-5} ft^2/s (at 50°F)
sigma = 2.06×10^{-5} (lb/ft)
ak2i = 1.14
ak2v = 0.98
ak2t = 1.6
akc10 = 1.39
akc20 = 1.39
akc30 = 1.43
vmnui = 0.7063×10^{-2} (ft^3/mol)
soluni = 0.1873×10^{-2} (lb/ft^3).

Wind data

The computer model reads the wind data (*ohmon.spl*, Block 2, Card 1) at each time step. This allows for changing the wind speed and direction in the simulation. A correction is needed because the wind speed on land and that on the river are different. If no better information is available, a value of 0.2 may be used for vwc (*ohmon.spl*, Block 2, Card 1).

Sample input data files

All file names to be opened for input and output will be in the file *ohmon.fnm*. Sample input data files included in this section are:

1. *ohmon.geo*
   River geometry, cross sections and branch geometry of the Ohio–Monongahela rivers.
2. *ohmon.igr*
   Boundary grid data for the Ohio–Monongahela rivers.
3. *ohmon.ice*
   Ice parameters, ice regions and ice thickness in the Ohio–Monongahela rivers. This file is needed even when the model is run for open-water conditions. Samples will be given for the ice-covered condition and the open-water condition.
4. *ohmon.flo*
   Water level and discharge at nodes from the unsteady flow model for the Ohio–Monongahela rivers.
5. *ohmon.bnd*
   Half-life index for shoreline grids of the Ohio–Monongahela rivers.

6. *ohmon.spl*
   Oil parameters, spin location, wind condition and ambient air temperature.
7. *ohmon.ndc*
   Information for converting unsteady flow computation results to what are needed in oil spill model flow computation for the Ohio–Monongahela rivers.
8. *ohmon.msc*
   River division data, exchange parameters for the two layers and information for coordinating transformation data for the Ohio–Monongahela rivers.

```
ohmon.fnmThu    Jan 24 08:59:15    1991 1

ohmon.fnm:
----------

  1ohmon.geo
  2oilprt.out
  7ohmon.flo
  8ohmon.bnd
  9ohmon.ndc
  11ohmon.sur
  13ohmon.sus
  12ohmon.spl
  14ohmon.ice
  20ohmon.msc
  22concen.dat
  29ohmon.igr
  28vel.pos
  30dep.pos
-------------------------------------

ohmon.geo:
----------

  24  16                                region 1
  12  22  32  44  45  64  89  104 108 121  131  138  139  141  150  165  177   194 204 208
  210 218 228 233
  1  16840.66   7741.73   -0.44720  0.89443     11      11       2       0    0.0     0
  2  18925.39   7018.47   -0.44720  0.89443     11      11       1       0    0.0     0
  3  20144.21   8923.44   -0.56714  0.82362     11      11       2       0    0.0     0
--------

  1        10
  0.0   660.0     540.0      660.0    540.0  596.0  600.0  596.0  650.0 596.0
  700.0 596.0     800.0      596.0    900.0  596.0  900.0  660.0 1274.0 660.0
  2        20
  0.0   665.0    1200.0      665.0   1280.0  660.0 1380.0  625.0 1659.0 625.0
  1800.0616.0    1900.0      594.0   2200.0  594.0 2420.0  580.0 2770.0 581.0
  2940.0583.0    3080.0      590.0   3140.0  590.0 3240.0  606.0 3300.0 606.0
  3380.0633.0    3830.0      635.0   3870.0  640.0 4030.0  645.0 4500.0 665.0
--------

  0
  23  5   region 2
```

ohmon.igr Thu Jan 24 09:01:241991 1

ohmon.igr

```
 1  15  19
 2  15  19
 3  15  19
 4  15  19
 5  14  19
 6  14  19
 7  14  19
 8  14  19
 9  14  19
10  14  19
11  14  19
12  14  19
13  14  19
14  14  19
15  14  19
16  14  20
17  14  20
18  14  20
19  14  20
20  14  20
21  14  21
22  15  22
23  15  22
24  15  23
25  15  23
26  16  23
```

ohmon.ice:

```
    0.035  0.84
0
    0.035  0.84
0
    0.035  0.84
0
    0.035  0.84
0
    0.035  0.84
0
    0.035  0.84
0
    0.035  0.84
0
    0.035  0.84
0
    0.035  0.84
0
    0.035  0.84
0
    0.035  0.84
```

```
  0
     0.035  0.84
  0
     0.035  0.84
  0

ohmon.floThu Jan 24 09:03:01   1991     1

ohmon.flo:
---------

   6.0 flow time step
branch    qu  qd  hu  hd region 1    1/   1/88 hour = 0.
   1   52810. 52810. 625.19 625.00
   2   51761. 52810. 625.25 625.19
   3   50721. 51761. 625.37 625.25
---------
  23  48876. 48878. 669.09 668.89
  24  48877. 48876. 669.30 669.09
   1
   2   open
branch    qu  qd  hu  hd region 2    1/   1/88 hour = 0.
   1   48877. 48876. 669.30 669.09
   2   48860. 48877. 669.45 669.30
   3   48850. 48860. 670.50 669.45
   4   48460. 48850. 670. 87    670.50
-------------------

-------------------------------------------------

ohmon.bnd:
---------

   1   1   81  1
   2   1   81  2
   1   82  84  2
   2   82  84  2
   3   82  84  2
   4   82  84  2
   1   85  34  2
   2   85  34  2
   1   343 358 2
   2   343 358 2
   3  343                              358        2
   4  343                              358        2
   1  359                              530        1
   2  359                              530        1
   1  531                              532        2
   2  531                              532        2
   3  531                              532        2
   4  531                              532        2
   1   533 536 1
   2   533 536 1
   1   537 538 2
   2   537 538 2
   3   537 536 2
   4   537 538 2
   1   539 740 1
   2   539 740 1
```

ohmon.splThu Jan 24 09:04:27 1991 1

ohmon.spl:

```
Ohio Monongahela
  No. 2 Fuel oil
240.0      288        1         1         1       03600.  -1.0       totime, ievery,
  400 705000.0      300.        84 1.411E-5 7.55E-4  .14   1.1   1.6   1.4  1.4 1.4
342650.-97800..7063E-02.1873E-02      7.88   465.0
  0.2     11.80   210.50    24.00
  0.2      4.21   100.50    20.00
  0.2      0.00     0.00    17.50
  0.2      2.53    40.50    15.50
  0.2      2.53    40.50    14.50
  0.2      0.00    00.00    18.00
  0.2      0.00    00.00    25.00
  0.2      3.37    60.50    29.50
  0.2      3.37    60.50    30.50
  0.2      2.53    90.00    29.50
  0.2      7.59   200.50    28.50
  0.2     10.96   230.00    28.00
  0.2     14.33   230.S0    27.50
  0.2     28.66   240.50    27.00
  0.2     36.25   250.50    27.50
  0.2     37.93   280.00    25.50
  0.2     33.72   280.S0    19.50
  0.2     26.13   270.50    13.50
  0.2     25.29   280.00     9.00
```

ohmon.ndc:

```
  Region 1:part 1
  1   12    1    2    3    4    5    6    7    8    9   10    11 12
  2   10   13   14   15   16   17   18   19   20   21   22
  3   10   23   24   25   26   27   28   29   30   31   32
  4   12   33   34   35   36   37   38   39   40   41   42    43 44
  5    1   45

  22   8  211  212  213  214  215  216  217  218
  23  10  219  220  221  222  223  224  225  226  227  228
  24   6  229  230  231  232  233  234
  Next we have located x-section
  1    2 2.11    1 0.09
  2    2 2.00    1 0.20


  231       25 2.50         24 1.00
  232       25 2.04         24 1.46
  233       25 1.50         24 2.00
  234       25 1.02         24 2.48
  Region 2: part 1
  1    8    1    2    3    4    5    6    7    8
```

```
ohmon.msc  Sun Jan 20 16:42:57    1991 1

part       full for rejrat = 1 ,inst for inst. rej., part for calculated;
0          =ipropt, >1 output vel. and depth in grid, opposite in inverse.
1.         =alpha, resurfacing
1.e-5           =beta, deposition
0.00001              =gamma, emulsification
0.028      =amngn
32.2       =gravac
0.01            =vbuoy
1.1        =alpc
0.03       =alpw
0.8        0.2  =ratsur, ratsus
0.2        =alevp, evap. modified coeff.
1000       200.      =ntxgrid, dx the x-grid number of working length
5          =nr
129.                                        s0
0.         0.         348200.    144000.    xmin,ymin,xmax,ymax
0.         0.         0.                    x0,y0,beta0
1741       46.                          ngrid(1), sbrn(1)
348200.    -36800.    432000.    139200.    xmin,ymin,xmax,ymax
348200.    139200.    -90.                  x0,y0,beta0
2621       0.0                          ngrid(2), sbrn(2)
378400.    -84800.    400000.    -36800.    xmin,ymin,xmax,ymax
378400.    -36800.    -90.                  x0,y0,beta0
2861       -11.5                        ngrid(3), sbrn(3)
315800.    -132000.   392400.    -84800.    xmin,ymin,xmax,ymax
392400.    -84800.    -180.                 x0,y0,beta0
3244       -40.5                        ngrid(4), sbrn(4)
52000.     -220000.   315800.    -104600.   xmin,ymin,xmax,ymax
315800.    -104600.   -180.                 x0,y0,beta0
4563       -132.                        ngrid(5), sbrn(5)
2288       3288
```

Additional input

Besides the input data files mentioned above, there are two additional sets of data to be input on the screen after the start of the simulation.

River combinations

The model is designed to simulate spills that occur either in the Monongahela River or in the Allegheny River. After the user starts running the oil spill model, the screen will show:

```
**************************************
* select river combination:          *
* for Ohio-Monongahela River input: 1 *
* for Ohio-Allegheny River input:   2 *
```

Choose 1 for an oil spill in the Monongahela River or 2 for a spill in the Allegheny River. If the spill is in the Ohio River, choose either 1 or 2. However, 2 will make take less computing time, since the data files on the geometry and shoreline boundary conditions are smaller.

Continuation runs

The model can be used either for a simulation from the beginning of a spill or for continuing a previously stopped simulation. The user will be required to choose from these two options after choosing the river combination. The screen will show the following:

```
*****************************************
* The model can be run from t = 0 or    *
* restarted after a stop                *
* Enter 0 or 1 and hit return           *
* 0 for a run starting from t = 0       *
* 1 to start from a previously stopped point *
* ------------------------------------- *
```

MODEL OUTPUTS

Output from the model can be directed to different devices, such as a console, a printer or files.

Velocity and depth distributions

Flow velocity and depth, both along the stream tubes and in the grids, are calculated in subroutine *veldep*. If needed the user can choose the printout option (ipropt> 1, *ohmon.int*, Block l, Card 2) to save all simulation results into corresponding files.

- *strm.vel:* Save coordinate (x,y) and velocity (v_x, v_y) at stream-tube locations.
- *strm.dep:* Save coordinate (x,y) and depth (h) at stream-tube locations.
- *grid.vel:* Save coordinate (x,y) and velocity (v_x, v_y) at grid box locations.
- *grid.dep:* Save coordinate (x,y) and depth (h) at grid box locations.

All of these data are used in advection and mixing calculations. They cannot be saved in the microcomputer version because of the limitation on the number of files to be opened. The arrangement of data files is shown as follows:

Data card of velocity for grids and stream tubes:

x y v_x v_y

Data card of depth for grids and stream tubes:

x y h

where coordinates and depth are in feet and velocity is in feet per second.

The cards for velocity and depth are repeated as many times as the distribution points. In this model, only the velocities and depths within the moving grid at each flow time step will be saved into files to save memory and computer time.

Simulation results

Oil spill simulation results will be output to files on the selected output frequency (ievery, *ohmon.spl*, Block 1, Card 2). These results include the following files:

- *oilprt.out:* Spill site and oil parameters. A summary of distributions of the oil, including updated total volume (for checking purposes), volume in the surface layer, volume in the suspended layer, total volume evaporated and oil evaporated in the current time step, total volume dissolved and volume dissolved during this time step, volume on land, volume deposited onto the riverbed, and volume emulsified and resurfaced.
- *ohmon.sur:* Locations and volumes of surface oil particles, including updated total particle number and the center of slick.

ohmon.sur: Block 1

Card 1
Example:
Ohio Monongahela Surface No. 2 Fuel Oil

Variable name	*Type and length*	*Column number*	*Description*
text	a20	11	River name
sur	a14	31	Indicate results of surface slick
fueltp	a20	45	Name of spilled oil

Card 2
Example:
881.25

Variable name	*Type and length*	*Column number*	*Description*
vave		–	Average volume of particles both on surface and in suspension at the beginning for graphics purpose (gal.)

Card 3
Example:
400 705000. 900. 0.81 0.141E–04 0.755E–03 0.706E–02 0.187E–02 0.000E+00

564000.000 141000.000 342650 –97800

Variable name	*Type and length*	*Column number*	*Description*
ntotal	Integer	–	Total number of particles defined in each layer (e.g. 400)
spvol	Real	–	Total volume of oil spilled
spgoil	Real	–	Specific gravity of oil
aniu	Real	–	Kinematic viscosity of water (ft^2/s)
sigma	Real	–	Surface tension of oil (lb/ft)
vmuni		–	Molar volume of oil (ft^3/mol)
soluni		–	Solubility of fresh oil (lb^5/ft^3)
amuni		–	Absolute viscosity of oil ($lb/ft^{2)}$
		–	Total volume of oil on water surface at the beginning of spill (gal.)
		–	Total volume of oil in suspension at the beginning of spill (gal.)

ohmon.sur: Block 2

Card 1
Example:
342650 –97800

Variable name	*Type and length*	*Column number*	*Description*
ipartx(1)	i8	–	*x*-coordinate of the spill site (ft)
iparty(1)	i8	9	*y*-coordinate of the spill site (ft)

Card 2
Example:
2300 391145 –77512 24.0000 –1.6 –0.5

Variable name	*Type and length*	*Column number*	*Description*
nwt1	Integer	–	Total number of surface oil particles at the present time
ipartx(1)	i8	–	*x*-coordinate of surface slick center (ft)
iparty(1)	i8	9	*y*-coordinate of surface slick center (ft)
ttt	Real	–	Completed simulation time (hr)
vwx	Real	–	Present *x* component of wind speed (mph)
vwy	Real	–	Present *y* component of wind speed (mph)

Card 3
Example:
391163 –85810 538.35 391160 –85399 150.81 391185 –84711 163.11391370

–85965 132.45

This card has four sets of values [x,y, vopsur(i)] to indicate the coordinates and volume of each particle; *x* and *y* in are in feet, and the volume of the i^{th} surface particle vopsur(i) is in gallons. This card will repeat for all particles.

Block 2 will be repeated as many times as desired output times.

- *ohmon.sus:* Locations and volumes of suspended oil particles, including the updated total particle number and the spill center. The output format is the same as *ohmon.sur.*
- *concen.dat:* One-dimensional cross-section averaged concentration distribution (including the surface layer and the suspended layer), indicating the volume concentration at different river miles.

concen.dat: Block 1

Card 1
Example:
& time, i0, dis0= 24.0000 2059 33.9545

where & is for a graphics purpose; time is the total length of the completed simulation (hr); i0 is the initial *x*-grid number of the moving grids; dis0 is the river mile of the downstream edge of the moving grids (mile).

Card 2
Example:
2.827 0.5278E-02

Variable name	*Type and length*	*Column number*	*Description*
dis	Real	–	River mile at which cross-section-averaged volume concentration is calculated
conc2	Real	–	Volume concentration at river mile distance (10^{-3})

Block 1 will be repeated as many times as the designed output number.

- *concen.sur*: One-dimensional surface concentration distribution, indicating the volume concentration at different river miles along the river. This file will not be available in the output for a microcomputer. The format of this file is the same as *concen.dat*.

The graphics output that corresponds to these outputs can be obtained by using the graphics program.

Sample output files

```
oilprt.out   Wed Jan 30 11:53:42    1991 1

oilprt.out:
-----------

1 Ohio Monongahela

                ******************
               *continuous spill*
               *at               *
               *342650.,-97800.  *
               *for 60. min.     *
                ******************
simulation period  =  240.0 hrs
-------------------------------------

characteristics of spill

no. of particles          : 400
oil spilled               : 705000. gals of No. 2 Fuel Oil
dt for spill simulation   : 300. secs.
specific gravity of oil   : 0.84 (api index = 37.0)
kinematic visco. of water: 0.1411E-04 sq ft/sec
surface tension           : 0.7550E-03 lbs/ft

  spreading coefficients
  k2i       k2v       k2t       c10       c20       c30
 1.14      1.10      1.60      1.40      1.40      1.40

molar volume              : 0.7063E-02 cu ft/mol
solubility of fresh oil   : 0.1873E-02 lbs/cu ft
viscosity of oil          : 0.00 gms/cm-sec
Manning's roughness of ice:0.000
```

```
api option is not selected--evap. constants are  c=   7.88 t0= 465.0

surface diffusion--default formulation is used

time, i0, iend, nhitb=
  8.00   2064   3064   1346

slick condition at the end of this time step

total volume (cu. ft) = 94244.5

total volume on land (cu. ft) = 44775.

total on surface = 46411.  total in suspension = 714.53

evaporation (cu. ft) this step = 18.694total evap.(cu. ft) = 2222.5

dissolved this step =    0.58905   total =    29.087
total resurfacing (cu. ft) = .12147E+06
total deposition (cu. ft) = 121.39
total emulsification (cu. ft) = 13582.
total out of range on surface (cu. ft = .66263E-02
total out of range in suspended (cu. ft) = .54000E-02

concen.dat   Thu Jan 24 09:12:37    1991 1

concen.dat:
```

```
6 time,  i0, dis0=  24.0000    2059     31.5455
    0.4180 0.5278E-02
    0.3801 0.1285E-03
    0.3378 0.1198E-01
    0.2152 0.6928E-04
    0.1616 0.4378E-01
    0.1193 0.1687E-01
0.7693E-01 0.3473E-01
0.2336E-01     0.1634
-0.1899E-01    0.1171
-0.7256E-01    0.3773
   -0.1261     0.1599
   -0.1944 0.9520E-01
   -0.2627 0.7579E-01
   -0.8132 0.7076E-01
   -0.85C6 0.7076E-01
   -0.9576      1.052
    -1.060 0.9058E-01
    -1.128     0.1246
    -1.213     0.2245
    -1.281      3.160
    -1.869      1.859
    -1.937      2.506
    -2.006      1.563
    -2.059      2.579
    -2.113      4.183
    -2.166 0.9436E-01
    -2.274 0.4299E-03
    -2.327      2.119
    -2.381 0.1234E-04
    -2.419      1.403
    -2.472 0.1794E-01
```

```
    -2.510      0.6395
    -2.564      0.1667
    -2.602      0.3221
    -2.639      0.2070
    -2.677      0.1014
    -2.715 0.5485E-01
    -2.753 0.6229E-01
    -2.791 0.7658E-01
    -2.833      0.1138
    -2.871 0.4878E-01
    -2.909 0.1256E-01
    -2.947 0.2762E-01
    -3.000 0.5685E-01

ohmon.surThu   Jan 24    09:10:02      1991          1

ohmon.sur:
```

Ohio Monongahela Surface No. 2 Fuel Oil

```
   881.250
400   705000.    300.   0.84    0.141E-04    0.75'E-030.706E-02    0.187E-020.000E+00
564000.000   141000.00
 342650  -97800
   3228  383560  -63631  24.0000      0.3     -1.7
 385603  -55130  127.61   385022  -55737  151.35  384943  -55816  122.80 385406  -55514  137.42
 385453  -55484   90.32   385005  -55790  130.41  384217  -56667  167.51 384269  -56384  102.60
 384204  -56198  145.88   384541  -S5888   99.56  385486  -55416  225.97 384341  -56130  230.82
 384681  -55980  115.19   384548  -56119  218.39  384121  -56382   91.33 384184  -56360  162.97
 384164  -56405   92.04   384390  -56438  167.40  384514  -S6237  216.95 384947  -55902  149.75
 384212  -56492  115.06   383893  -56521  114 22  384098  -56850   92.86 384082  -56556  170.92
 383831  -56706  102.75   384108  -56482  108.71  384059  -56695  209.84 383949  -56903  500.66
 383958  -56767  121.98   384161  -56739  100.85  383714  -57187  114.55 384053  -56653  131.79
 383848  -57152   91.06   383700  -57115  100.12  383734  -56833  118.72 384327  -56450  119.88
 384393  -56345  132.88   383628  -57093  152.93  383296  -57726  301.19 383217  -57443  321.61
 385530  -55327   90.76   383568  -57324  304.25  384432  -56297   96.78 383300  -57414  192.12
```

```
ohmon.sus:
```

Ohio Monongahela Suspended No. 2 Fuel Oil

```
881.250
400   705000.    300.   0.84    0.141E-04    0.755E-030.706E-02    0.187E-020.000E+00
564000.000   141000.00
342650   -97800
    324  383388  -63317  24.0000      0.3     -1.7
 381100  -60059  107.54   380927  -62207  103.10  381289  -62940  118.05 381496  -63364   88.44
 381612  -63445   93.64   383286  -64942  102.53  385900  -64900    1.47 385700  -55100    1.57
 385500  -55300    1.23   385500  -55500    4.27  385100  -55700    6.67 385300  -55700    0.57
 384500  -55900    1.30   384700  -55900    9.48  384900  -55900    1.15 384300  -56100    6.66
 384500  -56100    9.24   383900  -56300    0.08  384100  -56300   11.60 384300  -56300    5.42
 384500  -56300    1.51   383700  -56500    0.05  383900  -56500    3.79 384100  -56500    3.25
 384300  -56500    1.67   383500  -56700    0.06  383700  -56700    5.42 383900  -56700   21.05
 384100  -56700    3.49   384300  -56700    0.52  383500  -56900    9.22 383700  -56900   13.31
 383900  -56900    5.42   384100  -56900    0.58  383300  -57100   20.31 383500  -57100   13.78
 383700  -57100   10.03   383900  -57100    0.55  383300  -57300   21.70 383500  -57300    7.66
 383700  -57300    3.99   383100  -57500   25.84  383300  -57500   18.08 383500  -57500    1.74
```

CONCLUSION

This report describes the model formulation and implementation of a two-layer model, ROSS2, for simulating oil spills in rivers. The model considers the oil in the river as consisting of both the surface slick and suspended oil droplets mixed over the depth of the flow. The oil transformation processes considered in the model include advection, mechanical spreading, turbulent diffusion and mixing, evaporation, dissolution, shoreline deposition and sinking.

The model can be used for instantaneous or continuous spills, either on or under the water surface in rivers with or without an ice cover. Although it is developed for simulating oil spills, the model can be applied to spills of other hazardous materials.

The model has been implemented for the Ohio–Monongahela–Allegheny river system and the upper St. Lawrence River. A case study for the spill on the Monongahela River in January 1988 is presented along with detailed explanations of the program structure and its input and output. The simulation results compared well with field observations.

LITERATURE CITED

Berkey, E., R.L. Price, S.M. Creeger and W.M. Johnston (1989) Assessment of environmental effects from the January 2, 1988 diesel oil spill into the Monongahela River. In *Proceedings of Pittsburgh's Oil Spill, Pittsburgh, Pennsylvania.*

Blokker, P.C. (1964) Spreading and evaporation of petroleum products on water. In *Proceedings, 4th International Harbour Congress, Antwerp,* p. 911–919.

Butler, J., J. Morris and T. Slecter (1976) The fate of petroleum in the open ocean. In *Sources, Effects and Sinks of Hydrocarbons in the Aquatic Environment.* The American Institute of Biological Sciences, p. 287–297.

Cheng, R.T., V. Casulli and S.N. Milford (1984) Eulerian–Lagrangian solution of the convection–dispersion equation in natural coordinates. *Water Resources Research,* **20**(7): 944–952.

Coher, Y., D. Mackay and W.Y. Shiu (1980) Mass transfer rates between oil slick and water. *The Canadian Journal of Chemical Engineering,* **58**(October).

Cox, J.C., and L.A. Schultz (1981) The containment of oil spilled under rough ice. In *Proceedings of the 1981 Oil Spill Conference, American Petroleum Institute, Washington, D.C.,* p. 203–298.

Fannelop, T.K., and G.D. Waldman (1972) Dynamics of oil slicks. *American Institute of Aeronautics Journal,* **10**: 506–510.

Fay, J.A. (1969) The spread of oil slicks on a calm sea. In *Oil on the Sea* (D. Hoult, Ed.). New York: Plenum Press, p. 53–64.

Fay, J.A (1971) Physical processes in the spread of oil on a water surface. In *Proceedings of the Joint Conference on Prevention and Control of Oil Spills, Washington, D.C.,* American Petroleum Institute, p. 463–467.

Fingas, M., and M. Sydor (1980) Development of an oil spill model for the St. Lawrence River. Inland Waters Directorate, Water Management and Planning Branch, Technical Bulletin No. 116.

Fischer, H.B., E.J. List, R.C.Y. Koh, J. Imberger and N.H. Brooks (1979) *Mixing in Inland and Coastal Waters.* New York: Academic Press.

Gundlach, E.R., and M.D. Hayes (1978) Vulnerability of coastal environments to oil spill impacts. *Marine Technological Society Journal,* **12**(4): 18–27.

Hamilton, G.D., C.W. Soileau and A.D. Stroud (1982) Numerical modeling study of Lake Pontchautrain. *Journal of the Waterways, Ports, Coastal and Ocean Division, ASCE,* **108**: 49–64.

Hoult, D.P. (1972) Oil spreading on the sea. *Annual Review of Fluid Mechanics,* p. 341–367.

Hoult, D.P., and W. Suchon (1970) The spread of oil in a channel. Department of Mechanical Engineering, Massachusetts Institute of Technology, Cambridge, Massachusetts.

Hoult, D.P., S. Wolfe, S. O'Dea and J.P. Patureau (1975) Oil in the Arctic. Massachusetts Institute of Technology, Cambridge, Massachusetts, Report No. CG-D-96-75.

Huang, J.C. (1983) A review of the state-of-the-art of oil spill fate/behavior models. In *Proceedings of the 1983 Oil Spill Conference, American Petroleum Institute, Washington, D.C.*, p. 313–322.
Huang, J.C., and F.C. Monastero (1982) Review of the state-of-the-art of oil spill simulation models. Final Report submitted to the American Petroleum Institute, June.
Hung, S. C. (1991) Seaway emergency response plan. In *Proceedings, 1991 Oil Spill Conference, San Diego.*
Johnson, B. H. (1982) Development of a numerical modeling capability for the computation of unsteady flow on the Ohio River and its major tributaries. USA Waterways Experimental Station, Technical Report HL-82-20.
Larsen, P.A. (1969) Head losses caused by an ice cover on open channels. *Journal of Boston Society of Civil Engineers*, p. 45–67.
Leendertse, J.J. (1970) A water-quality simulation model for well-mixed estuaries and coastal seas. Volume I, Principles of computation. The Rand Corporation, Santa Monica, California, Report RM-6230-RC.
Lu, C.Y., and J. Polak (1973) A study of solubility of oil in water. Environmental Protection Service, Canada, Report EP5-4-EC-75-1.
Mackay, D., and C.D. McAuliffe (1988) Fate of hydrocarbons discharged at sea. *Oil and Chemical Pollution*, 5: 1–20.
Mackay, D., S. Paterson and S. Nadeau (1980a) Calculation of the evaporation rate of volatile liquids. *Proceedings of the 1980 National Conference on Control of Hazardous Material Spills, Louisville, Kentucky*, p. 361–368.
Mackay, D., S. Paterson and K. Trudel (1980b) A mathematical model of oil spill behavior. Environmental Protection Service, Fisheries and Environment Canada.
Miklaucic, E.A., and J. Saseen (1989) Oil spill, Floreffe, Pennsylvania—Case history and response evaluation. *Proceedings, Oil Spill Conference, San Antonio, Texas.*
Moore, S. F., R.L. Dwyer and A.M. Katz (1973) A preliminary assessment of the environmental vulnerability of Machias Bay, Maine, to oil supertankers. Parson Laboratory, Massachusetts Institute of Technology, Report No. 162.
Roache, R.J. (1972) *Computational Fluid Dynamics.* Albuquerque, New Mexico: Hermosa Publishers.
Sayre, W.W., and F.M. Chang (1969) A laboratory investigation of open-channel dispersion processes for dissolved, suspended, and floating dispersants. U.S. Geological Survey, Professional Paper 433-E, p. 71.
Shen, H.T., P.D. Yapa and M.D. Petroski (1990) Simulation of oil slick transport in Great Lakes connecting channels. USA Cold Regions Research and Engineering Laboratory, CRREL Report 90-1.
Shen, H.T., and P.D. Yapa (1988) Oil slick transport in rivers. *Journal of Hydraulic Engineering, ASCE*, **114**(5): 529–543.
Shen, H.T., and N.L. Ackermann (1980) Wintertime flow distribution in river channels. *Journal of the Hydraulics Division, ASCE*, **106**(HY5): 805–817.
Stolzenbach, K.D., O.S. Madsen, E.E. Adams, A.M. Pollack and C.K. Cooper (1977) A review and evaluation of basic techniques for predicting the behavior of surface oil slicks. Department of Civil Engineering, Massachusetts Institute of Technology, Cambridge, Massachusetts, Report No. 22.
Spaulding, M.L. (1988) A state-of the-art review of oil spill trajectory and fate modeling. *Oil and Chemical Pollution*, **4**: 39–55.
Tsahalis, D.T. (1979a) Theoretical and experimental study of wind and wave induced drift. *Journal of Physical Oceanography*, **9**: 1243–1257.
Tsahalis, D.T. (1979b) Contingency planning for oil spills: RIVERSPIL—A river simulation model. In *Proceedings of the 1979 Oil Spill Conference, Washington, D.C.* American Petroleum Institute.
Torgrimson, G.M. (1984) The on-scene-spill model: A user's guide. NOAA Hazardous Materials Response Branch, Technical Report (unpublished).
Vicory, A.H., and L. Ahles-Kedziora (1989) Interstate in-stream tracking of the January 1988 Ashland oil spill to the Monongahela and Ohio rivers. In *Proceedings of Pittsburgh's Oil Spill, Pittsburgh, Pennsylvania.*
Waldman, G.A., R.A. Johnson and P.C. Smith (1973) The spreading and transport of oil slicks on the

open ocean in the presence of wind, waves, and currents. Coast Guard Report No. CG-D-l 7-73, AD-763 926, July.

Weeks, W.F., and S.L. Dingman (1972) Thermal modification of river ice covers: Progress and problems. *Proceedings,The Role of Snow and Ice in Hydrology, Banff*, p. 1427–1435.

Yang, X.Q., P.D. Yapa, H.T. Shen and D.S. Wang (1990) Unsteady flow simulation for the Ohio River system. Department of Civil and Environmental Engineering, Clarkson University, Report 90-10.

Yapa, P.D., D.S. Wang, H.T. Shen, X.Q. Yang and J.B. Perry (1990a) An integrated oil spill model for Ohio–Monongahela–Allegheny river system (User's guide). Department of Civil and Environmental Engineering, Clarkson University, Report 90-11.

Yapa, P.D., H.T. Shen, X.Q. Yang, D.S. Wang and J.B. Perry (1990b) User's manual for an integrated oil spill model for St. Lawrence River. Department of Civil and Environmental Engineering, Clarkson University, Report 90-7.

APPENDIX A: DEFINITION OF FORTRAN VARIABLES

The program was written in FORTRAN 77 and was tested on the f77 compiler. In this appendix, important FORTRAN variables are given. For more detailed instructions on the usage of the program, refer to the main text. Descriptions of the main program, subroutines and preparation of data files are also given in the text. The program listing is provided in Appendix B.

Variable	*Symbol*	*Type*	*Description*
akc10	c_{10}	real	Fay's coefficient for gravity–inertial phase one-dimensional spreading
akc20	c_{20}	real	Fay's coefficient for gravity–viscous phase one-dimensional spreading
akc30	c_{30}	real	Fay's coefficient for surface tension– viscous phase one-dimensional spreading
ak2i	k_{2i}	real	Fay's coefficient for gravity–inertial phase axisymmetric spreading
ak2t	k_{2t}	real	Fay's coefficient for surface tension–viscous phase axisymmetric spreading
ak2v	k_{2v}	real	Fay's coefficient for gravity–viscous phase axisymmetric spreading
alevp	s_E	real	Coefficient for modifying evaporation due to emulsification (~0.2–0.5)
alpc	s_c	real	Weighting factor for the river current velocity to compute the surface drift velocity (~1.1)
alpha	a	real	Probability factor for re-entrainment of oil globules from the suspended layer to the surface layer
alpw	a_w	real	Weighting factor for the wind velocity to compute the surface drift velocity (~0.03)
amngn	$\overline{n}$	real	Manning's roughness coefficient for the riverbed
angle		real	Acute angle of the major axis of the slick with the x-axis (radians)
anice	n_i	real	Manning's roughness coefficient for ice at the ice/water interface
amiuo	μ	real	Absolute viscosity of oil (gm-cm/s)
amuni	μ	real	Absolute viscosity of oil (lbf-s/ft^2)
aniu	n_w	real	Kinematic viscosity of water (ft^2/s)
api	API	real	American Petroleum Institute index for oils
apitem		real	Temporary storage for API values
beta	β	real	Fractional empirical factor for bottom deposition of oil
cevp	C	real	Evaporation coefficient C
cordlb(m)		complex	Complex variable giving x and y coordinate locating cross section on reference shore
cordv(m,n)		complex	Coordinates at which vstrm(m,n) is acting
ddd	D_T	real	Horizontal diffusion coefficient
depth(n)	h	real	Depth of the river at the n^{th} grid box center (ft)
dstrm(m,n)		real	Flow depth at m^{th} cross section and n^{th} stream tube (ft)
difx	D_x	real	Diffusion coefficient in the x direction
dify	D_y	real	Diffusion coefficient in the y direction
dvdt	dv/dt	real	Rate of change of oil volume
dx		real	Width of the grid in x or y direction (since square grids are used, the widths are equal) (ft)

fevp1		real	Fraction of oil evaporated at the end of previous time step
fevp2		real	Fraction of oil evaporated at the end of present time step
fueltp		character	Type of oil
full		character	Character variable
gama	γ	real	Empirical fraction for oil exchange from surface to suspended layer
gravac	g	real	Gravitational acceleration (ft/s^2)
hlife(17)	λ	real	Half-life of the shoreline for oil retention (hr)
ibend(n)		integer	Index for the cross section; if 0, flow direction will be along the connection line of corresponding stream tubes in two neighboring cross sections; if 1, flow direction (shore or island)
idam(n)		integer	Particle numbers that have hit locks and dams; stored in the array where n is from 1 to ndam
idum(n)		integer	Temporary storage
ievery		integer	Frequency of obtaining output; e.g. value of 2 gives output every other time step
igrilb(i)		integer	Water-side j grid number (y direction) of the lower boundary of the river for the i^{th} grid in the x direction
igriub(i)		integer	Water-side j grid number (y direction) of the upper boundary of the river for the i^{th} grid in the x direction
igrlb(k,i)		integer	Land-side j grid number (y direction) of lower boundary of k^{th} island (if any) for the i^{th} grid in the x direction
igrub(k,i)		integer	Land-side j grid number (y direction) of the upper boundary of k^{th} island (if any) for the i^{th} grid in the x direction
ihitb(n)		integer	Particle numbers that have hit land; stored in the array where n is from 1 to nhitb
imovin(n)		integer	Particle numbers that are in the water; stored in the array where n is from 1 to nmovin
indprn		integer	Index for printout; if 0, no printout; if 1, printout
indxld		integer	Index for spreading; if 0, axisymmetric spreading; if 1, one-dimensional spreading
ipos		integer	Grid box number
ipol1(n)		integer	Beginning grid box number of the n^{th} ice region
ipos2(n)		integer	Ending grid box number of the n^{th} ice region
izrbx(n)		integer	x grid number of the n^{th} grid box to have zero velocity
izrby(n)		integer	y grid number of the n^{th} grid box to have zero velocity
jdum(11)		integer	Temporary storage
kintm		integer	Number of interpolations between two velocity points of two consecutive cross sections in the same stream tube
lcstsq(m)		integer	Last cross-section number of branch m
llmax		integer	Maximum i^{th} grid of the present moving grid
llmin		integer	Minimum i^{th} grid of the present moving grid
lmax		integer	Maximum i^{th} grid of the present oil slick
lmin		integer	Minimum i^{th} grid of the present oil slick
nbrnch		integer	Number of branches used in oil spill model
ndam		integer	Total number of particles that have hit locks and dams
nfirco(n)		integer	Next cross section connecting to cross section in question. For a divided channel around island, this represents the first cross section connected to in the lower division from the main channel cross section
ngridx		integer	Total number of grids in the x direction
nhitb		integer	Total number of particles that have hit land
nicerg		integer	Total number of ice regions

nicex1(n)		integer	x grid box of the starting point of ice region n
nicex2(n)		integer	x grid box of the ending point of ice region n
nicey1(n)		integer	y grid box of the starting point of ice region n
nicey2(n)		integer	y grid box of the ending point of ice region n
nmovin		integer	Total number of moving particles
nseco(n)		integer	For a divided channel around an island, this represents the first cross section connected to in the upper division from the main channel cross section (if no island, = 0; if lower division complete and returning back to upper division, = 888; if both divisions are complete and resuming main channel, = 999)
nsisct(n)		integer	Number of sounding depths used to describe the channel geometry at the n^{th} cross section
nstube		integer	Total number of stream tubes at the n^{th} cross section
ntpar		integer	Total number of particles
numcon(n)		integer	Condition number of cross section n. If all stream tubes continue to next cross section undivided, = 11; if stream tubes divide into two channels from main channel, = 12; if stream tubes from divided channels connect back to main channel, = 21
nzrvb		integer	Total number of boxes to assign zero velocities
parsur(n)		complex	x and y coordinate location of the n^{th} particle in the surface layer (ft, ft)
parsus(n)		complex	x and y coordinate location of the n^{th} particle in the suspended layer (ft, ft)
preldt		real	Time step for releasing new particles in case of continuous spill (in one spildt several preldt occur) (s)
qsct(n)		real	Discharge at the n^{th} cross section (ft^3/s)
radius(n)		real	Distance of the n^{th} particle from the spill centroid in case of axisymmetric spreadingor the distance of the n^{th} particle from the strip centroid in case of one-dimensional spreading
sctang(n)		real	Angle the n^{th} cross section makes with positive x axis (radians)
sigma	σ	real	Surface tension (lbf/ft)
slickr(n)		real	Slick radius of the n^{th} pie segment (ft)
solblt		real	Solubility of oil (gm/m^3)
soluni		real	Solubility of oil (lb/ft^3)
spaice		real	Surface area of spill under ice (ft^2)
sparea		real	Open surface area of spill (ft^2)
spcen		complex	x and y coordinates of the spill centroid (ft, ft)
spcen0		complex	x and y coordinates of the spill centroid at the beginning of simulation (ft, ft)
spgoil		real	Specific gravity of oil
spildt	Δt	real	Oil spill time step (s)
splrat		real	Rate of oil spill in case of continuous spill (ft^3/s)
spltim		real	Duration of oil spill in case of continuous spill (s)
spvol		real	Total volume of oil spilled (U.S. gal.)
text(n)		character	Storage array for character string
tice(m,n)		real	Thickness of ice at the m^{th} cross section an n^{th} sounding depth location (ft)
timet		real	Total time from the beginning of simulation to the end of present time step (s)
totime		real	Total time for which the simulation has to be performed (hr)
totevp		real	Total volume of oil evaporated until the end of present time step (ft^3)
typbnd(4,i)		real	Oil rejection rate from the shore. The dimension 4 is for the four

			shores (lower: 1, upper: 2, lower island: 3, upper island: 4). The dimension i represents the i^{th} grid in the x direction
t0evp		real	Initial boiling point of oil (K)
t0uni		real	Initial boiling point of oil (°R)
vbuoy	V_b	real	Buoyant velocity of the oil globules in the suspended layer (ft/s)
vcar(n)		complex	x and y components of velocity in the n^{th} grid box (ft/s, ft/s)
vmuni		real	Molar volume of oil (m^3/mol)
vmol		real	Molar volume of oil (m^3/mol)
volevp		real	Volume of oil evaporated during the present time step (ft^3)
volpie(n)		real	Volume of oil in the n^{th} pie multiplied by 8 (ft^3)
volspl		real	Total volume of oil spilled (ft^3)
vopsur(n)		real	Oil particle volume of n^{th} surface particle
vopsus(n)		real	Oil particle volume of n^{th} suspended particle
volspl		real	Imaginary original volume of oil spilled (m^3)
vpsur0		real	Initial particle volume in surface layer (ft^3)
vtsur0		real	Initial total volume in surface layer (ft^3)
vtsus0		real	Initial total volume in suspended layer (ft^3)
vstrm(m,n)		complex	x and y components of the stream velocity at the m^{th} cross section and n^{th} stream ube (ft/s, ft/s)
vwind		complex	x and y components of wind velocity (ft/s, ft/s)
vwmag		real	Magnitude of the wind velocity (ft/s)
vzero		real	Volume of the spill (ft^3)
wsct(n)		real	Water level at the n^{th} cross section (ft)
word		character	Character variable
yshift(n)		real	Distance the n^{th} particle is shifted in the negative y direction if there is an island (ft)
ywid(m,n)		real	Distance along the m^{th} cross section from the reference bank to the n^{th} sounding depth location (ft)
z(m,n)		real	n^{th} sounding depth for the m^{th} cross section (ft)
zd(n)		real	Reference datum for n^{th} section from which the sounding depth is evaluated(ft)

APPENDIX B: LIST OF PROGRAMS

The computer program is written in FORTRAN 77 and has been tested with several Fortran compilers. The program usage is discussed in the main text and Appendix A. Model output (results files) are described in the text. The main program, ROSS2, with all of the following subroutines will be saved on a floppy disk with input and output sample data for the users' reference.

ross2

advsur	advsus	areacl	bndloc	bndrej	calcij
check	check1	chif	ckout	con	conchk
disolu	emdam	emulfn	evapor	exchan	input
lumper	ohndc	orient	pievol	ploter	positn
presur	presus	random	rearrg	redepn	rejloc
reloca	shift	sprd1d	sprdax	strvol	ohvad
veldep					

REPORT DOCUMENTATION PAGE

Form Approved
OMB No. 0704 0188

1. AGENCY USE ONLY (Leave blank)	2. REPORT DATE	3. REPORT TYPE AND DATES COVERED
	August 1993	

4. TITLE AND SUBTITLE

A Mathematical Model for Oil Slick Transport and Mixing in Rivers

5. FUNDING NUMBERS

Contract No. DACA89-SS-K0019

Contract No. DTSL55-89-C-C0549

6. AUTHORS

Hung Tao Shen, Poojitha D. Yapa, De Sheng Wang and Xiao Qing Yang

7. PERFORMING ORGANIZATION NAME(S) AND ADDRESS(ES)

Department of Civil and Environmental Engineering
Clarkson University
Potsdam, New York

Water Resources Engineering Department
Luleå University of Technology
Luleå, Sweden

8. PERFORMING ORGANIZATION REPORT NUMBER

Special Report 93-21

9. SPONSORING/MONITORING AGENCY NAME(S) AND ADDRESS(ES)

U.S. Army Cold Regions Research and Engineering Laboratory
72 Lyme Road
Hanover, New Hampshire 03755-1290

St. Lawrence Seaway Development Corporation
Department of Transportation
New York 13772-0520

10. SPONSORING/MONITORING AGENCY REPORT NUMBER

11. SUPPLEMENTARY NOTES

12a. DISTRIBUTION/AVAILABILITY STATEMENT

Approved for public release; distribution is unlimited.

Available from NTIS, Springfield, Virginia 22161

12b. DISTRIBUTION CODE

13. ABSTRACT (*Maximum 200 words*)

The growing concern over the impacts of oil spills on aquatic environments has led to the development of many computer models for simulating the transport and spreading of oil slicks in surface waters. Almost all of these models were developed for coastal environments. A few river models exist. These models only considered the movement of surface oil slicks. In this study a two-layer model, ROSS2, is developed for simulating oil spills in rivers. This model considers the oil in the river to consist of a surface slick and suspended oil droplets entrained over the depth of the flow. The oil transformation processes considered in the model include advection, mechanical spreading, turbulent diffusion and mixing, evaporation, dissolution, emulsification, shoreline deposition and sinking. The model can be used for simulating instantaneous or continuous spills either on or under the water surface in rivers with or without an ice cover. The model has been implemented for the Ohio–Monongahela–Allegheny river system and the upper St. Lawrence River. This report describes the model formulation and implementation. A case study is presented along with detailed explanations of the program structure and its input and output. Although it is developed for simulating oil spills, the model can be applied to spills of other hazardous materials.

14. SUBJECT TERMS

Computer models
Oil slicks
Oil spills
Rivers

15. NUMBER OF PAGES

78

16. PRICE CODE

17. SECURITY CLASSIFICATION OF REPORT	18. SECURITY CLASSIFICATION OF THIS PAGE	19. SECURITY CLASSIFICATION OF ABSTRACT	20. LIMITATION OF ABSTRACT
UNCLASSIFIED	UNCLASSIFIED	UNCLASSIFIED	UL